A COMPARISON OF SOLAR WIND PARAMETERS MEASURED BY IMP 8, VOYAGER 1, AND VOYAGER 2

by

Stephen J. Simmerer

United States Military Academy

(1981)

Submitted to the Department of
Physics in Partial Fulfillment of
the Requirements for the
Degree of

MASTER OF SCIENCE
in Physics

at the

Massachusetts Institute of Technology

May 1993

Signature of Author Stephen J. Simmerer
Department of Physics
May 7, 1993

Certified by
Alan J. Lazarus
Senior Research Scientist
Thesis Supervisor

Accepted by G. F. Koster
George F. Koster, Chairman
Departmental Graduate Committee
Department of Physics

UNCLASSIFIED
SECURITY CLASSIFICATION OF THIS PAGE

REPORT DOCUMENTATION PAGE

Form Approved
OMB No. 0704-0188
Exp. Date: Jun 30 1986

1a REPORT SECURITY CLASSIFICATION UNCLASSIFIED	1b RESTRICTIVE MARKINGS
2a SECURITY CLASSIFICATION AUTHORITY	3 DISTRIBUTION/AVAILABILITY OF REPORT
2b DECLASSIFICATION/DOWNGRADING SCHEDULE	
4 PERFORMING ORGANIZATION REPORT NUMBER(S)	5 MONITORING ORGANIZATION REPORT NUMBER(S)
6a NAME OF PERFORMING ORGANIZATION Stephen J. Simmerer, MAJ	6b OFFICE SYMBOL (If applicable)
7a NAME OF MONITORING ORGANIZATION Massachusetts Institute of Technology	
6c ADDRESS (City, State, and ZIP Code) 3701 Stearns Hill Road Waltham, MA 02154	7b ADDRESS (City, State, and ZIP Code) 77 Massachusetts Avenue Cambridge, MA 02139
8a NAME OF FUNDING/SPONSORING ORGANIZATION US Army	8b OFFICE SYMBOL (If applicable)
9 PROCUREMENT INSTRUMENT IDENTIFICATION NUMBER	
8c ADDRESS (City, State, and ZIP Code)	10 SOURCE OF FUNDING NUMBERS

PROGRAM ELEMENT NO	PROJECT NO	TASK NO	WORK UNIT ACCESSION NO

11 TITLE (Include Security Classification)
A Comparison of Solar Wind Parameters Measured by IMP 8, Voyager 1, and Voyager 2 (U)

12 PERSONAL AUTHOR(S)
Stephen J. Simmerer MAJOR, US Army, Corps of Engineers

13a TYPE OF REPORT	13b TIME COVERED	14 DATE OF REPORT (Year, Month, Day)	15 PAGE COUNT
Thesis for MS Physics	FROM ____ TO ____	930507	138

16 SUPPLEMENTARY NOTATION

17 COSATI CODES			18 SUBJECT TERMS (Continue on reverse if necessary and identify by block number)
FIELD	GROUP	SUB-GROUP	

19 ABSTRACT (Continue on reverse if necessary and identify by block number)

This thesis analyzes measurements of four solar wind parameters (radial velocity, density, ram pressure, and flux density) as observed by three spacecraft: IMP 8 (Interplanetary Monitoring Platform 8, also called Explorer 50), Voyager 1, and Voyager 2. First, a brief discussion of the evolution of the solar wind within the solar system is presented in order to establish a basis for understanding observed trends in spacecraft data. Then following is an explanation and comparison of the data gathering instruments and collection methods of IMP 8 and the Voyager spacecraft including a discussion of the data analysis. Next, solar wind parameters are compared over four averaging periods: 25/27 days, representing the period of one solar rotation as seen by the Voyagers/IMP 8; 50/54 days, to coincide with two solar rotations; 100 days and 200 days, approximating four and eight solar rotations, respectively. Similarities and differences between spacecraft observations are discussed.

20 DISTRIBUTION/AVAILABILITY OF ABSTRACT	21 ABSTRACT SECURITY CLASSIFICATION
☐ UNCLASSIFIED/UNLIMITED ☒ SAME AS RPT ☐ DTIC USERS	UNCLASSIFIED
22a NAME OF RESPONSIBLE INDIVIDUAL Stephen J. Simmerer, MAJOR, US Army, EN	22b TELEPHONE (Include Area Code) / 22c OFFICE SYMBOL

DD FORM 1473, 84 MAR — 83 APR edition may be used until exhausted. All other editions are obsolete.

SECURITY CLASSIFICATION OF THIS PAGE
UNCLASSIFIED

A COMPARISON OF SOLAR WIND PARAMETERS MEASURED BY IMP 8, VOYAGER 1, AND VOYAGER 2

by

STEPHEN JON SIMMERER

Submitted to the Department of Physics
on May 7, 1993 in partial fulfillment of the
requirements for the Degree of Master of Science in
Physics

ABSTRACT

This thesis analyzes measurements of four solar wind parameters (radial velocity, density, ram pressure, and flux density) as observed by three spacecraft: IMP 8 (Interplanetary Monitoring Platform 8, also called Explorer 50), Voyager 1, and Voyager 2. First, a brief discussion of the evolution of the solar wind within the solar system is presented in order to establish a basis for understanding observed trends in spacecraft data. Then following is an explanation and comparison of the data gathering instruments and collection methods of IMP 8 and the Voyager spacecraft including a discussion of the data analysis. Next, solar wind parameters are compared over four averaging periods: 25/27 days, representing the period of one solar rotation as seen by the Voyagers/IMP 8; 50/54 days, to coincide with two solar rotations; 100 days and 200 days, approximating four and eight solar rotations, respectively. Similarities and differences between spacecraft observations are discussed.

Thesis Supervisor: Dr. Alan J. Lazarus

Title: Senior Research Scientist

Table of Contents

CHAPTER 1

INTRODUCTION

Of the several spacecraft that have been, or are currently collecting plasma data, this thesis is focused on IMP 8, Voyager 1, and Voyager 2. All three of these spacecraft were launched in the 1970's, beginning with IMP 8 and concluding with Voyager 1. To date, they have provided us with a wealth of plasma data spanning nearly two decades. IMP 8 and Voyager 2 continue to provide relevant data and, hopefully, will continue to do so for some years to come. Voyager 1, on the other hand, is no longer capable of measuring solar wind parameters in detail. Unfortunately, in 1980, three years after its launch, its plasma collecting instrument failed. Therefore, we have only about three years of Voyager 1 data with which to work. Even though there is a limited data base, Voyager 1 data have proven to be important. They provide a picture (albeit relatively short) of the solar wind from an area of the heliosphere which is distinct in radial distance but about the same longitude as Voyager 2.

A basic difference between the three spacecraft data sets is that IMP 8 provides data from 1 AU, as it orbits Earth, while the Voyagers record data from increasing radial distance from the sun as the spacecraft leave the solar system. For the first few years of their missions, the Voyagers remained very near the ecliptic plane, varying only a few degrees, but later in their missions, the spacecraft diverged as Voyager 1 headed north and then around 1990, Voyager 2 headed south. Both spacecraft were designed to pass close to Jupiter and Saturn while Voyager 2 was designed to additionally encounter Uranus and Neptune. Figures 1 and 2 provide the ecliptic and meridional projections, respectively, of the Voyagers' trajectories. Just after Voyager 1's encounter with Saturn in 1980, its plasma instrument malfunctioned. Up to that point in time the Voyagers had similar trajectories so we would expect Voyager 1 and

Voyager 2 to experience similar trends in solar wind, and to record many of the same solar events.

The Voyagers have been traveling out of the solar system at the rate of about 1.5 AU per year. At present, Voyager 1 is approximately 50 AU from Earth (radially) and about 27 AU above the ecliptic plane while Voyager 2 is about 38 AU from Earth (radially) but only about 5 AU below the ecliptic. Both Voyagers will continue their journey out of the solar system with Voyager 1 climbing above the ecliptic and Voyager 2 moving further below the ecliptic.

What is the solar wind and why should we study it? The solar wind is a plasma propagating radially outward from the sun, at non-relativistic speeds, averaging about 400 km/s. Plasma is an electrically conducting, ionized gas, containing protons, electrons, alpha particles, and several other ions. While the plasma instruments detect and record many of these ions, the data used in this thesis are proton specific. We study the solar wind because it helps us to understand the environment in which we live, the nature and dynamics of the sun, and what's beyond the limits of our solar system. All of this is important to our general understanding of dilute plasmas and how they interact with each other and with magnetized planets. We also get information about the sources of solar wind in the solar corona and some sense of events on the sun such as solar flares. Also, the dilute plasma itself is an interesting medium in which to study waves and shocks. This plasma, with its infinite boundaries is not accessible in the laboratory environment so we should take full advantage of its availability in space.

As the solar wind propagates radially outward from the sun, it encounters Earth's magnetic field, forms a bow shock, and slows to subsonic speed at the nose of the shock. The terrestrial magnetic field lines are forced backward and dragged back into the magnetotail thereby enclosing Earth in a

"magnetosphere". The boundary of the magnetosphere is the "magnetopause". Figure 3 depicts the solar wind/magnetic field interaction. As the solar wind encounters the bow shock a transition region called the "magnetosheath" is formed between the bow shock and the magnetopause. Plasma flows through the magnetosheath, around the magnetopause, and rejoins the ambient solar wind further downstream [Peratt, 1992].

On a larger scale, it is generally thought that the supersonic solar wind ends with the formation of a "termination" shock upstream (relative to the motion of the sun through the interstellar medium) beyond which the solar wind becomes subsonic. Some distance beyond this termination shock is the "heliopause", the boundary between the heliosphere and the very local interstellar medium (VLISM). The location of the heliopause is expected to be at the point where the dynamic pressure (ram pressure) of the solar wind equals the pressure of the VLISM. This distance has generally been estimated to be anywhere between 50 and 100 AU. Belcher et al. [1992] recently estimated the shock to lie between 80 and 95 AU, on the average, between 1990 and 1992. To complicate the problem, the location of the termination shock and the heliopause should change, i.e., move in and out, as the solar wind ram pressure changes. If we can find some accurate long-term averages of the solar wind parameters, we may be able to predict more accurately the location of the termination shock and heliopause.

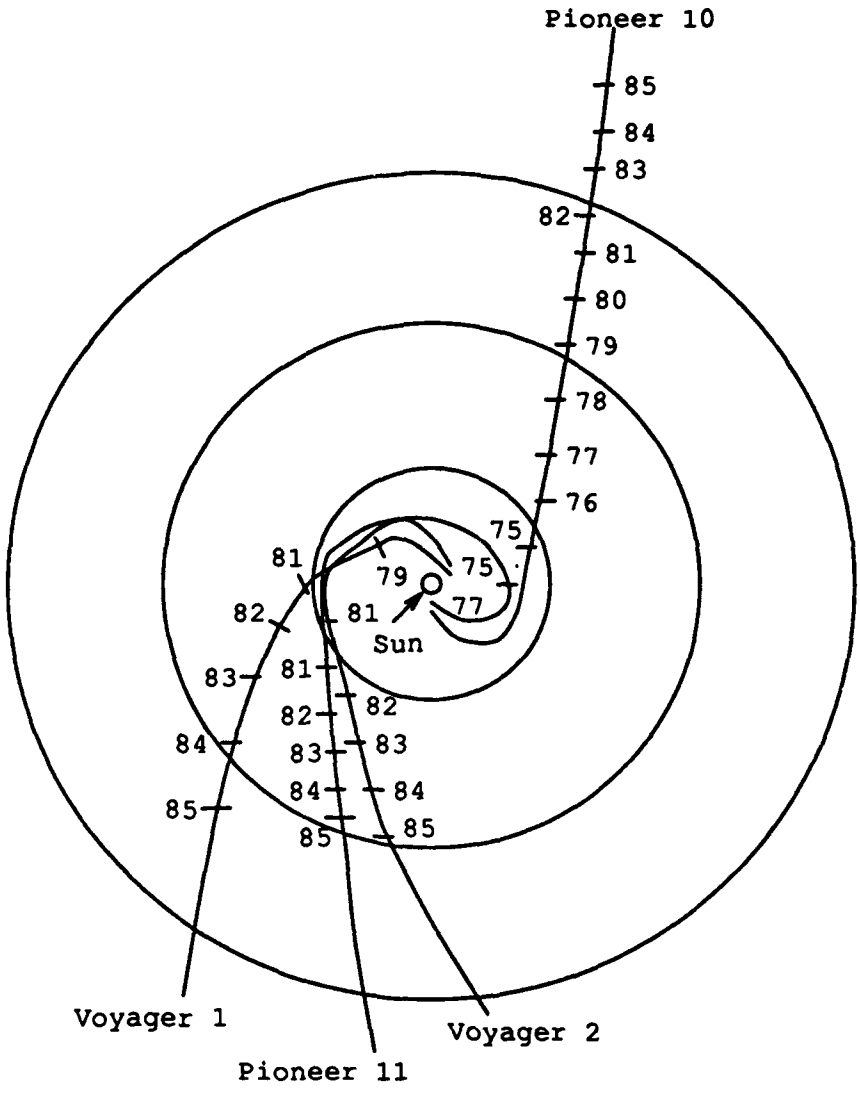

FIGURE 1. Ecliptic projection of the approximate trajectories of Pioneers 10 and 11 and Voyagers 1 and 2. Concentric rings are 10 AU apart. Times shown are approximate.

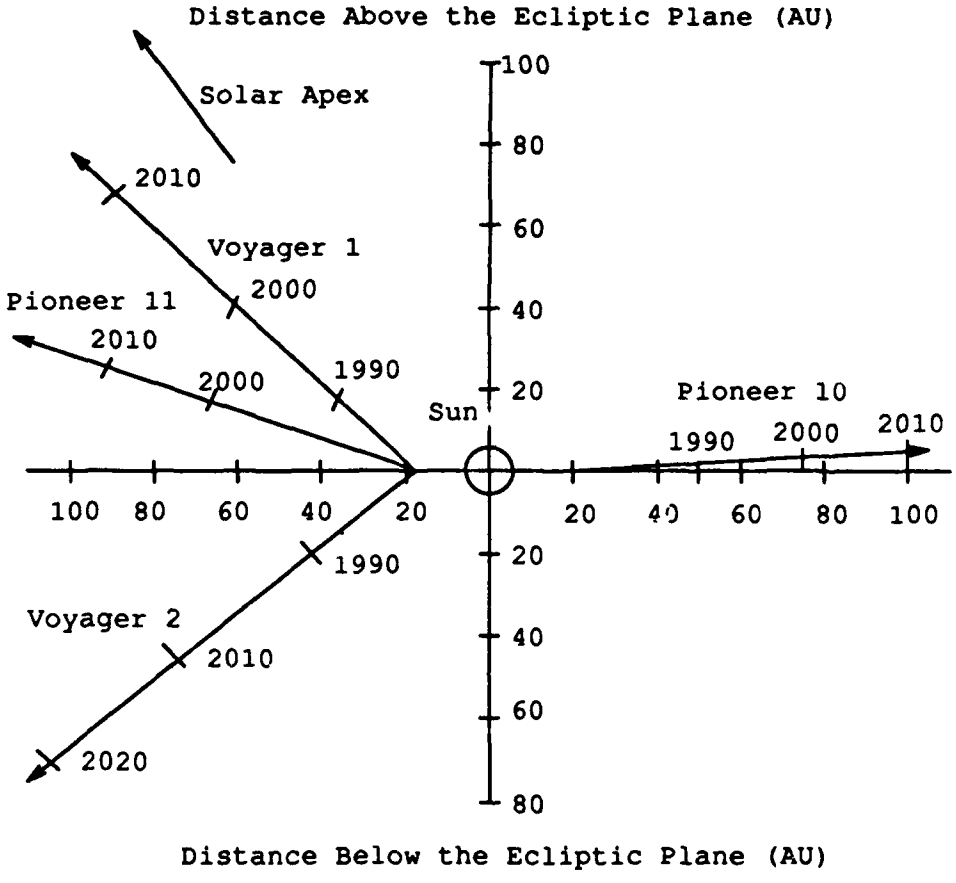

FIGURE 2. Meridional plane projection of the trajectories of the Voyagers compared to Pioneers 10 and 11. Solar apex is the direction of the sun's motion through the Very Local Interstellar Medium (VLISM). Figure adapted from Suess [1990].

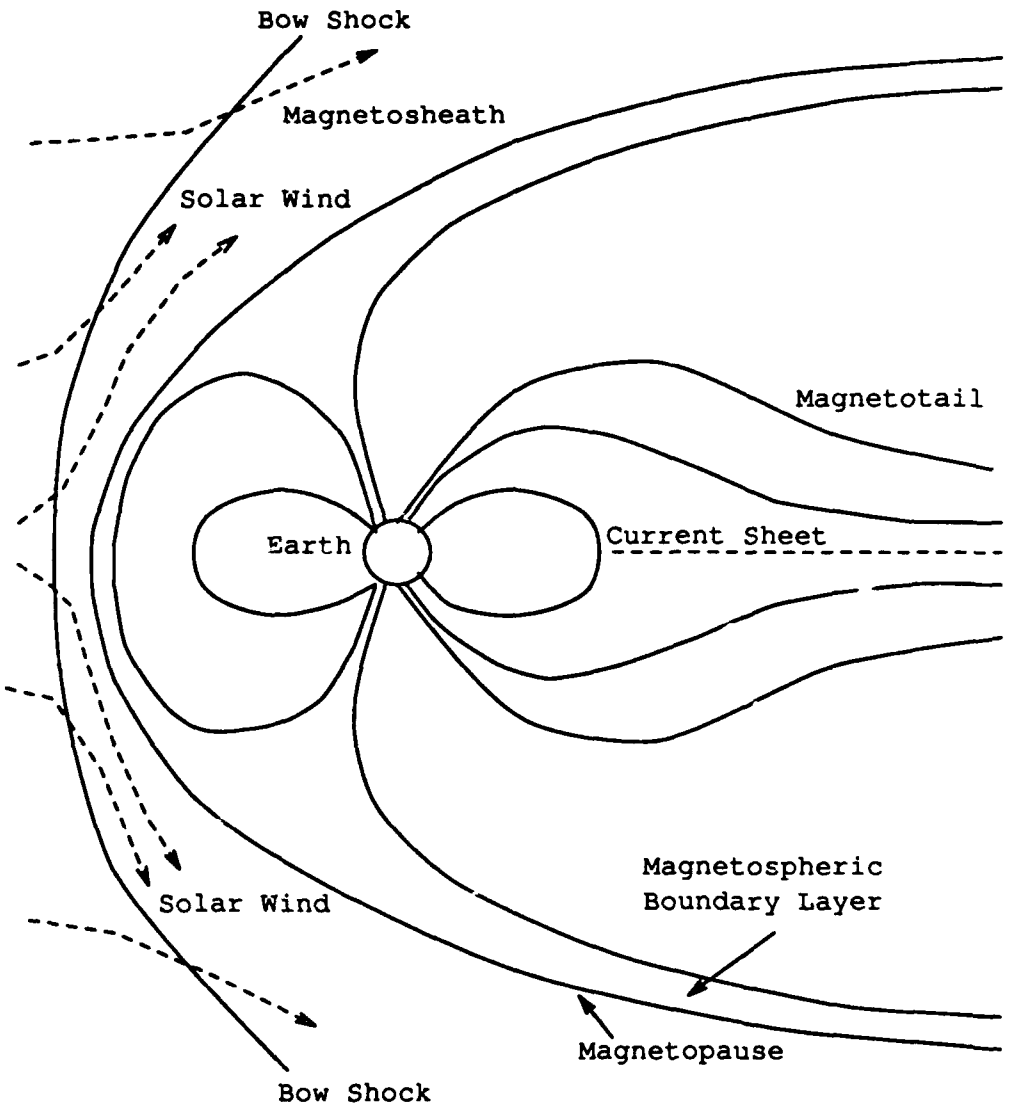

FIGURE 3. As the solar wind nears Earth's magnetic field, a bow shock forms. Earth's field lines are bent back forming the magnetosphere, magnetopause, and current sheet. The magnetopause is the boundary between shocked solar wind and the magnetosphere. Figure adapted from Peratt [1992].

CHAPTER 2

SPACECRAFT INSTRUMENTATION

IMP 8 was launched in October of 1973 into an Earth orbit varying between 30 and 40 Earth radii. With a nearly 12.3 day orbital period it gathers solar wind data at approximately one astronomical unit (AU) (1AU is approximately 150 million kilometers) from the sun, in a trajectory near the plane of the ecliptic [Farquhar, 1990]. Since its launch, IMP 8 has measured solar wind parameters for nearly two 11-year solar cycles. There were solar maxima around 1980 and 1991 and solar minima around 1976 and 1986. This long-term measurement provides us with a good baseline for comparing solar wind parameters throughout the solar cycle. Figure 4 shows the IMP 8 orbit with respect to Earth. As can be seen, IMP 8 periodically passes through the earth's magnetosphere and magnetosheath. During this period, which lasts about five days, IMP 8 continues to record data. Accordingly, these periods, as well as data taken therein, are removed before any analysis of pure solar wind is made.

IMP 8 collects plasma data using three modes: the "tracking" mode, the "non-tracking mode", and the "acquisition mode". The tracking mode is generally for use during the time when the spacecraft is in interplanetary space. The non-tracking mode is used during periods when IMP 8 is within Earth's magnetosphere and the proton fluxes are low. The acquisition mode is the initial mode in which the instrument scans the entire energy range until a peak current is found. When the peak is determined, the instrument switches to the tracking mode. Since we are not using the data inside the magnetosphere or magnetosheath, we are interested only in the tracking mode.

The spacecraft is equipped with a Faraday cup plasma collector/analyzer which measures particles with an energy/charge ratio between 50V and 7.6kV in a series of steps using 24 different energy windows. In the tracking mode,

the spacecraft searches for the peak solar wind flux. When the peak is determined, measurements are made using eight energy levels (windows) around that peak.

The spacecraft is spin-stabilized and rotates once about every 2.69 seconds. As the craft rotates, one of the 24 energy levels is applied to the modulator grid in the form of a DC voltage and an AC square wave is added to produce an "energy window". Any particles with energy/charge ratios greater than the applied potential will enter the detector. Those particles with insufficient energy to overcome the applied potential will be repelled. As the total potential varies in time between the DC baseline potential and the applied square wave potential, some particles are repelled and some make it to the collector plate to be counted. Those that reach the collector are recorded as a current. The modulated component of the current is a measure of the number of particles within the established energy window (channel). As the craft rotates for a second time, a different square wave potential is applied and the current is again measured. This process continues until all eight energy ranges (windows) have been used. The result is one spectrum [Bridge et al., 1967].

The Voyager spacecraft is three-axis stabilized and its instrumentation is slightly different from IMP 8's. While Faraday cups are used, there are more of them and they are configured differently than IMP 8's Faraday cup. The Voyagers have four sensors referred to as the A, B, C, and D cups. The A, B, and C cup-normals are arranged on a 20° half-angle cone whose axis points towards Earth (approximately towards the sun) while the D cup points at right angles to that axis. All four cups measure proton energy/charge ratios ranging from 10 V to approximately 6 kV. The D-cup is configured in order to measure particles moving in the direction approximately perpendicular to the spacecraft-Sun line, such as drifting or rotating particles that would be expected

during encounter periods [Bridge et al., 1977].

The Voyagers take measurements in a different manner than the IMP 8 spacecraft. Because the Voyager spacecraft are three-axis stabilized, not spin-stabilized, more plasma detectors are needed to determine the direction of flow. Each of the A, B, and C cups measures a component of velocity from which an overall velocity can be calculated. There are two modes of operation: 16 wide-window channels (the low resolution mode), and 128 channels with narrower windows, which is the high resolution mode. The low resolution mode is used when detail is not as important for better time resolution and the high resolution mode is used when greater detail is required [Bridge et al., 1977].

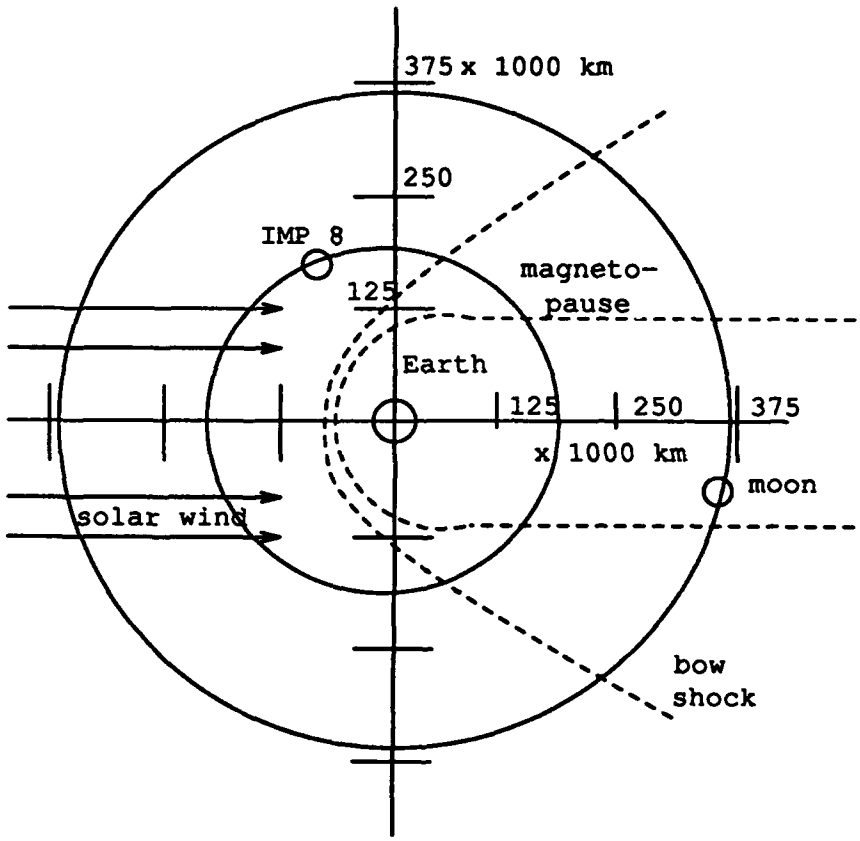

FIGURE 4. A view of IMP 8's trajectory as seen looking down on Earth's North Pole. The solar wind creates a bow shock around the earth. IMP's trajectory takes it through this shock and Earth's magnetosphere once every orbit for about five days. IMP's orbital period is about 12.3 days. Figure adapted from Farquhar [1990].

CHAPTER 3

SOLAR WIND PRODUCTION

The solar wind is produced by the sun in a very complex process which is not fully understood. Generally, the wind is categorized as either quasi-stationary or transient with either high or low speed streams. The quasi-stationary wind's features persist for periods of time, lasting as long as several months. The transient wind is produced by coronal mass ejections (CME) and solar flares which are relatively unpredictable and are short-lived bursts of plasma. The high speed quasi-stationary streams come from regions of the corona, called coronal holes [Neugebauer, 1991]. Bohlin [1977] concisely defined coronal holes as "fairly large-scale, cool, low density areas at both low latitude and the polar caps, encompassing weak, predominately unipolar magnetic fields which extend away from the sun as diverging, open lines of force, and which give rise to high-speed solar wind streams that cause geomagnetic storms". Figure 5 illustrates the relationship between coronal holes, magnetic field lines, high speed and low speed solar wind.

If solar wind is the result of expanding hot coronal plasma, what heats the corona? According to Neugebauer [1991], magnetic fields are primarily responsible for transferring the energy necessary for this heating. The magnetic fields are energized by two processes: convection and microflares. In the outer part of the sun, heat is transferred to the surface via convection, imparting energy to the magnetic field. Microflares also add energy to the magnetic field. These microflares occur within supergranules, which extend about 30,000 km in diameter. Supergranules are composed of many granules which are smaller areas of the sun's surface containing very strong magnetic fields. Microflares occur very often with about 1000 seen every second on the surface of the sun. The energy of each microflare is estimated to be about 10^{26} ergs.

The energy produced by these two processes generates hydromagnetic waves which propagate out to the corona, thereby increasing the plasma's thermal energy. This is enough energy to accelerate the plasma, causing it to escape at speeds between 250 and 2000 km/s [Neugebauer, 1991].

The winds described above are solar cycle dependent. The solar cycle refers to a periodic change in the activity of the sun's magnetic field. The cycle is approximately 11 years in duration, ranging from the period of the maximum number of sun spots called solar maximum, to the period of the minimum number of sun spots, called solar minimum. Counter-intuitively, it is during solar minimum that we see more high speed streams at lower latitudes than we see near the period of solar maximum due to the fact that near the period of solar maximum, coronal holes tend to recede poleward, causing high speed streams to emerge predominately at high latitudes. These coronal holes change shape quickly, on the order of less than one solar rotation. Around solar maximum increased solar flare activity and sporadic coronal mass ejections also contribute to solar wind production [Smith, 1991]. During solar minimum the coronal holes extend to regions close to the equator, causing high speed streams to emerge near the equator, as well as at higher latitudes, and persist for several rotations. As the sun rotates and plasma continuously streams out of the corona, the magnetic field lines remain anchored to their point of origin in the sun. As plasma streams radially away from the sun, the magnetic field lines are dragged outward, and since they remain attached to the sun, they becoming curved, resembling a pinwheel, as depicted in Figure 6.

As plasma propagates radially outward from the sun at different speeds, the faster streams catch up to the slower streams. The magnetic field lines carried by the plasma streams intersect and form a boundary, called an interface. The area around this interface is called an interaction region. At the interface, there

is no penetration of one plasma stream into another because the plasma streams are good conductors. Surface currents, $\vec{J}$, are produced on the plasmas in order to create induced magnetic fields which keep the net magnetic field inside the plasmas constant. A repulsive force $\vec{J} \times \vec{B}$, is produced, keeping the plasmas from penetrating each other. Near the sun, the interface regions form at very small angles, and since there is no penetration, the plasma streams essentially "slide" off each other and change direction. As the streams propagate further away from the sun, the interface regions form at larger angles and the plasmas cannot merely slide off each other any more. Instead, both forward moving and reverse shocks are created. This shock formation process reduces the speed of the faster plasma and increases the speed of the slower plasma, thereby reducing the variation in the stream speeds. The density and temperature of the plasma, on the other hand, increases on both sides of the interface region. For this reason, at large distances from the sun, after being processed through several interaction regions, the solar wind is much less variable but regions of relatively high density and temperature can still be found.

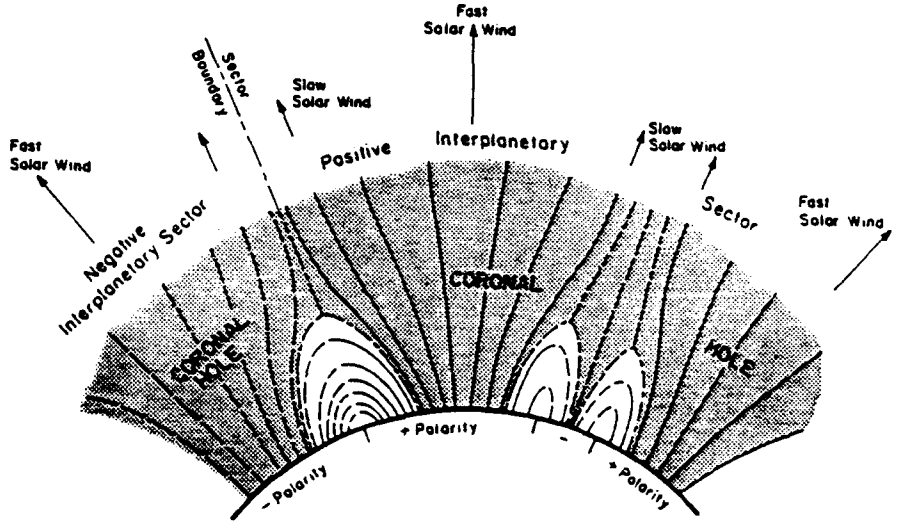

FIGURE 5. Coronal holes are low density regions containing single polarity magnetic field lines which open into space. They provide passageways into space through which high speed solar wind passes. Low speed quasistationary streams emanate from areas between adjacent coronal holes. Figure from Hundhausen [1977].

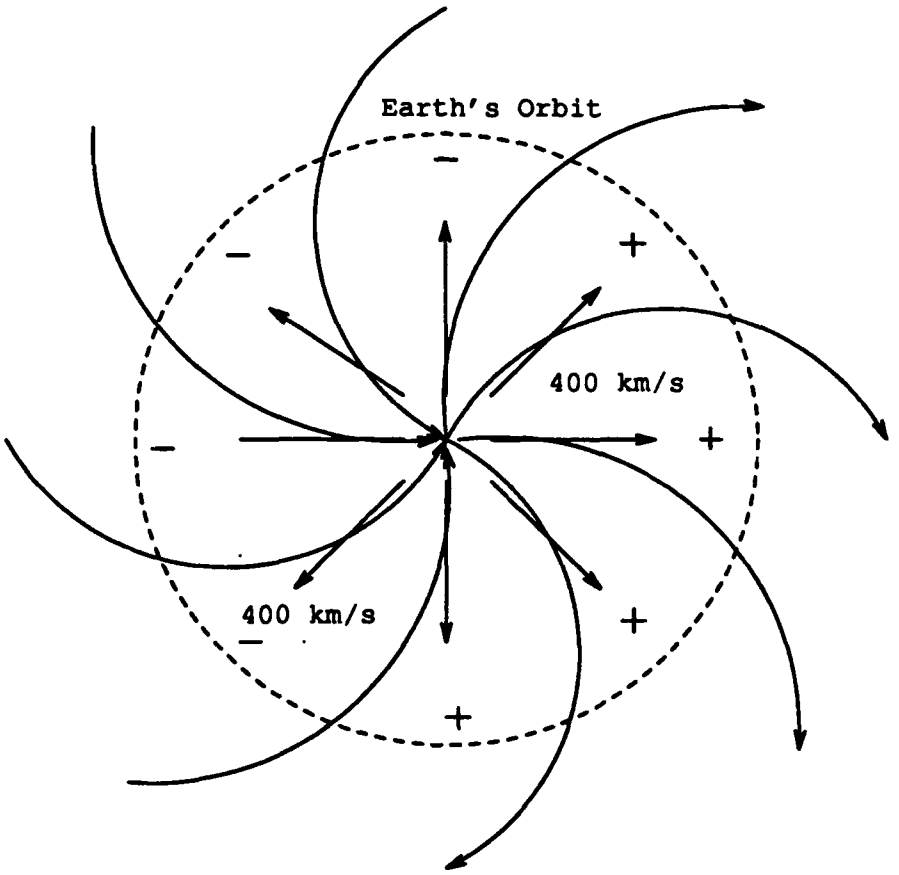

FIGURE 6. Archimedean spiral depicting how escaping solar wind drags magnetic field lines with it. Intersecting plasma streams produce interaction regions. Solar wind propagates radially outward at an average speed of about 400 km/s. Figure adapted from Parker [1963].

CHAPTER 4

DATA ANALYSIS

This chapter is the focal point of this thesis and is divided into several sections. The first Section, 4.1, will provide a summary of the data used and highlight efforts to eliminate errors from the data itself. Section 4.2 will explain how averages of the solar wind parameters were made and the criteria for selectively eliminating other erroneous data. A short discussion on the variation in velocity hourly averages is provided in Section 4.3 in order to give the reader an idea of the fluctuations in the solar wind and also to introduce the data contained in the appendices to which many references will be made in later parts of this Chapter. Section 4.4 covers the same thing for density hourly averages. Sections 4.5 and 4.6 will explain how velocity and density, respectively, were corrected for differences in radial distance.

This thesis will examine four averaging periods: 25/27 days, 50/54 days, 100 days, and 200 days. These periods approximate one, two, four, and eight solar rotations, respectively. This range of averaging periods was selected to provide a look at both shorter and longer term trends in the solar wind. For purposes of this thesis, I parametrized the solar wind in terms of four quantities: radial velocity, density, dynamic pressure, and flux density. Each of these parameters will be analyzed and discussed for the four averaging intervals in Sections 4.7-4.10.

4.1. GENERAL METHODOLOGY

The purpose of this analysis is to determine average trends in the solar wind by using data from multiple spacecraft and to explain differences in the solar wind as measured by them over the four averaging intervals mentioned above. The 27 day interval was used for IMP 8 because it represents the approximate (synodic) period of one solar rotation as seen from Earth while 25

days is the approximate (sidereal, i.e., as seen from the fixed stars) period for one solar rotation as seen by the Voyagers from a distance of several AU. The difference between the synodic and sidereal periods occurs because the sun's rotation is in the same direction as is the earth's orbital motion. While the synodic period is a function of radial distance from the sun as well as a function of heliographic latitude, and is approximately equal to 26.9 days at the sun's equator, the sidereal period is 25.38 days [Gurnette and Woolley, 1961]. So, for a short period after launch, from the Voyagers' locations, the sun rotated at the synodic rate. But as the Voyagers traveled further away from the sun, the sun's period of rotation effectively decreased and rapidly approached the sidereal period. Therefore, the approximation of a constant 25 day solar rotation period was used in calculating average parameters measured by Voyager 1 and Voyager 2. The sun's period, as a function of radial distance, will be derived below.

We shall first look at the radial dependence of the synodic period. Since the spacecraft is launched from Earth, it has the same azimuthal component of velocity as does Earth around the sun. As the spacecraft moves radially away from the sun, its azimuthal velocity, V_ϕ, decreases in order to conserve angular momentum: $\vec{L} = m(\vec{R} \times \vec{V})$ (See Figure 7). Thus, as V_ϕ decreases, the period of the sun's apparent rotation also decreases. Eventually, the spacecraft reaches a distance from the sun where its period of rotation about the sun becomes so long that the sun's rotation period approaches the sidereal period. More precisely,

$$\omega_{synodic} = \omega_{sun} - \omega_{spacecraft}$$

and since $\omega = \frac{2\pi}{T}$, where T is the period, we can write this as

$$\frac{1}{T_{synodic}} = \frac{1}{T_{sun}} - \frac{1}{T_{spacecraft}}$$

From the conservation of angular momentum we have

$$m_{sc}(\vec{R}_1\ V_{\phi_1}) = m_{sc}(\vec{R}_2\ V_{\phi_2})$$

where

R_1 = distance of spacecraft from sun before launch

R_2 = distance of spacecraft from sun after launch

V_{ϕ_1} = azimuthal velocity of spacecraft before launch

V_{ϕ_2} = azimuthal velocity of spacecraft after launch

m_{sc} = mass of spacecraft

This gives

$$\frac{V_{\phi_1}}{V_{\phi_2}} = \frac{R_2}{R_1}$$

We can calculate the period of the spacecraft after launch as follows:

$$T_{sc} = \frac{2\pi R_2}{V_{\phi_2}}$$

Let T_E be the earth's (and spacecraft's) orbital period before launch. Taking the ratio of the periods, we get

$$\frac{T_E}{T_{sc}} = \frac{V_{\phi_2}}{V_{\phi_1}} \times \frac{R_1}{R_2}$$

substituting for the ratio of velocities gives

$$\frac{T_E}{T_{sc}} = (\frac{R_1}{R_2})^2$$

solving for T_{sc} we get

$$T_{sc} = T_E(\frac{R_2}{R_1})^2$$

solving for $T_{synodic}$ and substituting in the expression for T_{sc} we get

$$T_{synodic} = \frac{1}{\frac{1}{T_{sun}} - \frac{1}{T_E(\frac{R_2}{R_1})^2}}$$

Using the following values we can calculate $T_{synodic}$ at various radial distances from the sun:

$$T_{sun} = 25.38 \text{ days}$$

$$T_E = 365 \text{ days}$$

$$R_1 = 1 \text{ AU}$$

For $R_2 = 2$ AU we get

$$T_{synodic} = 25.83 \text{ days}$$

For $R_2 = 3$ AU we get

$$T_{synodic} = 25.58 \text{ days}$$

For $R_2 = 4$ AU we get

$$T_{synodic} = 25.49 \text{ days}$$

So, we can see that when the spacecraft is only 4 AU from the sun, the apparent rotation period of the sun is already reduced to very near the sidereal period. Therefore, it is not long before the spacecraft begins "seeing" approximately the sidereal period of the sun.

As mentioned previously, the sun does not rotate as a rigid body and thus, the synodic period is also a function of heliographic latitude and could be calculated as follows:

$$T = 26.9 + 5.2(\sin^2\alpha)$$

where α is the heliographic latitude [Gurnette and Woolley, 1961]. Since the sun's period of rotation varies with latitude, the simplifying assumption was made to use the sun's period as measured at the equator, i.e., $\alpha = 0$. This produces a synodic period of 26.9 days at the sun's equator. Furthermore, since

we don't know what the periods of the solar wind sources might be, a standardized model is needed. So the approximations were made to use a 27 day solar rotation period as seen by IMP 8 and a 25 day period as seen by the Voyagers.

Besides the 25/27 day averaging intervals, three other intervals were calculated: 50/54, 100, and 200 days. These intervals represent approximately two, four, and eight solar rotations, respectively. While the 100 and 200 day averages provide insight into the long term trends, the shorter periods (25/27 and 50/54 day intervals) provide a better resolution of the solar wind and are useful in helping to explain differences in measurements between the spacecraft.

One strength of this study is the extensive data bases used. Since its launch in 1973, IMP 8 has collected data through two solar maxima and two solar minima. All of the IMP 8 averages used in this paper were calculated using over 67,100 hourly averages (from 1973 day 309 to 1992 day 252). Note that day 1 is defined as January 1. A few of the hourly averages were produced using one spectrum but most were produced using many spectra, some using as many as 100. These 67,000+ hourly averages represent about 42% of the time that IMP 8 has been collecting data. About 35% of IMP 8's orbit is spent in the magnetosheath and magnetosphere, so about 53,000 hourly observations were not usable. The remaining 25% of the available hourly averages is missing because either the spacecraft did not record any data or the data were edited out because of errors of some sort, such as obviously incorrect values (e.g., spikes in velocity or density) or format errors resulting from data processing. Nevertheless, the size of the data base made available by IMP 8 is significant.

Figure 8 (top panel) is a plot of IMP 8 hourly averages for the second-half of 1977. The periodic spikes shown represent the high speed streams IMP 8 encountered as the sun rotated, causing the plasma stream to sweep past IMP

8's location. Periods of missing data, indicated by straight lines, are normally indicative of IMP 8's presence in the magnetosphere and magnetosheath. Points have been added to this plot in order to help visualize the periods of missing data. The period between 1977.61 and 1977.62 is an example of a period when IMP 8 was in the magnetosheath and/or magnetosphere. This period corresponds to about five days, which is the approximate duration of IMP 8's presence in the magnetosphere/magnetosheath.

The Voyager 1 database, on the other hand, does not cover such a long time span. The spacecraft collected and transmitted plasma data from launch in 1977 until 23 November 1980 (day 328), when its solar wind experiment high voltage supply malfunctioned. Limited as it is, this data set represents 19,277 hourly averages. This corresponds to 68% of the 28,152 hours available between 1977 day 250 and 23 November 1980. Like the IMP 8 data set, the Voyager 1 data base was edited to remove erroneous data points, encounter periods, and instrument malfunctions. The larger periods eliminated, with the reason for deletion, are listed in Appendix F.

Figure 8 (middle panel) is a plot of the Voyager 1 hourly averages from 1977.5 to 1980. From this figure we can determine the time between periodic spikes. These spikes represent the high speed streams coming from coronal holes. As the coronal hole evolves, the high speed stream does, too. From one solar rotation to another, the high speed stream probably does not originate from exactly the same place in the corona. This explains why the interval between high speed stream spikes does not equal 27 days. For example, two large velocity spikes occur between 1977.724 and 1977.876 with a smaller spike near 1978.81. The time interval between the two larger spikes is about 55.5 days, nearly the amount of time for two solar rotations. The smaller spike is not centered between the two larger ones but is about 31.4 days after the first

spike and about 24.1 days before the next one. These three high speed streams may all have originated from the same coronal hole. If this assumption is correct, it is clear that there is some structural change in the solar wind source from rotation to rotation.

Voyager 2 data consisted of hourly averages from 1977-1992 (1977 day 234 to 1992 day 163). The data set was scoured in the same manner as the IMP 8 and Voyager 1 data sets to remove bad data points such as velocity and density spikes which were generally singular in nature. Additionally, periods were removed when Voyager 2 encountered the magnetospheres of the planets Jupiter, Saturn, Uranus, and Neptune, as well as the repetitive crossing of the Jovian magnetotail. The exact times of these encounters are given in Appendix F. The resulting data base consisted of 74,600 hourly averages, representing about 57% of the possible time between 1977 day 234 and 1992 day 163.

Figure 8 (bottom) is a plot of Voyager 2 hourly averages of velocity. Like the Voyager 1 data, there are velocity maxima appearing as the spacecraft measures high speed streams. Notice that this velocity profile is similar to that for Voyager 1 as expected since the spacecraft were only .01 AU apart radially on January 1, 1978.

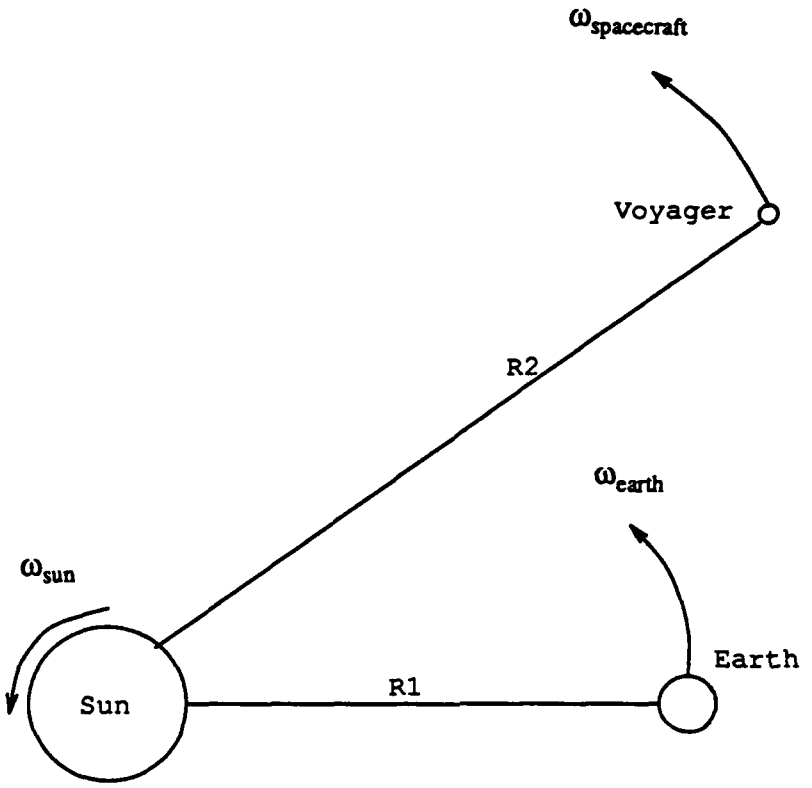

Before Launch: $\omega_{apparent} = \omega_{sun} - \omega_{earth}$

After Launch: $\omega_{apparent} = \omega_{sun} - \omega_{spacecraft}$

FIGURE 7. Before launch the spacecraft has the same angular velocity around the sun as Earth. From Earth, the apparent (synodic) period of the sun is about 26.9 days at the heliographic equator. After launch, the spacecraft's angular velocity, ω, decreases to conserve angular momentum. Ths sun's period as perceived by the spacecraft decreases as a function of distance from the sun, and rapidly approaches the sidereal period of 25.38 days.

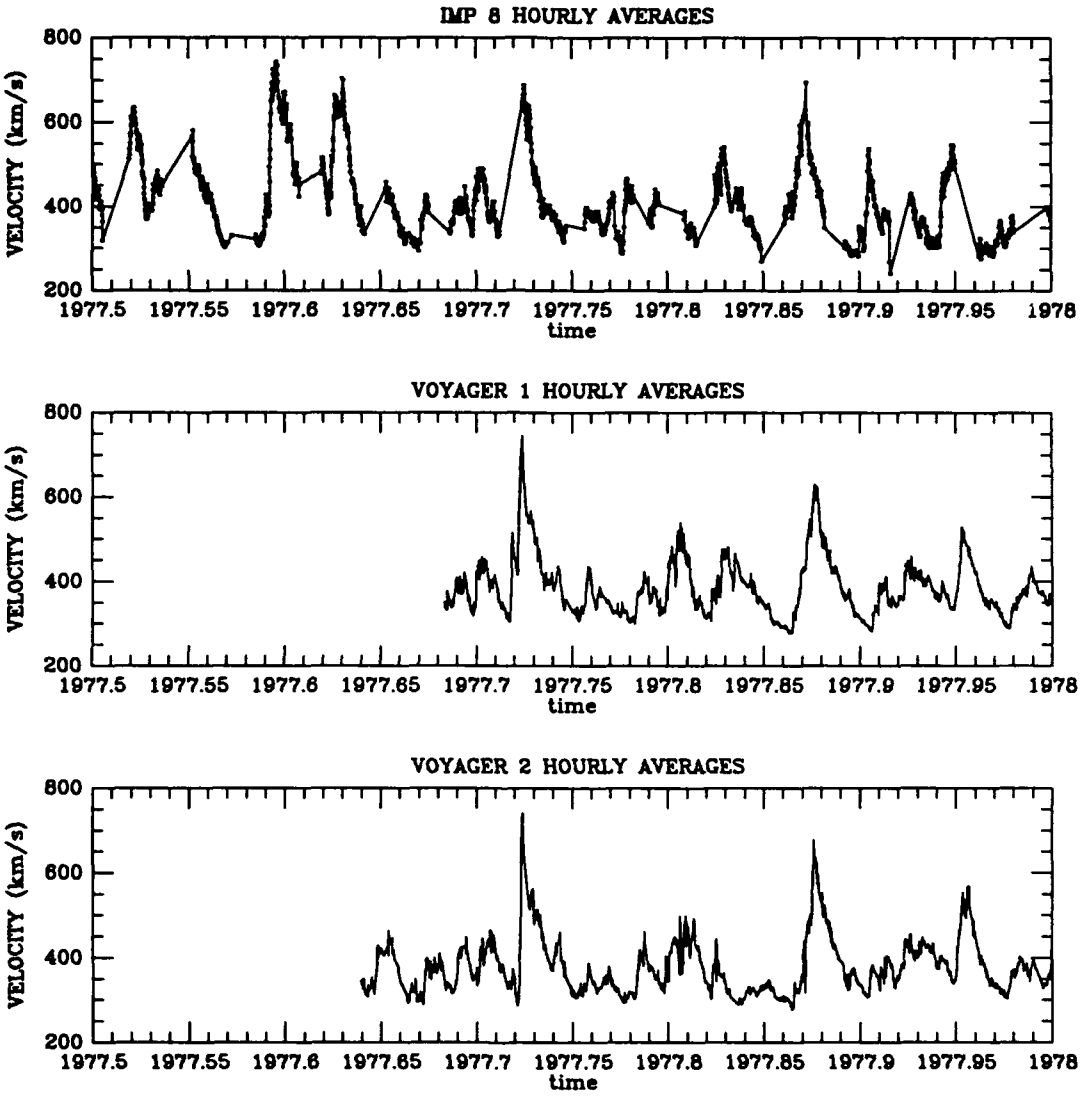

FIGURE 8. Hourly Averages of Velocity for IMP 8 (Top), Voyager 1 (Middle), Voyager 2 (Bottom). Points added to IMP 8 data to enhance visibility of data gaps.

4.2. COMPUTATION OF AVERAGE PARAMETERS

To produce the 25-200 day average parameters, the hourly-average data were used and a weighting technique was applied. Each hourly average consisted of a least one data point (spectrum) but most contained several data points. Hourly averages were weighted in proportion to the number of spectra that were used to compute them. So, the hourly averages using more spectra were weighted more heavily in computing both average parameters and average times. For example, an hourly average made of five spectra was weighted five times as much as an hourly average containing only one point. The average was then obtained by summing all values and then dividing by the total number of spectra used. In the example below, the average velocity is computed using the given data in two ways: first, it is computed using the weighting method and second, by considering both hourly averages to be equally weighted. The difference in average values obtained between the two methods is considerable.

YEAR	DAY	HOUR	NUM	VEL
1973	240	01	10	425
1973	240	02	1	500

the (weighted) average velocity would be calculated as below:

$$\frac{(10 \times 425) + (1 \times 500)}{11} = 431.8 \text{ km/s}$$

The (non-weighted) average velocity would be calculated as:

$$\frac{(425 + 500)}{2} = 462.5 \text{ km/s}$$

There are consequences associated with this weighting technique and it may not have been the best method to use. For example, given a 25 day averaging interval containing 100 hourly averages, evenly distributed, we would have four hourly averages each day. Let each of the hourly averages on the first day of

the interval be made from ten spectra while the other hourly averages in the following 24 days be made from only one spectrum each. The average time would be calculated to lie near the beginning of the averaging interval, between days five and six. Actually, since each day had the same number of hourly averages and each of these were equally valid observations, then an average time calculated to be at the middle of the interval would have been more representative of this example data set. A comparison of actual data to see how many points were skewed more than 20% from the center of the averaging interval yielded the following results: about 17% of IMP 8's data points averaged over 27 days were located more than 20% from the center but this dropped to 9% or less for 50, 100, and 200 day intervals; 15-20% of Voyager 1 data points were more than 20% from the center; and nearly 10% of Voyager 2's 25-day average points were more than 20% from the center but this dropped to less than 6% when averaged over 50, 100, and 200 days. The problem boils down to this: what kind of data should be considered as one "unit"? In this thesis, the individual spectrum was considered a unit of data. In retrospect, the hourly average probably should have been considered as the basic data unit.

To compute a specific averaged interval, 25 days for example, a start time (the first day of the data) was given from which the end time was calculated by counting out 25 days. During this period, all data in between the start and end times were weighted, summed, and then averaged, producing one average data point for each desired parameter. The old end time then became the new start time and another 25 days was counted out to establish the new end time. The average values were then calculated. This process continued until the end of the data set was reached. Using this method, if both start and end times fell within the same data gap (i.e., there was no data in the interval), no average

value was calculated (instead of assigning an average value of zero). Another consequence of this method was that some of the average values were made using a very small number of spectra because the interval happened to fall mostly within a data gap and contain only a very small bit of data at one end (or both ends) of the interval. In extreme cases such as these, the averaged data point was thrown out. In the future, there probably should be some criteria established by which an averaged data point is thrown out unless there is "enough" data within a specified time interval. Whatever constitutes enough data will have to be determined.

The program used to calculate average intervals used a set of criteria to eliminate erroneous data points. Any points where the radial velocity was less than 200 km/s or greater than 2000 km/s were deleted. If there was a difference between moment and fit densities greater than 20%, that point was deleted. Moments and fits refer to the two methods used to calculate parameters. These two methods are summarized below.

The data used to obtain the results in this thesis are based upon data from a "mission" tape. The mission tape data was produced by taking a spectrum every five minutes instead of using every spectrum available. This procedure reduced the total number of data points but allowed rapid processing.

Given a spectrum like the one shown in Figure 9, a non-linear least squares fitting program was used to obtain a satisfactory fit to the measured currents. In Figure 9, the measured current is plotted along the ordinate and the energy channels are plotted along the abscissa. The proton velocity distribution function was assumed to be an isotropic Maxwellian (Gaussian) convected with a bulk velocity $\vec{V}$. The measured current in a particular energy window is related to an integral over velocity space of the velocity distribution function. Because the angular acceptance of a sensor is much broader than the angular width of

the supersonic distribution function, the measured current can be modelled by a one-dimensional integral in the z-direction where z is the normal to the plane of the modulator grid in the sensor. Because the distribution function is narrow compared to the cup acceptance in the x and y directions, the integrations over the other two dimensions are well approximated by integrating from $-\infty$ to ∞, which can be done analytically. The result is that the current in channel j is given by:

$$I_j = Aqn \int_{v_{z,low\,j}}^{v_{z,high\,j}} v_z f(v_z,V_z)dv_z$$

where

$f(v_z,V_z)$ = the normalized velocity distribution function

$$= \frac{1}{w\sqrt{\pi}} \int_{v_{z,low\,j}}^{v_{z,high\,j}} v_z\, e^{\frac{-(v_z-V_z)^2}{w^2}} dv_z$$

A = area of cup aperture

q = charge

n = proton density

v_z = component of proton velocity along z direction

V_z = component of bulk velocity along z direction

w = most probable thermal speed

To start the iterative fitting process, the program must be provided with approximate values of density, bulk velocity, and thermal speed. The initial values are the results of moment calculations. The fitting program uses this input to calculate a value of χ^2 where

$$\chi^2 = \sum_j [I_j - \frac{1}{qA} \int_{v_j}^{v_{j+1}} v_z f(v_z,V_z)dv_z]^2$$

and j is the channel number. After calculating χ^2, its change with respect to

new values for density, bulk velocity, and thermal speed are also calculated. These new values are used as input for a second iteration. A new value is then calculated for χ^2 and compared to the first value found for χ^2. This iterative process continues until a satisfactory fit is obtained, as defined by a change in χ^2 of 10% or less. The values of density, bulk velocity, and thermal speed obtained with the final fit are used as parameter values.

Moment parameters are calculated by summing currents over each energy channel without knowing an explicit velocity distribution. Currents in each channel are calculated from:

$$I_j = qA \int_{v_j}^{v_{j+1}} v_z f(v_z) dv_z$$

where

v_j = low velocity for channel j

v_{j+1} = high velocity for channel j

then

$$\int_{v_j}^{v_{j+1}} f(v_z) dv_z \approx \frac{I_j}{qA\bar{v}_{z,j}}$$

where

$$\bar{v}_{z,j} = \frac{(v_j + v_{j+1})}{2}$$

Since

$$n = \int_{-\infty}^{\infty} f(v_z) dv_z$$

then it follows that

$$n \approx \frac{1}{qA} \sum_j \frac{I_j}{\bar{v}_{z,j}}$$

The Bulk Velocity is

$$V_z = \frac{\int_{-\infty}^{\infty} v_z f(v_z) dv_z}{\int_{-\infty}^{\infty} f(v_z) dv_z}$$

and, therefore, can be approximated as

$$V_z \approx \frac{\bar{v}_z}{n} \int_{-\infty}^{\infty} f(v_z) dv_z \approx \bar{v}_z \frac{1}{qAn} \sum_j \frac{I_j}{\bar{v}_{z,j}} \approx \frac{1}{qAn} \sum_j I_j$$

Starting with the definition of thermal speed

$$w^2 = \frac{2 \int_{-\infty}^{\infty} (v_z - V_z)^2 f(v_z) dv_z}{\int_{-\infty}^{\infty} f(v_z) dv_z}$$

and using the approximations from above yields the final expression for thermal speed

$$w^2 \approx \frac{2}{qAn} \sum_j (v_{z,j} - V_z)^2 \frac{I_j}{\bar{v}_{z,j}}$$

These values of density, bulk velocity, and thermal speed are used in calculating hourly average moment parameters.

For a more thorough discussion on methods of analysis, see Vasyliunas [1971].

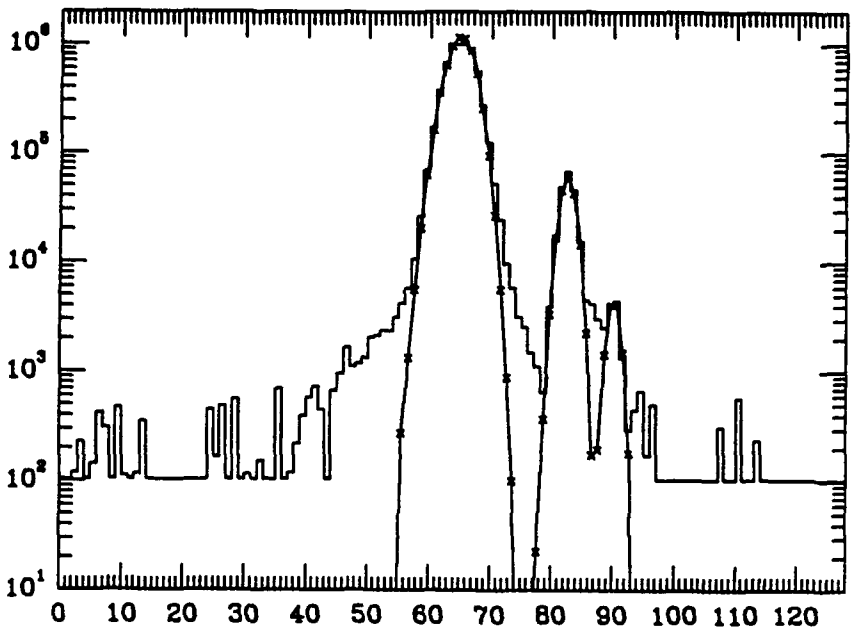

FIGURE 9. Sample current spectrum from one cup fitted by three convected, isotropic, Maxwellian velocity distributions. Channel number is plotted along the abscissa and current is plotted along the ordinate. The proton current distribution is centered at channel 65. Other ions are fitted near channels 82 and 90. The proton distribution is moving with a convected velocity component along the cup normal of about 330 km/s; the proton density is about 17.8 cm^{-3}; and its thermal speed is 19.4 km/s.

4.3. VELOCITY HOURLY AVERAGES

The hourly averages of velocity for IMP 8, Voyager 1, and Voyager 2 are presented in Appendix A. The period covered is 1978 to 1981 (the second half of 1977 was shown in Figure 8) and includes all available Voyager 1 data. Looking at these graphs, it is obvious that generally the velocity profiles for Voyager 1 and Voyager 2 are nearly the same, especially from 1978.5 to 1981. There appears to be a one-to-one correlation between the high speed streams measured by Voyager 1 and Voyager 2 and there is usually a one-to-one correspondence between the streams measured by the Voyagers and IMP 8. For example, the high speed stream measured by IMP 8 on 1978.01 was recorded by both Voyager 1 and Voyager 2 approximately 1978.02. This delay is explained by the fact that it takes some finite time for the plasma to propagate out to the Voyagers' locations. (In 1978.02 Voyager 1 was located 2.001 AU from the sun and Voyager 2 was located 1.983 AU from the sun). A second example is seen about 1978.9 when IMP 8 measured a high speed stream of about 630 km/s. The Voyagers measured a high speed stream about 700 km/s near 1978.94, a difference of about 14 days. This time lag is what we would expect due to the difference in distance from the sun between IMP 8 and the Voyagers at that time (about 3.7 AU). It would have taken about 10.2 days for plasma traveling at 630 km/s to reach the Voyagers after passing IMP 8. There was some additional delay due to the longitudinal difference between IMP 8 and Voyager 2. At that time, the longitudinal difference was about 55°. Assuming that the plasma velocity and stream structure was constant in time, the additional propagation delay would simply be the time that it took the sun to rotate 55°. This is readily calculated, assuming a 25.38 day rotation, to be about 3.8 days (See Figure 10). This makes the total expected propagation delay to be about 14 days, in accordance with the observed delay. Note that

the stream measured by the Voyagers is faster than the stream measured by IMP 8, indicative of some change in the stream. The stream measured by the Voyagers may have been a combination of two streams detected by IMP 8 about 1978.89 and about 1978.9. The first stream may have had a higher velocity than the second, causing it to catch up to the lower velocity stream as it reached the Voyagers' location. We do not know the velocity of the stream measured by IMP 8 at 1978.89 because there is a data gap at that time.

In general, the propagation time (for a given velocity stream) to Voyager 2 was greater than that for Voyager 1 until near the end of 1977 because Voyager 2 had traveled further from the sun (See Figure 1). However, Voyager 1 moved faster than Voyager 2 and the two spacecraft reached the same radial distance about day 347 of 1977. Since that time, Voyager 1 has continued to travel radially outward faster than Voyager 2. Consequently, Voyager 1 detected the same high speed streams increasingly later than Voyager 2. This is fairly evident beginning in 1978.

As the Voyagers' radial distance from the sun increased, there was a general flattening of the velocity profiles around 390 or 400 km/s with an occasional spike near 600 km/s, especially after 1980. The individuality of the high speed streams were lost through the effect of processing through the interaction regions mentioned in Chapter 3.

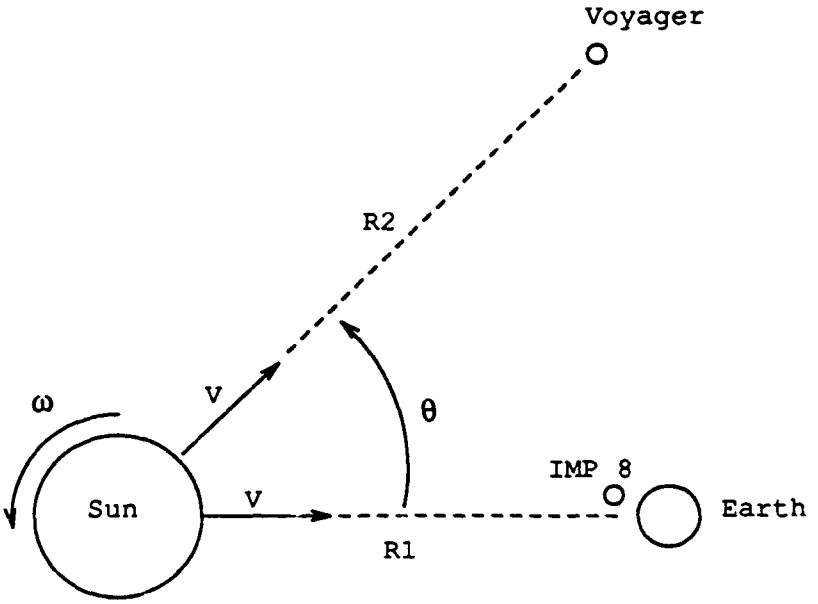

FIGURE 10. Assuming a plasma stream is constant in time, the propagation time for plasma to reach IMP 8 is $T_1 = \frac{R_1}{V}$. Considering longitudinal effects, the time delay for plasma originating from the same coronal hole to reach Voyager is $T_2 = \frac{R_2}{V} + \frac{\theta}{\omega}$, where ω is the angular rotation speed (about 13°/day) of the sun, assuming a period of 25.38 days, and θ is the longitude angle between IMP 8 and Voyager.

4.4. DENSITY HOURLY AVERAGES

The hourly averages of density for IMP 8, Voyager 1, and Voyager 2 are presented in Appendix B. Density does not remain constant as the solar wind propagates outward from the sun. Therefore, the densities have been normalized to 1 AU in order to facilitate comparison of IMP 8 densities with Voyager densities. Because IMP 8 remains in a near-Earth orbit, varying only about .1% from 1 AU, it is assumed to be at a constant distance of 1 AU from the sun and, consequently, its density has not been normalized.

In uniform, spherically symmetric flow, density decreases as R^{-2}, where R is the radial distance from the flow source. We know that solar wind does not flow uniformly because of the temporal dependence of solar dynamical processes and the disruptive nature of interaction regions. However, if we assume that the solar wind flows in accordance with this simple model, we can correct for density in a simple way. Belcher et al. [1992], studied this problem and found that solar wind density can be accurately modeled as varying with distance from the sun as

$$R^{-2.10 \pm .03}$$

Therefore, even though the solar wind is not spherically uniform, density falls off very nearly as the simple R^{-2} model and we, therefore, can use this approximation without introducing significant error.

This normalization approximation gives the approximate value of the density when the plasma passed 1 AU. The normalized ram pressure is $P = N \times R^2 \times V^2$. The ram pressure, also known as dynamic pressure, is the force per unit area exerted by the moving protons. The units of pressure used in this thesis are nanopascals (nPa), where 1 nPa = 1×10^{-8} dyne/cm^2. The normalized flux density is $F = N \times R^2 \times V$. Flux density represents the number

of protons passing through a unit area per second. With these data sets normalized, we can compare the solar wind parameters as measured by the two Voyager spacecraft with IMP 8.

Like velocities, the densities measured by the Voyager spacecraft are more similar to each other than to those from IMP 8. Generally, the two Voyager spacecraft measure the same density variations but with some differences in magnitudes. After 1979, there is a marked change in the density structure as measured by the Voyagers. The number of very large density spikes has decreased and there are seen several regions of very low density. These density phenomena result from processing plasma streams through several interaction regions. As explained in Chapter 3, density increases on both sides of the interface regions, accounting for the continued large density regions. The areas of very low density, called rarefaction regions, are caused by faster streams moving away from slower streams, reducing the density of the region between the streams. Some examples of these rarefaction regions are especially apparent in 1980.

4.5. PROJECTED VELOCITIES

Appendix C contains plots of hourly average velocity projected back to a distance of 1 AU. The data have been modified to account for the time taken to propagate to the point in space where they were measured. The projected data provide some idea of what the stream structure looked like when it passed 1 AU (the same distance from the sun as IMP 8). The propagation time was computed as follows:

$$\text{time lag (days)} = \frac{K \times (R-1) \times D}{V}$$

where

$$K = 1.5 \times 10^8 \text{ km/AU}$$

$$R = \text{spacecraft distance (AU)}$$

$$D = \frac{1 \text{ day}}{86400 \text{ s}}$$

$$V = \text{velocity (km/s)}$$

As an example, the time to propagate to 10 AU, while moving at a constant 450 km/s, is nearly 39 days. At 30 AU, the propagation time is about 116 days. The propagation time was then subtracted from the actual time of measurement to yield the time that the plasma should have crossed 1 AU. As a result, IMP 8 and both Voyagers will appear to have measured the same high speed streams at the same time. Note that later in the mission, notably after 1978.5, there is a "leaning" effect created by this normalization process. Because the propagation time is inversely proportional to the velocity of the stream, the slower streams will be pulled back further than the high speed streams. In the latter half of 1980 this effect is readily apparent.

It is especially important to realize that the stream structure produced by this projection process is not exactly the structure which crossed at 1 AU

because the streams have been processed through several interaction regions, resulting in velocity changes. This adjustment process, however, provides us with some idea of what the stream structure looked like at 1 AU.

There have been no adjustments to account for longitudinal differences between the spacecraft. Since Voyager 1 and Voyager 2 followed very nearly the same trajectory until the time of the Voyager 1 failure, the longitude of Voyager 1 and Voyager 2 are approximately the same. Since Earth orbits the sun once in a year and the Voyagers are generally heading radially outward from the sun, the angle between IMP 8 and the Voyagers varies between 0° and 180°. Therefore, the maximum time difference that can arise when the two spacecraft measure the same stream is about 13 days, or half of one solar rotation period. This time difference is important when averaging over 25 or 50 days but is not so important when averaging over 100 or 200 day intervals. In retrospect, data probably should have been adjusted to account for longitudinal differences between the spacecraft.

4.6. PROJECTED DENSITIES

Projected density is shown in Appendix D. As mentioned, the Voyager densities were normalized to 1 AU in order to make comparisons with IMP 8 measurements. Not only was the density drop-off accounted for but the propagation time was taken into effect, too, using the same procedure as explained in Section 4.5. The leaning effect associated with this projection process is not very evident in 1977 but becomes apparent beginning in the second half of 1978. This effect is so great that some data are overwritten by other data. This overwriting of data is due to velocity variation and each density datum is moved back in time by a different amount. Consequentially, the plots become difficult, at best, for use in determining density values. The Voyager 1 data on or about 1980.6 are a good example of this. We will use these plots to the best of our ability when trying to compare values of one spacecraft's measurement with another while keeping this shortcoming in mind.

4.7. 25/27-DAY AVERAGES

This section examines 25 day averages for the Voyagers and 27 day averages for IMP 8. These intervals approximate one solar rotation as seen by the respective spacecraft. These periods are the shortest averaging intervals used in this thesis and, consequently, provide the best resolution of the solar wind structure. In this analysis, we will first look at the period 1977-1981 because it includes all of the Voyager 1 data which are available. The period 1973-1993, comparing IMP 8 and Voyager 2, will be presented next.

Figure 11 is a plot of 25/27 day averages comparing solar wind (proton) parameters as measured by IMP 8, Voyager 1 and Voyager 2. From the top down are flux density, ram pressure, density, and radial velocity. IMP 8 data are indicated as dotted lines with square points; Voyager 1 data are indicated as dashed lines with open triangles; Voyager 2 data are represented as solid lines with filled-in triangles.

4.7.1. VELOCITY

The velocities vary between 350 km/s and 550 km/s, generally. Because the period covered is only four years, we cannot see the effect of the full solar cycle but the effects of the 1980 solar maximum are apparent: the velocities of all three spacecraft fall to a minimum at this time. This decrease occurs because coronal holes retreat to the sun's polar regions during this period, resulting in low speed streams dominating near the heliographic equator.

At this time resolution, there are significant differences between the Voyagers and IMP 8 between 1979.2-1979.7 and 1980.3-1980.5. The data between 1978.2-1978.4 show good agreement between IMP 8 and Voyager 2. (There are no data for Voyager 1 during this period). The first period in question, 1979.2-1979.7, shows that the Voyagers agree with each other and disagree with IMP 8 until 1979.5, but after 1979.6 all three spacecraft disagree with

each other. This disagreement is probably the result of both longitudinal and latitudinal differences between the spacecraft. Between 1979.2 and 1979.7 Voyager 2 stayed near 6° below the heliographic equator and Voyager 1 remained near the heliographic equator. IMP 8, on the other hand, moved from - 6° to + 7.5° during this time period. About 1979.7 (see Figure A-4) Voyager 1 recorded a maximum hourly average velocity over 804 km/s while Voyager 2 recorded a maximum of about 945 km/s. At the time of this measurement, the angle (longitude difference) between IMP 8 and the Voyagers was about 145°. Because the Voyagers were on the opposite side of the sun from IMP 8 and at different heliographic latitudes, they probably encountered different stream structure than IMP 8 did. Comparing the Voyagers' measurements of this high speed stream, we notice that Voyager 2 recorded the stream a little earlier than Voyager 1 did. This is because Voyager 2 was closer to the sun than Voyager 1 and the stream had a higher velocity at Voyager 2's location, causing it to propagate faster. Furthermore, the stream probably was a time-varying stream because it was not seen again during the next solar rotation.

Since all the parameters, including time, were averaged according to the number of data points (the consequences of this technique were discussed in Section 4.2), a time interval having significantly more data at one end, or having measured a very high speed stream near an end will have an average time skewed toward that end. In the subject period's case, the data gap covered three 25 day averaging periods. The first interval started just before the data gap, thereby skewing the average time of that point near the beginning of the 25 day period. The second interval occurred entirely within the period of missing data, producing no data, and consequently, causing a gap in the curve between the points shown about 1979.42 and 1979.61. The third interval started about .02 years before the data gap ended, thereby skewing the average

point to near the end of the period. Therefore, due to the data gap and then the high speed stream, the average time of measurement for Voyager 2 was slightly later than the average time of measurement for Voyager 1.

The second period in question, 1980.3-1980.5, shows agreement in velocity between the Voyagers but not IMP 8. The data indicate a low IMP 8 average velocity of about 350 km/s while both Voyagers measured an average of about 440 km/s. There are no significant data gaps in the Voyager data during this period but there are periodic gaps in the IMP 8 data, resulting mostly from edited magnetosphere and magnetosheath periods. During this period, IMP 8 records minima of about 300 km/s and the Voyagers record higher minima, of about 350 km/s. This period covers three 27-day averaging intervals: the first starts about 1980.28 and ends about 1980.35; the second goes from 1980.35 to 1980.425; and the third ranges from 1980.425 to 1980.5. Looking at the 27 day IMP 8 averages, we see that the point at about 1980.4 is the one which disagrees with the Voyagers. This point was made from the hourly average data in the interval 1980.35-1980.425, which includes two data gaps. The velocity data which are present are very low, generally about 300-350 km/s. The Voyager data for the same period record a low of about 350 km/s and a high of about 500 km/s at the end of the interval. This higher hourly average velocity may have resulted from longitudinal and latitudinal differences between the spacecraft. In 1980.5, IMP 8 was located about 4° above the heliographic equator while Voyager 2 was located about 5° below it. Also, there was a difference in longitude of approximately 90° between the Voyagers and IMP 8 in 1980.4. Therefore, it is possible that the Voyagers encountered different solar wind streams than IMP 8 did, accounting for the differences in average velocity.

4.7.2. DENSITY

Moving to the panel above velocity in Figure 11, we see the density profiles for the spacecraft. Density varies roughly between 3 and 17 protons/cm^3, with IMP 8 recording the greater variation. In general, IMP 8 measured higher density than either of the Voyagers, with an unusually high average occurring near 1978.1. This period may be an example of how streams differ in longitude and/or time. At the time of measurement, there was a 52° difference in longitude between the Voyagers and IMP 8. The stream recorded by IMP 8 had a vastly different structure than that recorded by the Voyagers. By the time the sun rotated through 52°, the stream structure could have changed and the density decreased, thereby explaining why the Voyagers did not record the same data as did IMP 8. Also, gaps in the IMP 8 data may have contributed to the difference. Between 1978 and 1978.2 there are six gaps in the IMP 8 data (see Figure D-2). Notice that these gaps often occur at times when the density profile is moving toward a minima. This excludes low density data from the averaging process, thereby producing a higher average density.

There are several differences seen between 1979.5 and 1981. Most of these can be explained using the same arguments of data gaps or higher hourly averages. For example, the difference seen about 1979.5, when IMP 8 recorded a density of about 10 protons/cm^3, Voyager 1 about 6 protons/cm^3, and Voyager 2 about 3 protons/cm^3, may be explained by a data gap in the Voyager 2 data between 1979.45 and 1979.6. Also, IMP 8 measured a large density spike about 1979.495 while Voyager 1 did not. Besides data gaps and longitudinal differences, there may be another explanation for some of the differences between spacecraft measurements. The answer may lie with solar wind velocity gradients. This issue will be considered later in Section 4.7.6.

4.7.3. DYNAMIC PRESSURE

Dynamic pressure is shown in the second panel from the top of Figure 11. Pressure is seen to vary between about 1 and 4 nanopascals (nPa), with IMP 8 generally recording a higher pressure. Since dynamic pressure is computed as $N \times V^2 \times R^2$, the differences seen between the spacecraft are a direct result of the differences explained in the velocity and density profiles. Note that average dynamic pressure values were calculated by taking the average of the product of density and velocity squared, $\langle nV^2 \rangle$.

4.7.4. FLUX DENSITY

Flux density, $N \times V^2 \times R$, is presented in the top panel of Figure 11. It is seen to vary between about 1 and 5×10^8 protons–cm^{-2}–s^{-1}. Note that average flux density values were also calculated by taking the average of the product of density and velocity squared, $\langle nV^2 \rangle$. Notice that IMP 8 data produces the highest flux density averages with the largest differences seen around 1978.1. Since flux density is a function of density and velocity the differences are a result of the differences explained in velocity and density.

4.7.5. LONG-TERM VARIATIONS

Figure 12 presents 25/27 day averages for the period 1973 to 1993 for IMP 8 and Voyager 2. (Voyager 1 is excluded because we already examined this data in the previous sections and found that the Voyager spacecraft data are generally very similar.) The effects of the 11-year solar cycle are obvious here. We expect to see a decrease in solar wind velocity near low latitudes near solar maximum and an increase in velocity near low latitudes near solar minimum because of the evolution of coronal holes throughout the solar cycle, as explained in Chapter 3. We are satisfied by looking at the velocity profile near the solar minima of 1976 and 1985 and the solar maxima of 1980 and 1991. During the solar minimum of 1976, IMP 8 records solar wind moving between

500 and 600 km/s. After that time, the velocity decreases to around 400 km/s during the solar maximum of 1980. Velocity then gradually increases to about 450 to 600 km/s around the solar minimum of 1985 and decreases again approaching the 1991 solar maximum.

The velocity profiles of IMP 8 and Voyager 2 follow the same trends between 1981 and 1993 (the period 1977-1981 will not be discussed here since it was already covered earlier) except during the period 1986-1988. During this period, Voyager 2 recorded a very constant velocity of about 380-400 km/s for more than one year. IMP 8, on the other hand, measured very periodic velocity peaks ranging between 380 km/s to over 500 km/s. What caused this period of nearly constant velocity as measured by Voyager 2 from 1986-1987? Several scientists have examined this and have arrived at possible answers. Miyoke [1988] studied the period between 1985 and 1986 using observations from IMP 8, Sakigake, Suisei, and Giotto spacecraft. He found that in May and June of 1986 Sakigake measured high speed streams in excess of 600 km/s while located about 5-7° above the heliographic equator. At the same time, IMP 8 measured lower speed streams (about 400 km/s) while located between -5 and 0°. Later that year, around August and September, when IMP 8 was located about 5-7° above the heliographic equator, it measured high speed streams in excess of 600 km/s but Sakigake did not because it was located between 0 and 5° above the heliographic equator. Miyoke suggests that these velocity differences were caused by latitudinal velocity gradients in the solar wind.

These latitude velocity gradients may have been the result of changes in the coronal neutral sheet (current sheet) during this period. The current sheet can be described as the boundary between solar magnetic field lines of opposite polarity. According to Lazarus et al. [1988], the current sheet can be an indication of the boundary between fast and slow solar wind regions. Of course,

there are an enormous number of regions where there is an interface between magnetic field lines of opposite polarity, creating local current sheets. But if we model the sun's magnetic field as a single dipole, the resulting current sheet is the one we are after. As the solar cycle evolves from maximum to minimum, the coronal holes extend to lower latitudes, thus the axis of the sun's dipole moves, thereby changing the location of the current sheet. Throughout the solar cycle, the location of the current sheet can vary significantly. According to Gazis [1993] and Suess et al. [1993], in 1986 the current sheet declined to about 10° from the heliographic equator. The current sheet's location at this time is much lower than in 1980 when it was tilted about 70° to the heliographic equator [Suess et al., 1993]. The measurements made by Voyager 2 and IMP 8 about 1986.5-1987.5 are consistent with the explanation given above: Voyager 2 measured low, nearly constant velocity plasma streams about 380 km/s while located near the heliographic equator and IMP 8 measured 27 day average velocities peaking over 530 km/s while located at 7.5° above the heliographic equator.

Figure 13 depicts the variation in the solar wind velocity with heliographic latitude between 1977 and 1993. The top panel provides the velocity profile of Voyager 2 superimposed on a plot of its variation in heliographic latitude. The latitude scale is on the left ordinate and velocity is indicated on the right ordinate. Time is plotted along the abscissa. The bottom panel provides the same information for IMP 8 except it also includes the plot of Voyager 2's latitude variation, in order to facilitate comparison between the two spacecraft. Note that the latitudinal variation of IMP 8 is between a maximum of 7.5° above the heliographic equator to a minimum of 7.5° below the heliographic equator with a period of exactly one year, coinciding with the earth's rotation around the sun. As Earth's heliographic latitude varies between -7.5° and +7.5°

during the year, IMP 8's heliographic latitude also varies by the same amount. From the top panel, we can see that shortly after launch in 1977, Voyager 2 reached its maximum distance above the heliographic equator of nearly 10°. It then descended to a minimum of almost - 6° between 1979.5 and 1980 when it began a long slow ascent back towards the heliographic equator. About 1985.5 Voyager 2 reached the heliographic equator and continued its ascent to about 4° near 1990 when it began its final descent through the heliographic equator. Between 1986 and 1987, Voyager 2 remained near the heliographic equator, ranging between 0° and 2° above it while IMP 8 continued its latitudinal variation between ±7.25°. Since Voyager stayed near the heliographic equator, it measured only the low speed streams present during this period when the current sheet was near the heliographic equator. IMP 8's measurements are consistent with Miyoke's [1988] study.

The density variations are shown in the second panel from the bottom of Figure 12. Over the long-term, the density variation is between 1 and 19 protons/cm^3. The largest differences are seen between 1984 and 1986, around 1988, and again about 1990. IMP 8 consistently measured higher densities than Voyager 2. Correspondingly, dynamic pressure (second panel from top) varied between .5 and 6.5 nPa and flux density (top panel) ranged between .5 and 7 x 10^8/cm^2–s. Variations in pressure and flux are the direct result of the variations in density and velocity. Note that there has been a change of scale in order to accommodate the dynamic pressure range of values.

4.7.6. LATITUDE GRADIENTS

As discussed in earlier sections, coronal holes are usually the sources of high speed solar wind [Neugebauer, 1991]. I examined inferred magnetic field and coronal hole data compiled by McIntosh et al. [1991], to correlate high speed streams with coronal holes. The correlation showed that it is relatively

easy to associate a coronal hole with a high speed stream detected by IMP 8 during solar minimum when many coronal holes extend to the heliographic equator. On the other hand, it is not so easy to identify a coronal hole as the source of high speed plasma near solar maximum. More detailed results of this work are summarized in Appendix E. Perhaps more readily confirmed is the phenomena of high speed sources producing latitude gradients, thereby accounting for many of the velocity differences between IMP and the Voyagers. This is discussed below.

Using the IMP 8 data, it is possible to identify times when there was an apparent latitudinal gradient in velocity. If a gradient existed then we should be able to explain the velocity differences recorded by Voyager 2 by comparing its latitudinal location with that of IMP 8. Looking at Figure 13, there are several periods when gradients seemed to exist: 1979-1980; 1986-1988; 1989-1990; and 1991-1992, for example. Sometimes the sources of high speed wind appeared above the heliographic equator and at other times they appeared below the heliographic equator. The first period noted, 1979-1980, is interesting because velocity increased from about 415 km/s to a peak of near 515 km/s as IMP 8 descended from 7.5° above the heliographic equator to 7.5° below it. Between 1986 and 1988, the source appeared to be changing from above, to below, and then back to above the heliographic equator. During this period, IMP 8 started at 7.5° above the heliographic equator and measured solar wind moving about 535 km/s. As IMP 8 descended, velocity decreased to about 390 km/s at the point where the spacecraft was 4° below the heliographic equator, then velocity jumped to near 500 km/s as IMP 8 reached 7.5° below the heliographic equator. The gradient seemed to shift again to above the heliographic equator as velocity increased while IMP 8 ascended through the heliographic equator and reached a peak of nearly 505 km/s at the point where the

spacecraft was 7.5° above. Between 1989 and 1990, velocity increased with decreasing latitude indicating a southern source and then increased with increasing latitude between 1991 and 1992, indicating a northern source.

If these velocity gradients actually existed, then we should be able to predict the velocities measured by Voyager 2. For example, the peak velocity measured by IMP 8 between 1979 and 1980 of about 525 km/s occurred when IMP and Voyager 2 were near the same heliographic latitude, about -5°, implying a source in the south. Therefore, we would expect that Voyager would have also recorded a velocity peak of a similar magnitude at the same time. As seen in Figure 13, Voyager measured a peak velocity of about 470 km/s at this time, about 55 km/s less than that measured by IMP 8. However, a short time later, after Voyager descended further to about -6°, the spacecraft did record a significant average velocity peak of nearly 565 km/s. At the same time, IMP neared it maximum latitude and recorded a lower velocity, equal to about 440 km/s. So, when both spacecraft were below the heliographic equator, they both measured high average velocities and when they ascended toward the heliographic equator, the average velocities decreased. These spacecraft measurements are consistent with the presence of a high speed source in the south.

Between 1986.5 and 1988 there is more evidence supporting the existence of high speed sources above and below the heliographic equator. For example, IMP 8 measured average solar wind velocity of 535 km/s about 1986.5 at its peak above the heliographic equator. At the same time, Voyager was about 2° above the heliographic equator and measured about 415 km/s solar wind. While there was a large difference (120 km/s) in velocities measured at the same time, it is noteworthy to mention that either shortly earlier or later when IMP was near 2° above the heliographic equator (which was the same location as Voyager 2), IMP recorded a much lower velocity of about 390 km/s, nearly

matching the velocity recorded by Voyager 2, a result consistent with the presence of a high speed source near the heliographic equator. About 1987.1, IMP 8 recorded a velocity peak of about 495 km/s when it reached -7.5° heliographic latitude while Voyager 2 recorded average velocity of only 375 km/s while it was still located near +2° latitude. These measurements indicate a high speed source in the south. IMP 8 measured another velocity peak of about 505 km/s near its maximum latitude about 1987.8, indicating a source in the north while Voyager 2 measured a velocity of about 470 km/s at about the same time as it neared 3.5° above the heliographic equator, also indicating a source in the north.

In 1989.1, IMP 8 measured a velocity peak about 560 km/s when it reached its minimum latitude, implying a source in the south. About the same time, Voyager 2 recorded an average velocity peak of about 505 km/s when it was about 4° above the heliographic equator, indicating a source in the north. These last two measurements may imply the presence of short lived high speed sources both above and below the heliographic equator.

A similar series of measurements were made between 1991 and 1992. During this period, a high speed source appeared to exist above the heliographic equator as IMP 8 recorded increasing velocity with increasing latitude. As it reached its maximum latitude, IMP 8 recorded average velocity peaks of about 560 km/s with large velocity fluctuations over this period. As IMP descended through the heliographic equator, the velocity decreased, still consistent with a source above the heliographic equator. But, if a source existed in the north, we would have expected Voyager 2 to detect lower velocity streams since it was below the heliographic equator at that time and was moving increasingly lower. However, at first Voyager 2 measured higher velocity (about 495 km/s) as it descended to about -3°, but descending further, it began

to follow the decreasing velocity trend recorded by IMP 8. A possible explanation for these measurements is that there were multiple high speed sources that varied with longitude and with time.

Figures 14, 15, and 16, respectively, are plots of density, dynamic pressure, and flux density varying with latitude. These are presented to show that using the same type of analysis used for velocity, periods of gradients in these three parameters can be identified. For example, there appears to be a gradient in density (Figure 14) in the south about 1982, 1988, 1992, and a northern gradient can be seen about 1991.8 and 1992.2. Figure 15 shows a dramatic increase in dynamic pressure as a function of latitude with a northern source suspected around 1991.2 and 1992. Large fluxes around 1978, 1982, 1990, and 1992, seem to be dependent on low latitude, while between 1991 and 1992, large fluxes are measured with higher latitudes. High speed streams are indicated in Figure 13 about 1979 and 1981 but flux remains low during these periods, as shown in Figure 16. While high speed streams were prevalent at IMP 8's location between 1986 and 1988, flux remains moderate. Velocity fell to a low about 1988 but flux was high. Between 1991 and 1992 both velocity and flux were high. This data suggests that flux is not constant, i.e., flux is not necessarily higher in regions where there are high speed streams and lower where there are low speed streams.

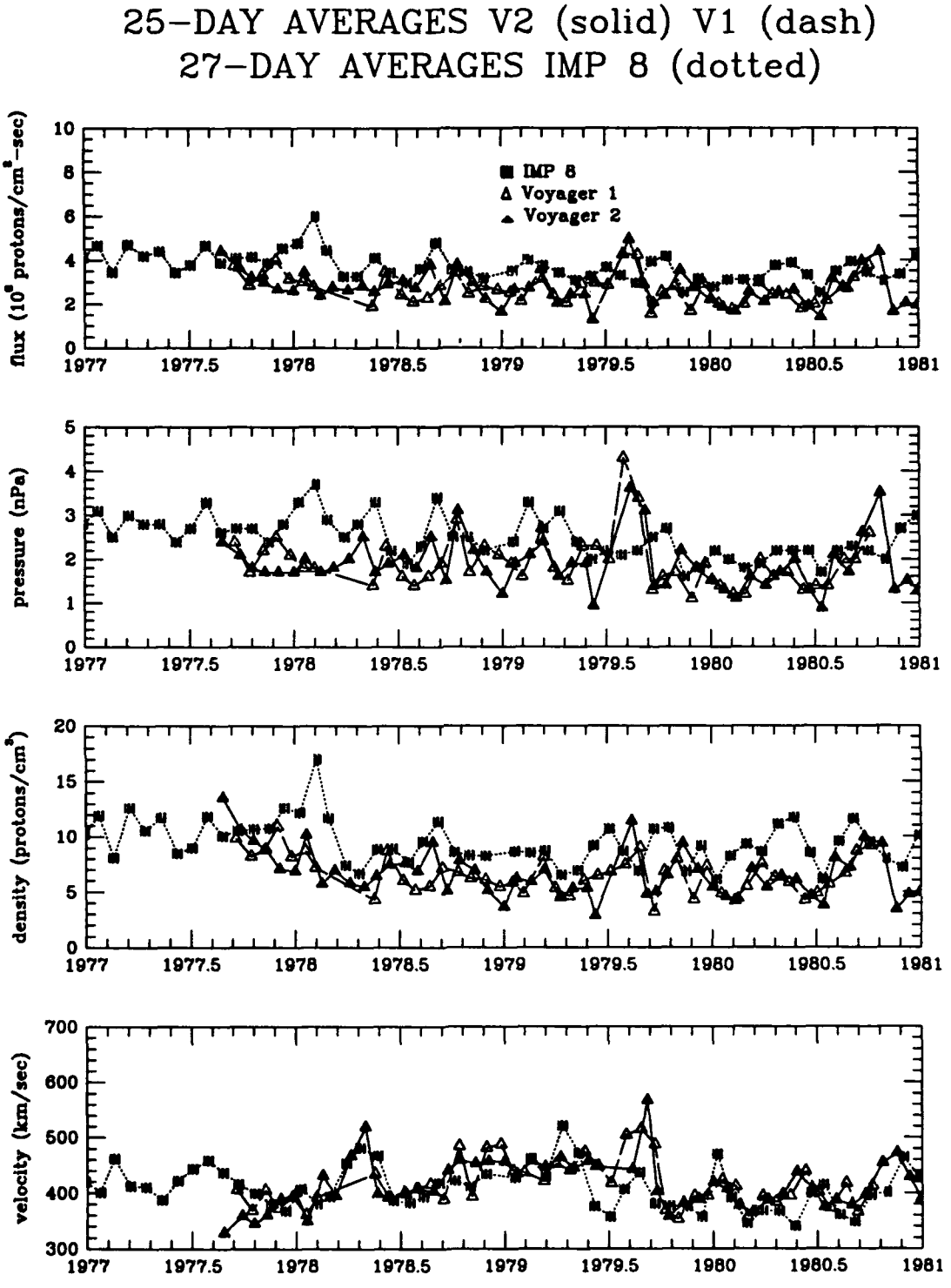

FIGURE 11. 25/27 Day Averages of flux density, ram pressure, normalized density, and velocity. All parameters adjusted for propagation time.

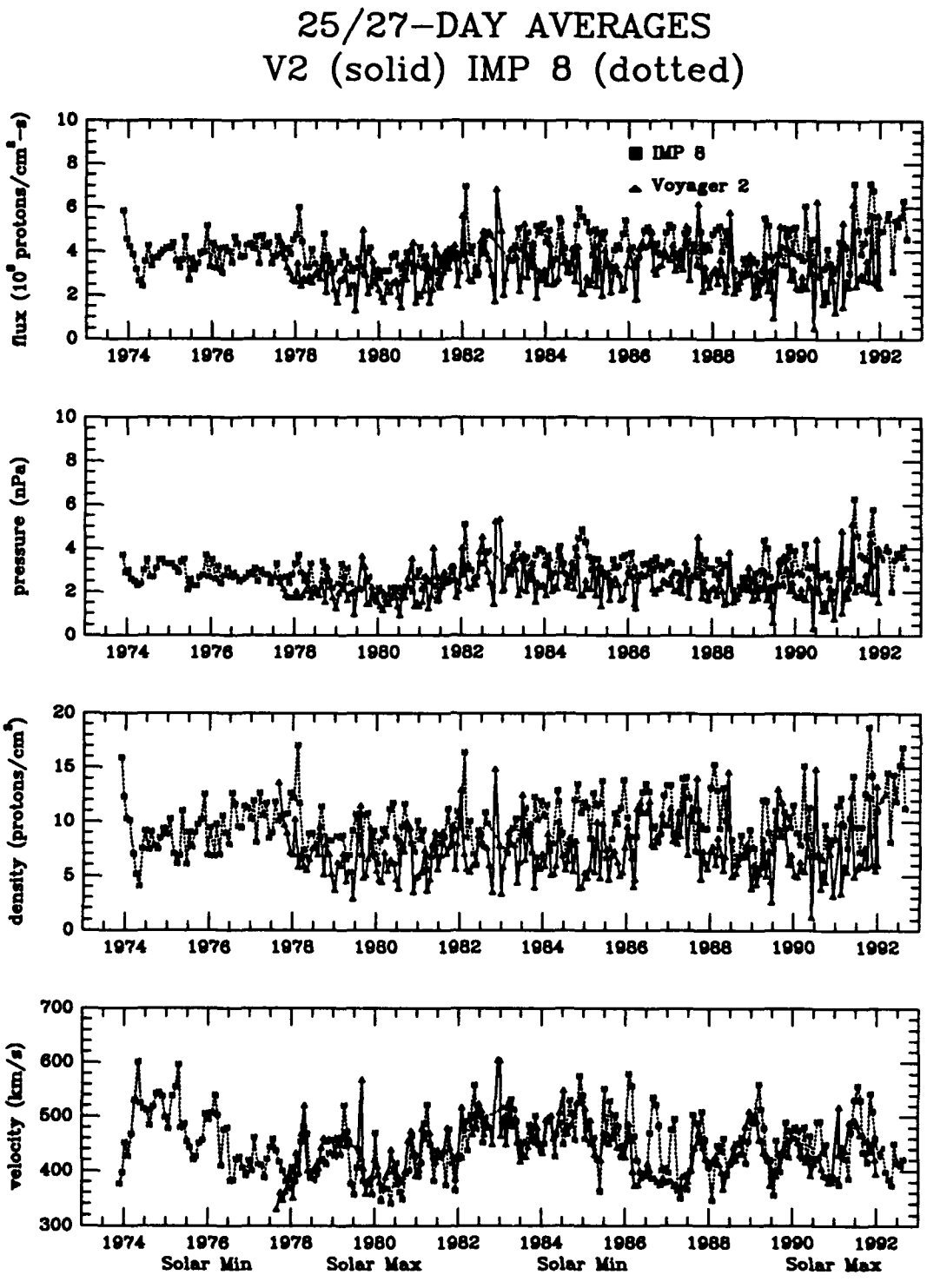

FIGURE 12. 25/27-Day Averages for Voyager 2 and IMP 8. V2 data adjusted for propagation time.

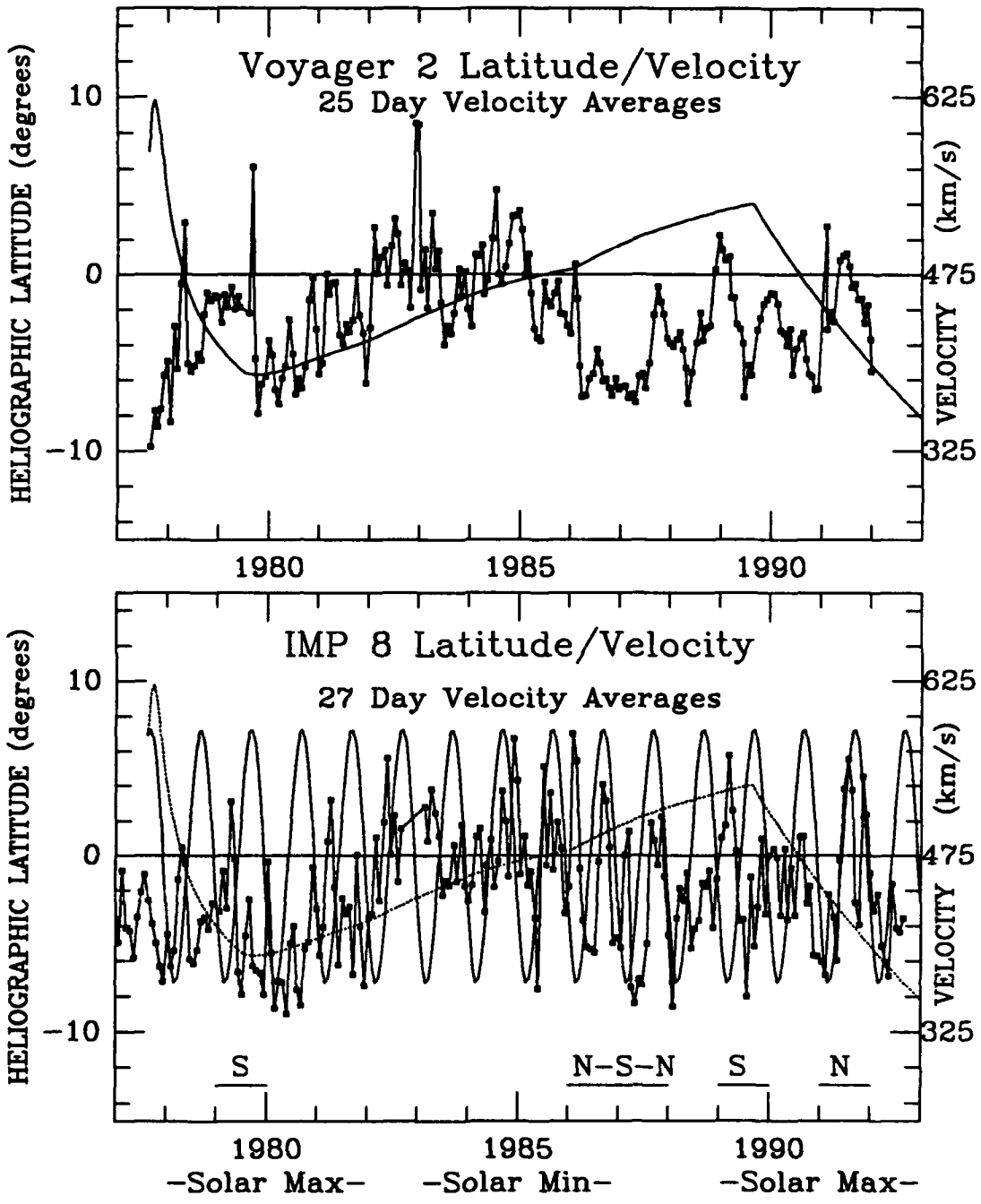

FIGURE 13. Heliographic latitude and velocity vs. year for Voyager 2 (top), IMP 8 (bottom). Velocity corrected for propagation time. Latitude not corrected for propagation. High speed source locations indicated by N (north) or S (south).

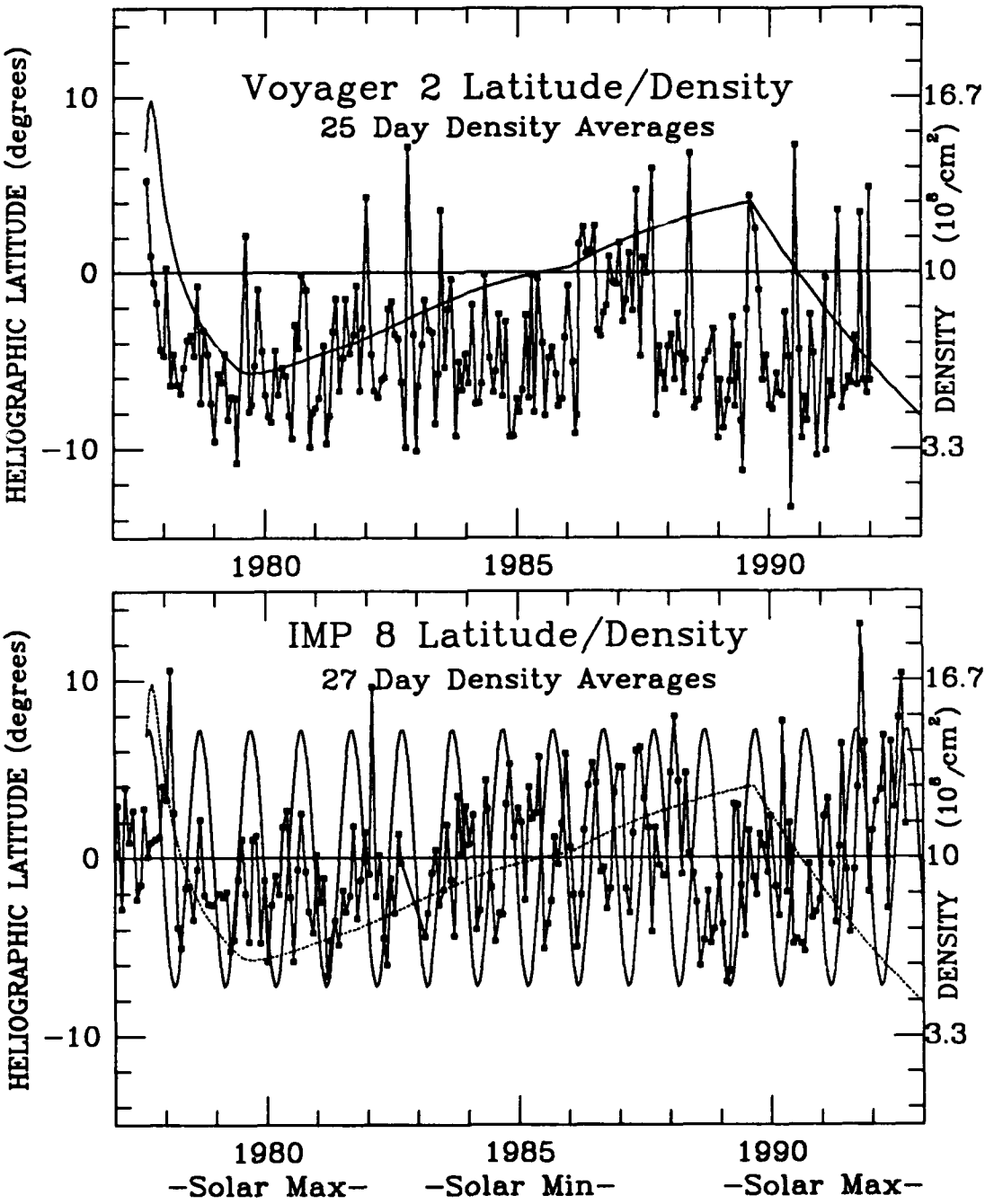

FIGURE 14. Heliographic latitude and density vs. year for Voyager 2 (top) and IMP 8 (bottom). Density corrected for propagation time; latitude not corrected.

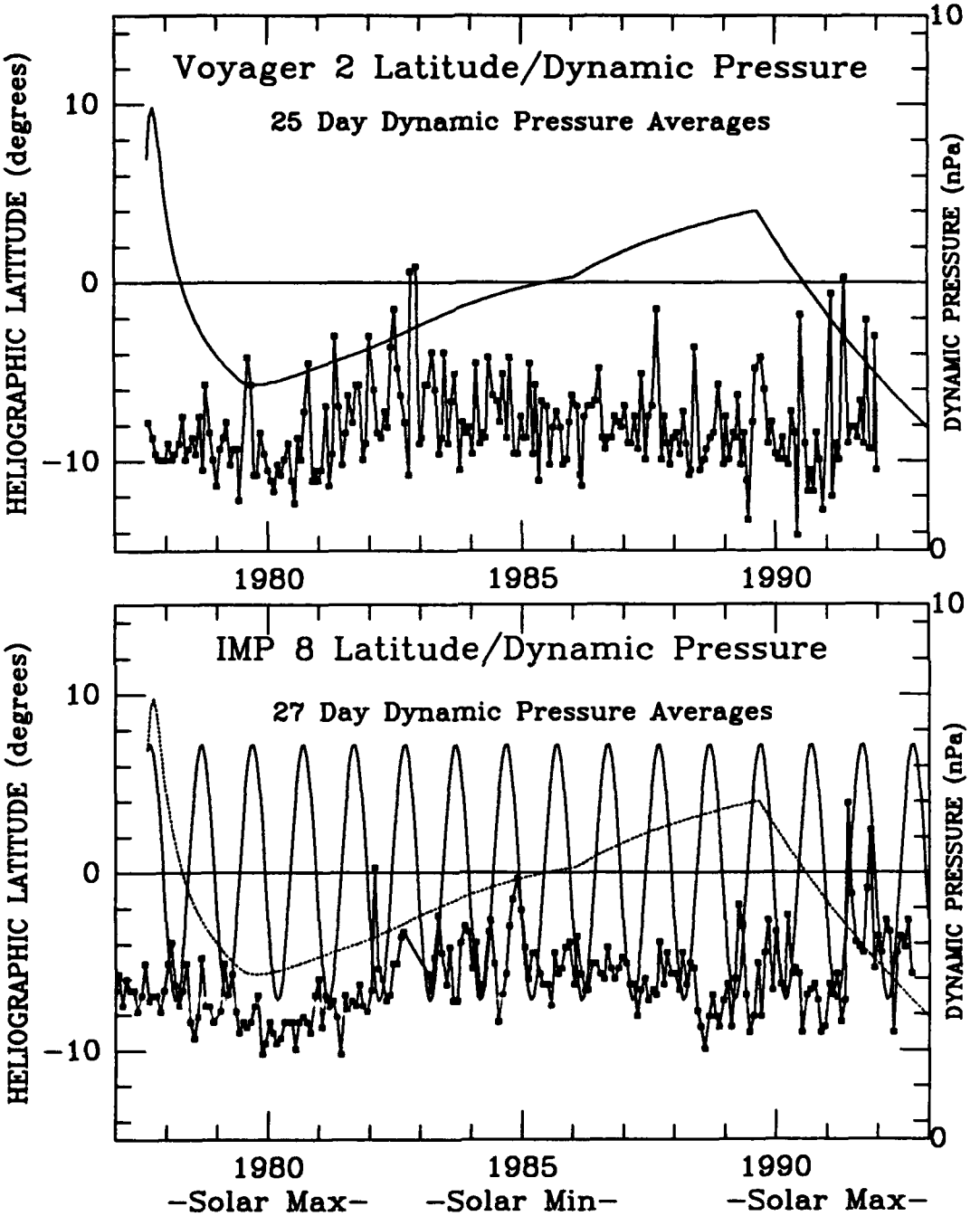

FIGURE 15. Heliographic latitude and dynamic pressure vs year for Voyager 2 (top) and IMP 8 (bottom). Pressure corrected for propagation time; latitude not corrected.

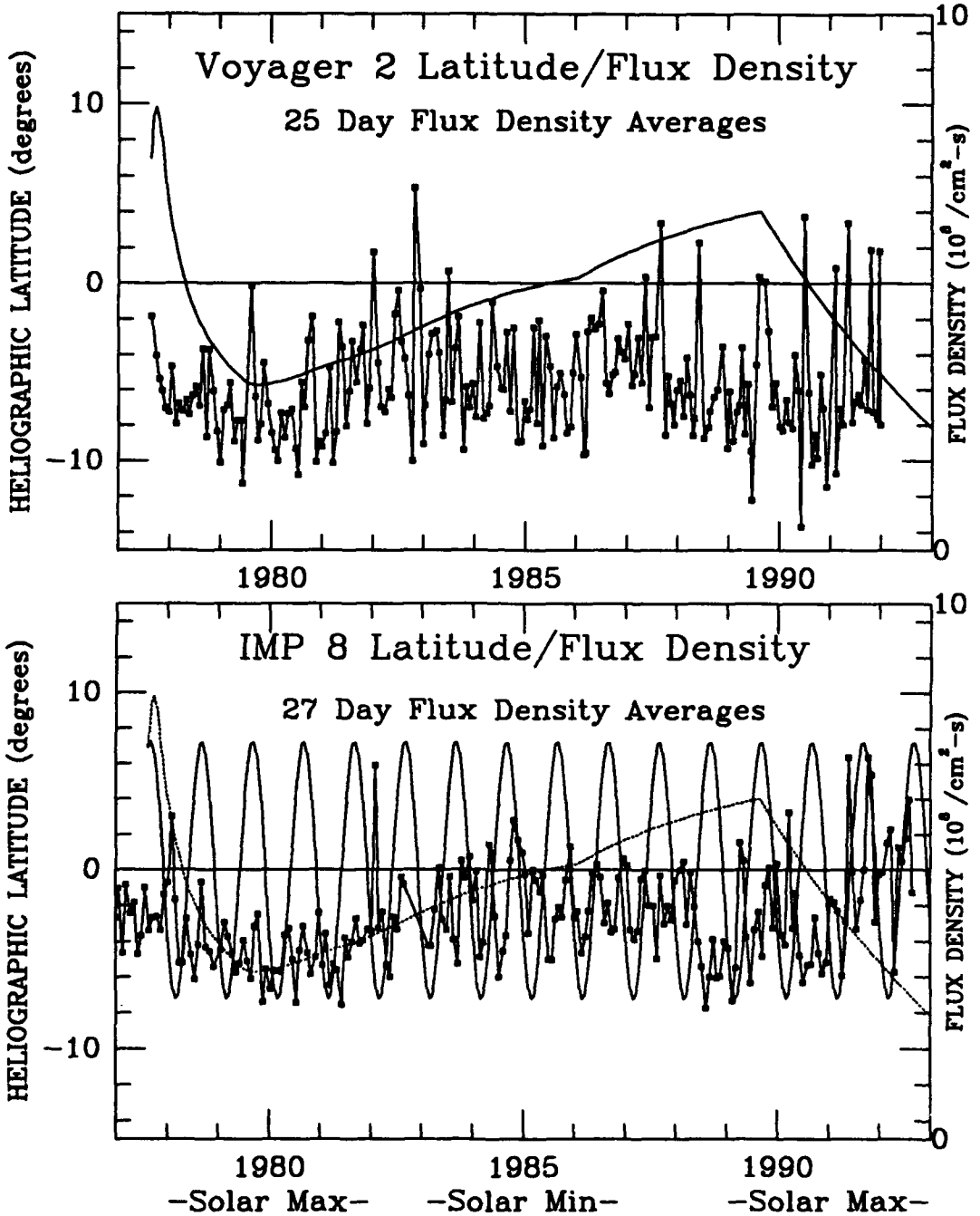

FIGURE 16. Heliographic latitude and flux density vs. year for Voyager 2 (top) and IMP 8 (bottom). Flux corrected for propagation time; latitude not corrected.

4.8. 50/54-DAY AVERAGES

In this section, solar wind parameters were averaged over 50 day intervals for Voyager 1 and Voyager 2 and 54 day intervals for IMP 8. These intervals approximate two solar rotations, as seen by the respective spacecraft and are used to provide a picture of long- term trends while keeping the loss of resolution relatively low. As alluded to in Section 4.7, the longer the averaging interval, the greater is the loss of resolution of the solar wind temporal structure. The longer averaging intervals, such as 54 days, obscure detail, especially the extreme low and high speed streams and are sensitive to transient solar wind. Therefore, I chose not to look at even shorter averaging periods because I did not want to focus too closely on localized phenomena and lose the long-term perspective.

Figure 17 is a plot of 50/54 day averages comparing solar wind (proton) parameters as measured by IMP 8, Voyager 1 and Voyager 2. The parameters are the same as those in Figure 11. IMP 8 data are indicated as dotted lines with square points; Voyager 1 data are indicated as dashed lines with open triangle points; Voyager 2 data are represented as solid lines with filled-in triangles. The period covered is 1977-1981 because it coincides with the complete Voyager 1 data set. The period between 1973 and 1993 comparing just IMP 8 and Voyager 2 will be presented separately.

4.8.1. VELOCITY

The velocity profile varies from a minimum of 360 km/s to a maximum of about 500 km/s during this period, a little less variation than that shown in the 25/27 day averaging periods, because some of the extreme values have been averaged out. As in the 25/27 day analysis, some effects of the solar cycle are evident. The velocity reached a minimum around 1980, the period of solar maximum. Prior to the solar maximum, velocity was higher, reflecting the

presence of higher speed streams near the heliographic equator.

The larger of the differences that remain were measured during the following two time periods: 1979.3-1979.8 and 1980.3-1980.5. These two intervals are generally the same as those identified in Section 4.7.1. and the underlying reasons for the differences in hourly averages were explained therein. But there are other differences seen here worth mentioning. Specifically, the first period start and end times have been shifted slightly and the amount by which the average values differ has been reduced, especially the average velocity peak reported by Voyager 2 about 1979.7. These differences were caused by averaging over a longer time interval. The first interval now spans between 1979.3 and 1979.8, having been shifted later by .1 year. The difference seen between 1979.2 and 1979.3 in the 25/27 averages has been nearly eliminated in the 50/54 day averages. This is an example of the fact that the solar wind changes in time. Because the solar wind did not remain constant during that period, its small scale structure was averaged out by using a longer averaging time interval. The remainder of the first period, 1979.3-1979.8, is similar to that shown in Figure 11 except that the range of average values has been reduced. Voyager 2 recorded a 25 day average velocity of about 560 km/s but that has been reduced to only 490 km/s by averaging over 50 days. The same effect is evident on the velocity minima. For example, IMP 8 reports a 54 day average velocity of about 390 km/s around 1979.55, up from a 27 day average velocity of 360 km/s. The second period in question, 1980.3-1980.5, also matches a period discussed previously, where the Voyagers agree and IMP records a different value. Comparing this period in Figure 17 to the 25/27 day results we see again a reduction in the range of average values.

4.8.2. DENSITY

There are greater differences in the density profiles of IMP and the

Voyagers than that seen in the velocity profiles. But averaging over 50/54 days has narrowed the average density range. Considering all three spacecraft, density now varies between 4 and 14 protons/cm^3. While there are still a few periods where there were significant differences between Voyager 1 and Voyager 2, generally, they measured the same densities throughout this four year period. The greatest differences between the Voyagers' average densities occurred between 1978.5 and 1978.7 and between 1979.7 and 1980 but these differences are smaller that that observed for the 25 day intervals. The difference seen about 1978.5 is only about 33% now while the 25 day average difference for that same period was about 80%. There was a large difference, as much as 100%, between the Voyagers' 25 day averages between 1979.4 and 1979.5 that is not seen in the 50 day averages. This change is due to the fact that a data point calculated to lie at about 1979.62 was deleted because it contained only about 700 spectra while the other data points near that time were calculated using about 3000 spectra. This interval happened to occur during a large data gap in the Voyager 2 data. Consequently, there was not much hourly average data used to compute average values. The second period in question, between 1979.7 and 1980, may be another example of how time varying streams' plasma parameters change when averaged over longer time intervals. Between 1979.7 and 1980, the 25 day average differences were as large as 100% but this has been reduced to about 40% using the new averaging interval. One explanation for the differences between the Voyager data around 1978.5 is the fact that Voyager 2 measured a density hourly average of over 54 protons/cm^3 about 1978.55 while Voyager 1 measured a smaller average density of only 34 protons/cm^3 a couple of days later. The stream structure could have been modified due to processing through additional interaction regions because Voyager 1 was about .2 AU further from the sun that Voyager 2 was

about 1978.5, or maybe Voyager 1 measured a different stream of plasma than did Voyager 2.

IMP 8, on the other hand, consistently measured higher densities than the Voyagers. The differences were as much as about 40% near 1979 and 60% about 1980.3. Beyond this consistent difference, there was an event around 1978.1 when IMP measured an average density of nearly 14.5 protons/cm^3 and the Voyagers recorded a much lower density of about 8 protons/cm^3. This consistent difference is a more significant problem to be resolved. It may be the result of differences in the analysis or processing of the data sets. A fitting routine called XJC was used to calculate fit parameters for the Voyager data used in this thesis. Another fitting program, called LABCUR, which takes into account the detailed response of the Faraday cups, produces fit densities about 7% greater than that produced by XJC. The reasons for the differences are beyond the scope of this thesis, but it is important to realize that the difference exists. Another reason for density differences may lie with the calibration of the IMP 8 instrument. There appears to be a calibration error which causes densities to be about 8% too high. By correcting for these two factors, density differences between the IMP 8 and Voyager spacecraft may be reduced to about 20%.

4.8.3. DYNAMIC PRESSURE

Dynamic pressure is indicated in the second panel from the top of Figure 17. Pressure varied between about 1 and 3.6 nPa for the Voyagers and between 1.8 and 3.5 nPa for IMP 8. Differences between IMP 8 and the Voyager averages are a direct result of the differences described for velocity and density.

4.8.4. FLUX DENSITY

Flux is plotted in the top panel of Figure 17. Flux varied from a low of

about 1.7 x 10^8/cm^2–s to a high of about 4.5 x 10^8/cm^2–s for the Voyagers while IMP 8 varied between 3 and 5.5 x 10^8/cm^2–s. Flux differences are the result of the differences discussed above for velocity and density.

4.8.5. LONG-TERM VARIATIONS

50/54 day averages for the period 1973-1993 are shown in Figure 18. We will focus on the period of 1981-1993 as in Section 4.7.5. The most readily obvious differences seen here compared to the 25/27 day averages is that there is less extreme variation between the spacecraft data. The reduced variation is the result of averaging time varying parameters over longer periods. The differences that remain after using this larger averaging period are generally more significant because they have persisted over longer periods of time or originally were of a very large (or very small) magnitude.

The effect of the solar cycle on solar wind velocity is visible at this time resolution. IMP 8 recorded velocity peaks of more than 550 km/s before the 1976 solar minimum. Both spacecraft measured peaks near 520 km/s near the 1985 solar minimum and slower wind near the solar maxima of 1980 and 1991, as expected.

Velocity profiles for the two spacecraft follow the same trends with no major differences except for a large spike about 1983 measured by Voyager 2 and the gradient related differences between 1986 and 1988. Long term values for this averaging interval are between 360 km/s and 550 km/s.

Density varied between about 5 protons/cm^3 and 17 protons/cm^3, a narrower range than for the 25/27 day averaging interval. IMP 8 density measurements are still greater than Voyager 2, and in some cases, significantly different. There are several periods when IMP measured nearly double (and sometimes more) the density measured by Voyager 2: 1980.5, 1984, 1985, 1988, 1990, and 1991-1992.

Dynamic pressure varied between 1 and 5 nPa, a slightly reduced range than that for 25/27 day averages. Flux varied slightly less using this averaging period, with a range of about 2 to 7 x $10^8/cm^2$–s.

4.8.6. LATITUDE GRADIENTS

Latitude gradients are easier to look for using this averaging period because of the reduced number of data points, and consequently, the reduced variation in velocity. Figure 19 shows that velocity gradients appeared to exist below the heliographic equator during the following periods: 1979.2, 1981.2, 1989.2, and 1991.5. On the other hand, evidence exists for a high speed source above the heliographic equator in 1986.5 and 1987.8. The period around solar minimum, from about 1982 to about 1986, was not examined for the existence of gradients because high speed sources are too numerous during this period in the solar cycle.

Comparing the Voyager 2 velocity measurements with the IMP trends often provides consistent evidence for gradients. For example, in 1979.2, IMP was at -7.5° and measured 475 km/s solar wind, a value much higher than that measured shortly prior to and immediately after this time. Voyager 2 reached its minimum of about -6° slightly later, around 1979.7, and recorded nearly the same velocity, 480 km/s, implying a southern source of high speed plasma. Again we see evidence supporting a southern source in 1981.2 when IMP measured 475 km/s solar wind at about -4.3°. Voyager 2, at the same time, was also at -4.3° and also measured 475 km/s solar wind.

In 1989 the velocity measurement of IMP 8 and Voyager 2 peaked but at this time the spacecraft were no longer near the same latitude. IMP's velocity profile between 1989 and 1989.2 would indicate a source existed below the heliographic equator. However, Voyager 2 measured a peak in velocity at the same time while it was nearly 4° above the heliographic equator, implying a

northern source. Since Voyager's latitude remained the same (to within one degree) during this period, the velocity profile should have continued to reflect higher velocities but it did not. Between 1989.2 and 1989.5 both spacecraft observed a decrease in velocity to a minimum of about 385 km/s (Voyager) and 405 km/s (IMP). By this time, the spacecraft were both located above the heliographic equator at about 4°. These observations are partially explained by a change in the solar wind structure during this period and perhaps multiple high speed sources. Maybe a gradient spanned across the heliographic equator instead of remaining either above or below it.

Around 1991.5, both spacecraft recorded velocity peaks in the solar wind. At this time Voyager was nearly 4° below the heliographic equator and moving down while IMP was about 4° above the heliographic equator and was moving upward. Note that IMP began sensing a high speed stream just as it began its ascent from -7.5° and recorded a velocity drop as it approached its position 5° above the heliographic equator. Both spacecraft recorded decreases in velocity after 1991.5 as both descended. These measurements are consistent with the presence of a high speed source below the heliographic equator during this period.

The next two periods are beautiful, distinct examples of high speed sources in the north. About 1986.5, IMP measured an average velocity of approximately 505 km/s when it reached 7.5° above the heliographic equator. The average velocity dropped to about 400 km/s as IMP descended toward the heliographic equator. Voyager 2 measured very constant solar wind (about 385 km/s) during this period for reasons explained in Section 4.7.5. Around 1987.8, IMP recorded another increase in velocity to 495 km/s as it ascended from -7.5° to its maximum of 7.5°. Then velocity decreased to 355 km/s as the spacecraft descended to -7.5° latitude about 1988. Voyager 2 also recorded an

increase in velocity to 455 km/s at the same time as it continued its ascent to about 3.5°. Shortly thereafter, velocity dropped to about 375 km/s near 1988.3. At this time, IMP was near -7.5° and Voyager was between 3° and 4° but both observed low speed streams. Therefore, it seems that the high speed source disappeared.

Figures 20, 21, and 22 show how density, dynamic pressure, and flux density, respectively, vary with latitude. As mentioned in Section 4.7.6, these plots can be used to identify periods when gradients seem to exist in density, pressure, and flux.

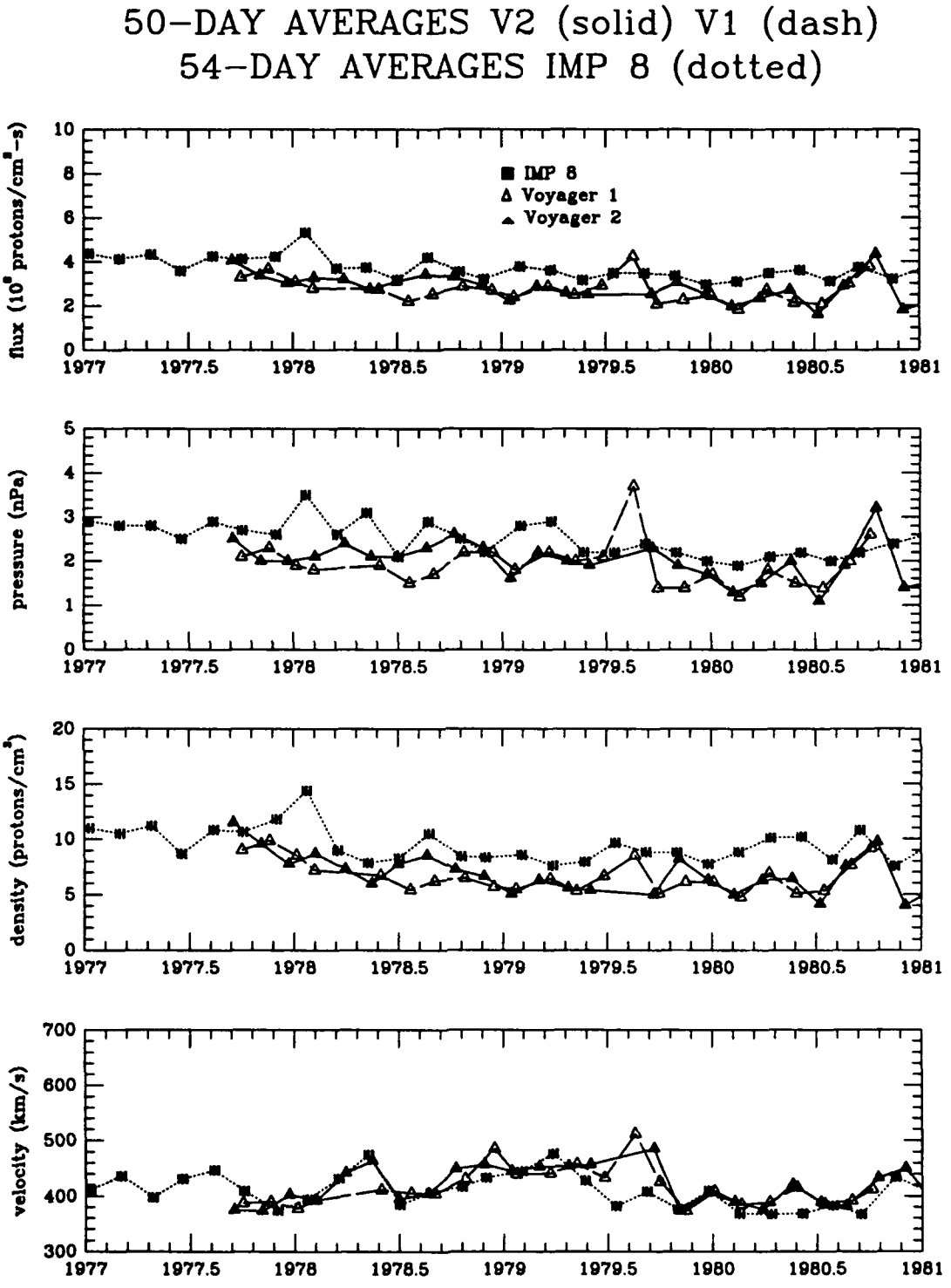

FIGURE 17. 50/54 Day Averages of flux density, ram pressure, normalized density, and velocity. All parameters adjusted for propagation time.

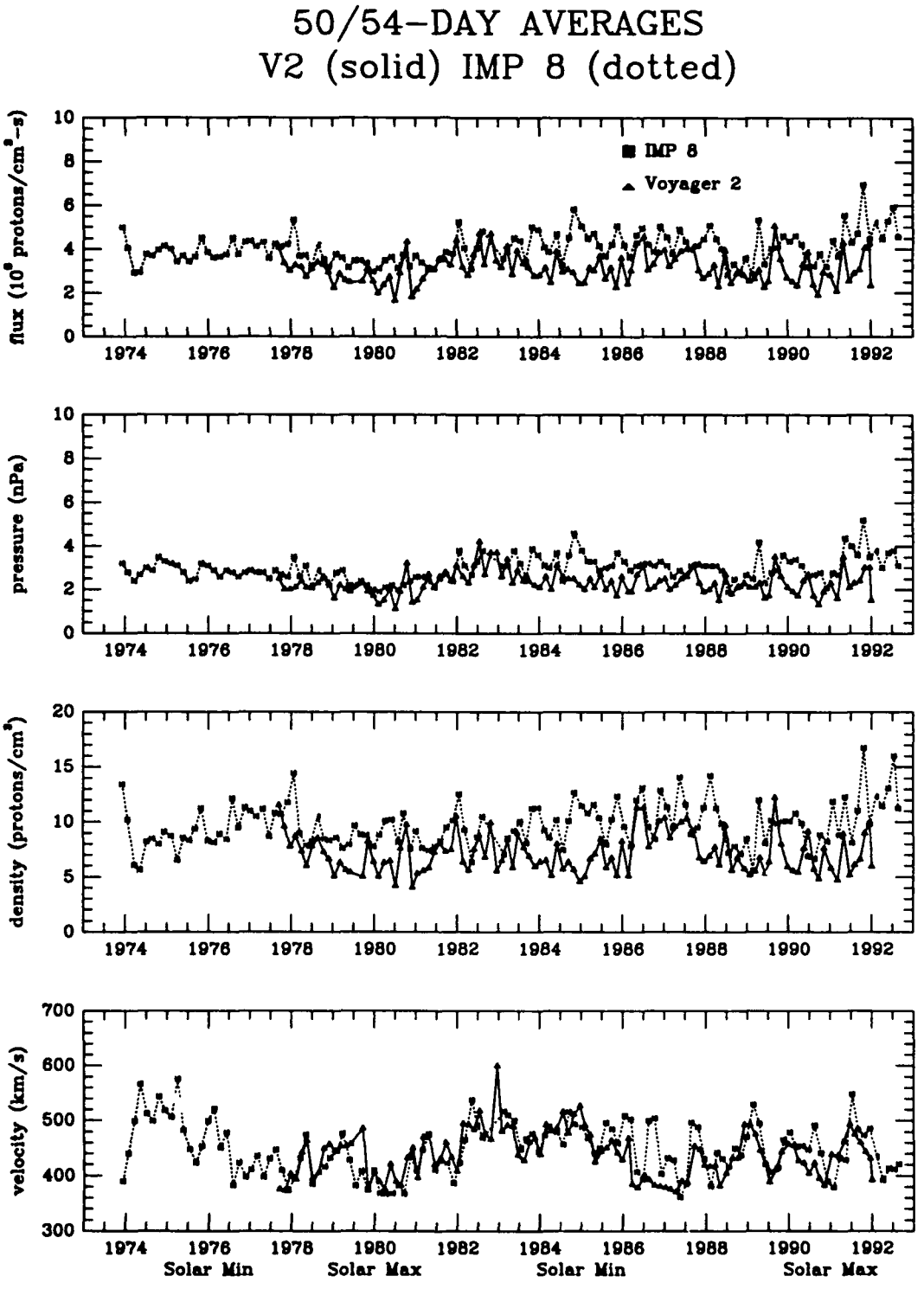

FIGURE 18. 50/54–Day Averages for Voyager 2 and IMP 8. V2 data adjusted for propagation time.

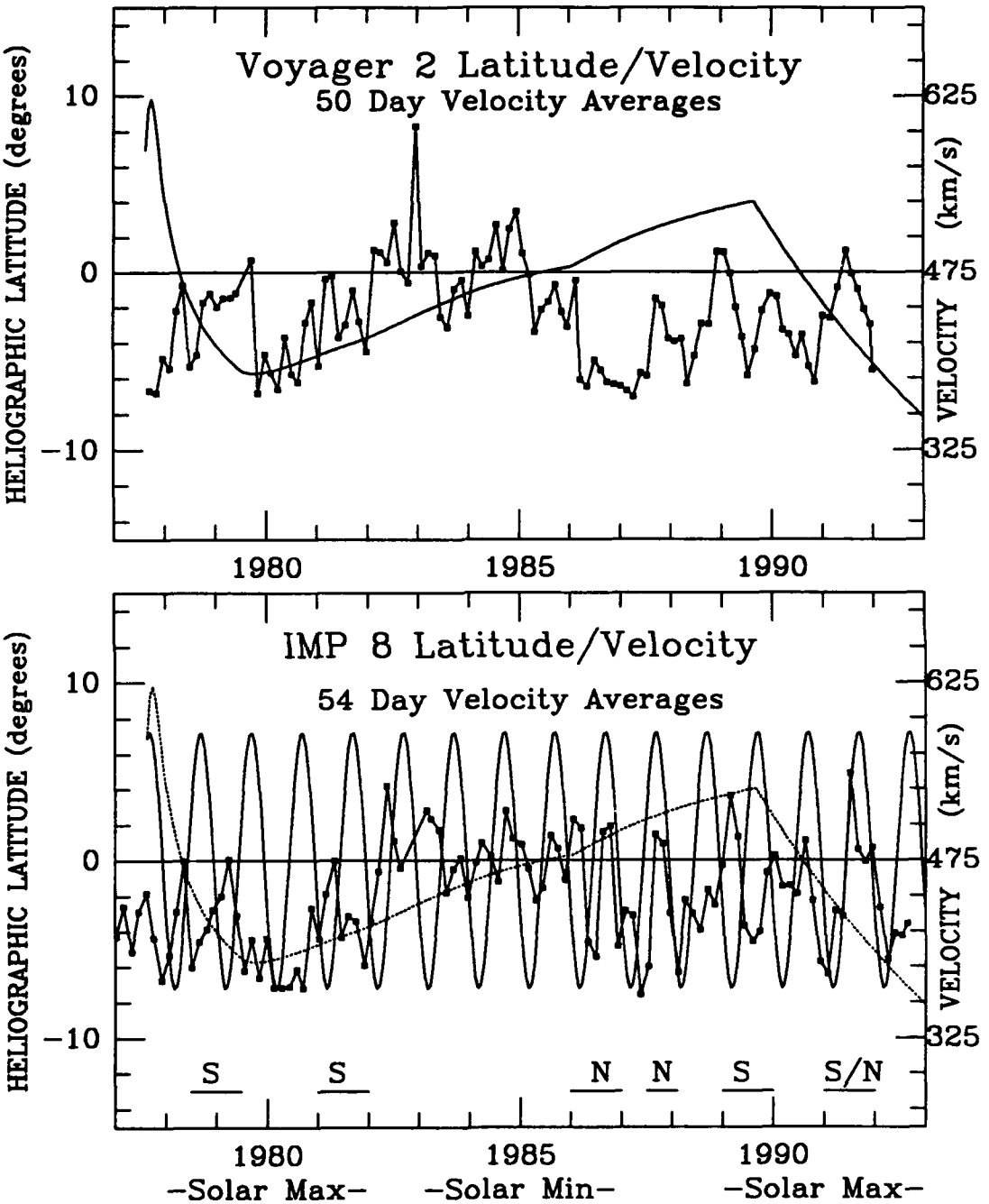

FIGURE 19. Heliographic latitude and velocity vs. year for Voyager 2 (top) and IMP 8 (bottom). Velocity corrected for propagation time; Latitude not corrected. High speed sources labeled as N (north) and S (south).

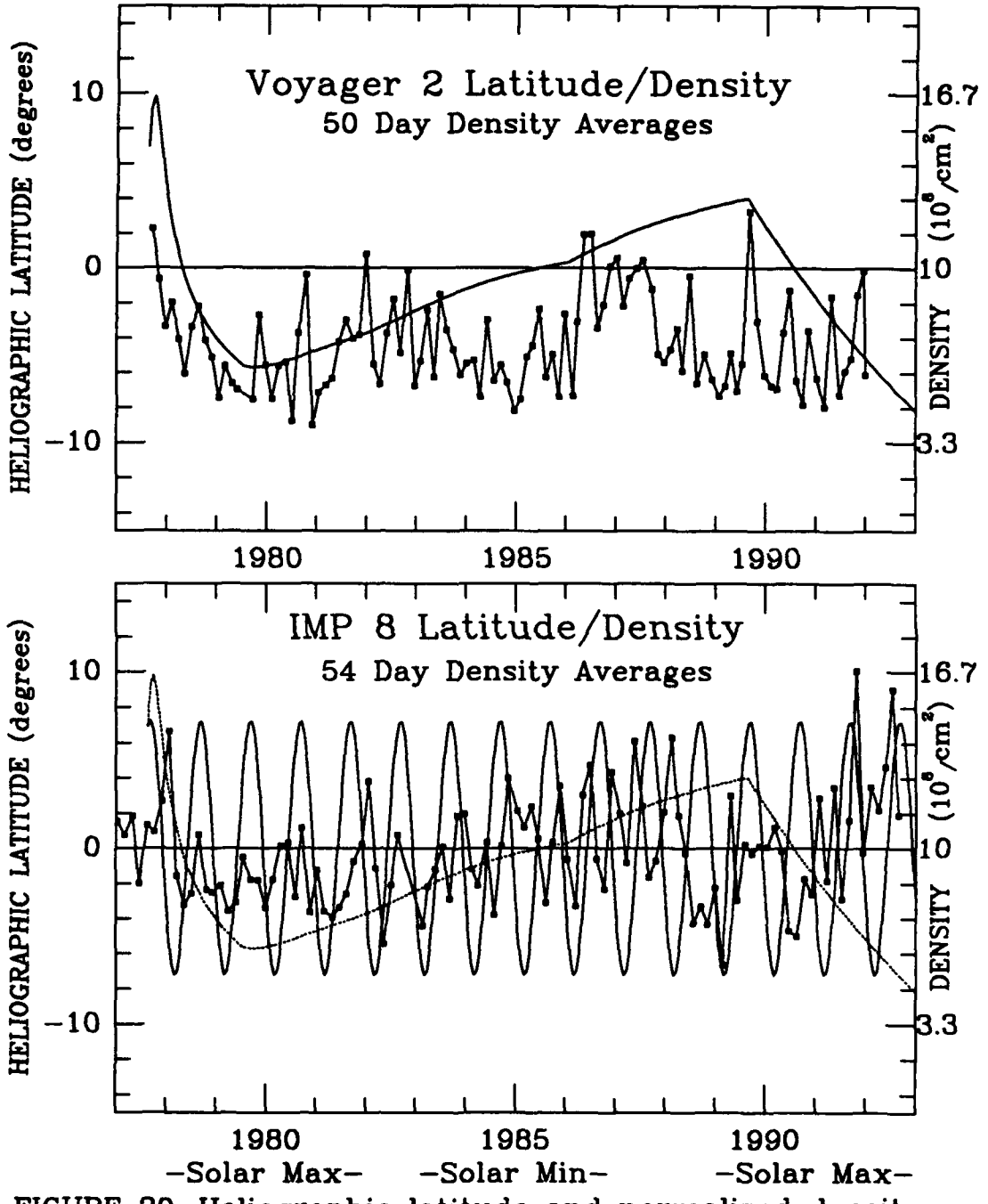

FIGURE 20. Heliographic latitude and normalized density vs. year for Voyager 2 (top), IMP 8 (bottom). Density corrected for propagation time; latitude not corrected.

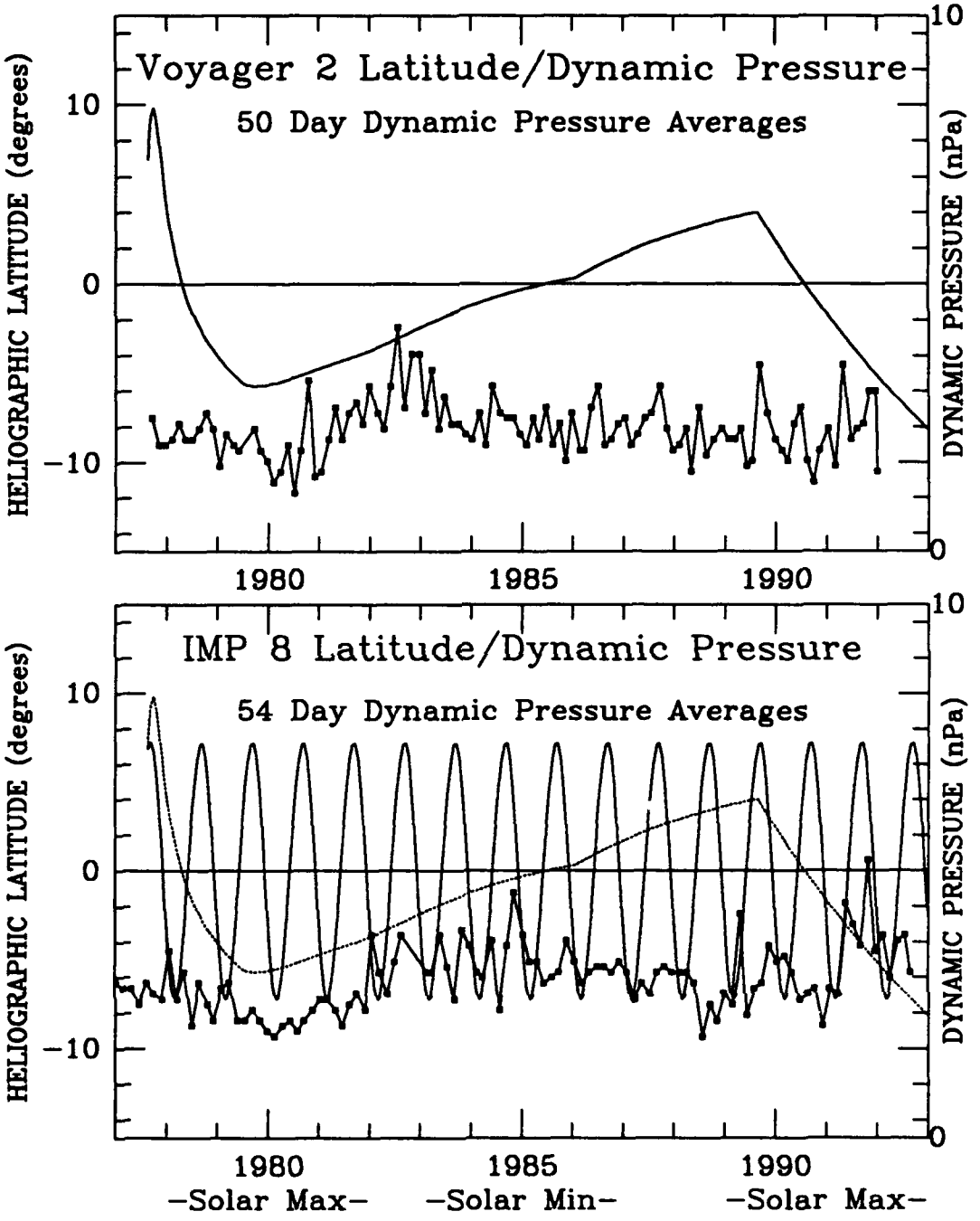

FIGURE 21. Heliographic latitude and dynamic presure vs. year for Voyager 2 (top) and IMP 8 (bottom). Pressure corrected for propagation time; latitude not corrected.

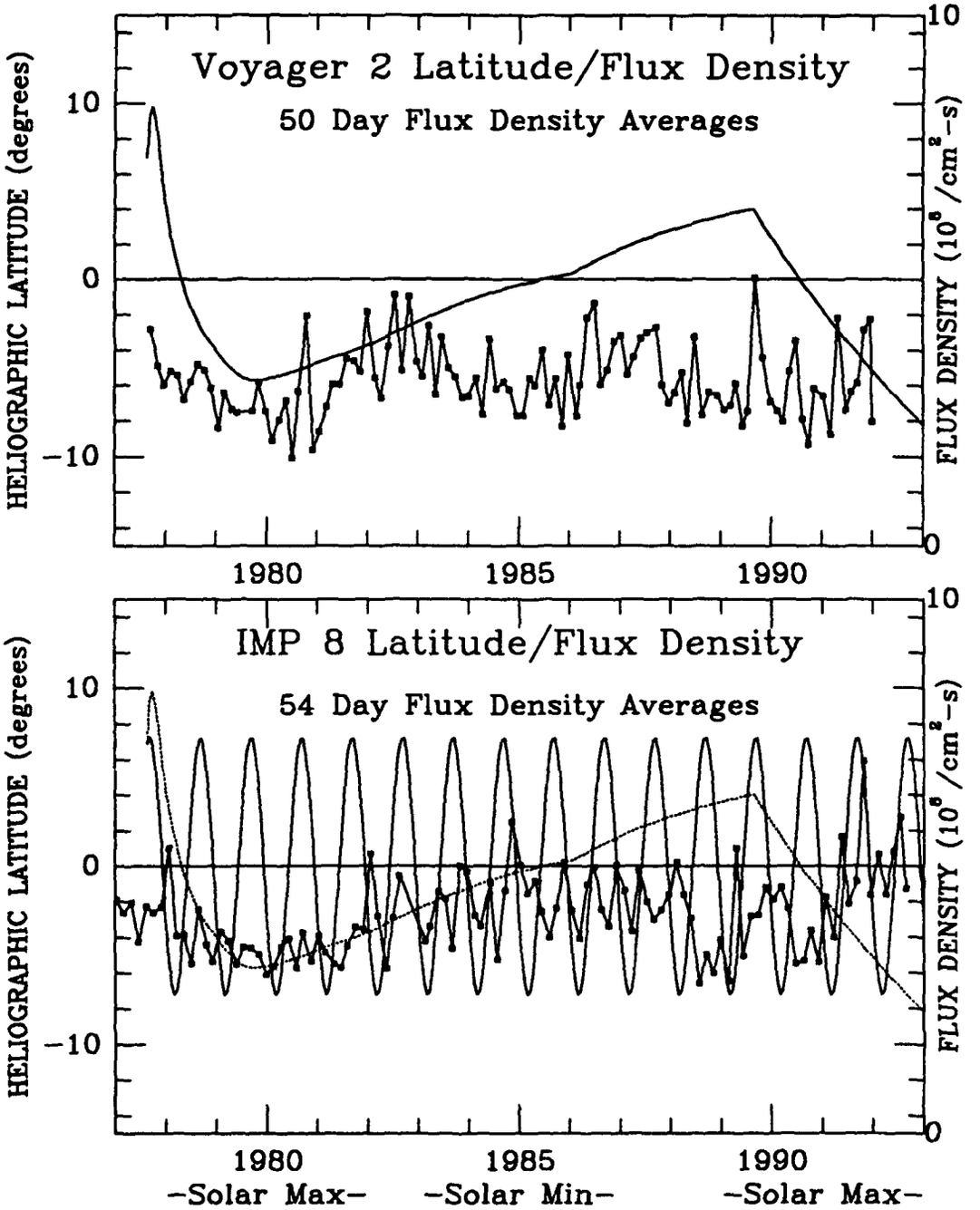

FIGURE 22. Heliographic latitude and flux density vs. year for Voyager 2 (top), IMP 8 (bottom). Flux density corrected for propagation time; latitude not corrected.

4.9. 100-DAY AVERAGES

This section examines solar wind parameters averaged over 100 day intervals, approximating four solar rotations. Using this averaging interval, there has been enough resolution lost such that most of the differences remaining are those that were caused by data gaps of a long duration not common to all data sets, and/or large, persistent solar wind structures not seen by all three spacecraft.

4.9.1 VELOCITY

Figure 23 provides the usual parameters averaged over 100 days. Velocity ranges between 350 km/s and 480 km/s. It is apparent that there is essentially no difference between the average velocities measured by the Voyagers. But there are differences remaining between IMP 8 average values and Voyager average values. Basically, these differences occur in the same periods that were seen in Figures 11 and 17. These periods are 1978.7-1979; 1979.4-1979.8; and 1980.2-1980.6. The differences in the first, second, and third periods have been reduced to about 10%, 15%, and 5%, respectively, from that seen in previous sections. As mentioned in the introduction to this section, these differences remain because they were not caused by minor fluctuations in the solar wind but by a combination of long duration data gaps and/or long duration (or very large) solar wind structures common to the Voyagers but not measured by IMP 8. For a more detailed discussion for the differences found in these periods, see Sections 4.7.1 and 4.8.1.

4.9.2. DENSITY

Average density varies between about 5 and 13.5 protons/cm^3. The one significant difference remaining between the Voyagers occurs about 1978.6 where Voyagers differ by about 33%. This difference is the same as that seen in the 50 day averages, the result of the differing solar wind structure as

explained in Section 4.8.2.

The most interesting (and unexplained) difference between densities is that IMP measured densities 30-50% (and sometimes 100%) greater than the Voyagers. The average difference is about 38%. The reason for this is probably the result of the choice of fitting program used and a calibration error, as discussed in Section 4.8.2.

4.9.3. DYNAMIC PRESSURE

The range of dynamic pressure values continues to narrow with the increased averaging interval. Now pressure is seen in Figure 23 to vary only between 1.4 nPa and 2.4 nPa for the Voyagers and between 2 and 3 nPa for IMP 8.

4.9.4. FLUX DENSITY

The same narrowing effect is seen with flux values. Flux varies between 2 and 3.5 x $10^8/cm^2$–s for the Voyagers and between 3 and 5 x $10^8/cm^2$–s for IMP 8, as seen in Figure 23.

4.9.5. LONG-TERM VARIATIONS

Figure 24 presents 100 day averages for 1973-1993. Velocity ranged between 360 km/s and 550 km/s during this period, with only minor variation between spacecraft, except for the periods where high speed sources are suspected of causing velocity gradients. These periods, 1985.5-1987.5 and 1990.5-1991, were discussed in Section 4.7.6. (the start and end times of these intervals differ slightly from those mentioned in Section 4.7.6 due to the effect of averaging over a different number of days but the periods stated in this section are based upon the apparent gradients as seen in Figures 13 and 19). Note that two data points, occurring 1982.645 and 1983.141, were edited out because the number of spectra used to compute the averages were about 1/4th (5948) and 1/25th (874) the number of spectra which should have been used (about

25,000). In other words, these two averaging intervals covered periods which were missing so much data that the average result is probably not truly representative of the solar wind during that time.

Average density measured by IMP 8 varied between 7 and 13 protons/cm^3 while Voyager measured a lower average value of between 5 and 10 protons/cm^3. As a rough calculation, assuming the average IMP measurement is 10 protons/cm^3 and the average Voyager measurement is 7.5 protons/cm^3, the average difference is about 33%.

Average dynamic pressure varied between 2.0 and 4.2 nPa for IMP 8 and between 1.4 and 3.4 nPa for Voyager.

Flux density average values varied between about 3 and 5.5 x $10^8/cm^2$–sec for IMP 8 and between 2 and 4.5 x $10^8/cm^2$–sec for Voyager.

4.9.6. LATITUDE GRADIENTS

At this time resolution, the effect of high speed sources, producing velocity gradients, can still be seen in all but one period. In section 4.8.6, five times were identified when gradients appeared: 1979.2, 1981.2, 1989.2, and 1991.5 (southern gradients); and 1987.8 for a northern gradient. Looking at Figure 25, gradients are still detectable at 1979.2, 1987.8, 1989.2, and 1991.5 but the one in 1981.2 is not very distinguishable any longer.

Figures 26, 27, and 28 provide the same information as those in Sections 4.7.6. and 4.8.6. except the data presented here is averaged over 100 day intervals. It could be argued from Figure 26 that there were density gradients visible about 1978, 1988, 1990, and around 1992. The same could be said about pressure gradients from Figure 27 around 1990 and 1991.5. Figure 28 shows that flux was higher in the southern latitudes in 1978 and 1982, and higher in the north about 1991.8.

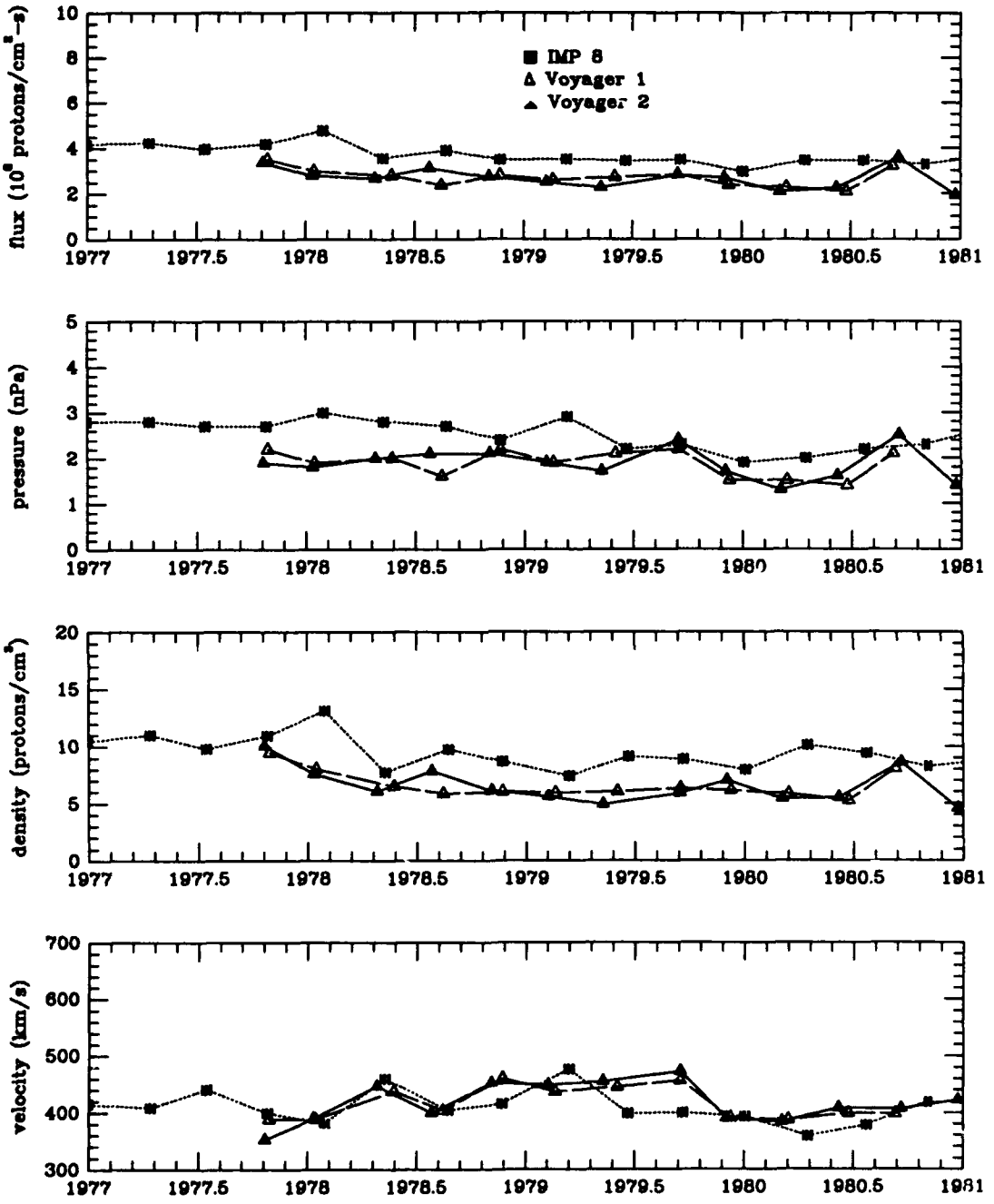

FIGURE 23. 100 Day Averages of flux density, ram pressure, normalized density, and velocity. All parameters adjusted for propagation time.

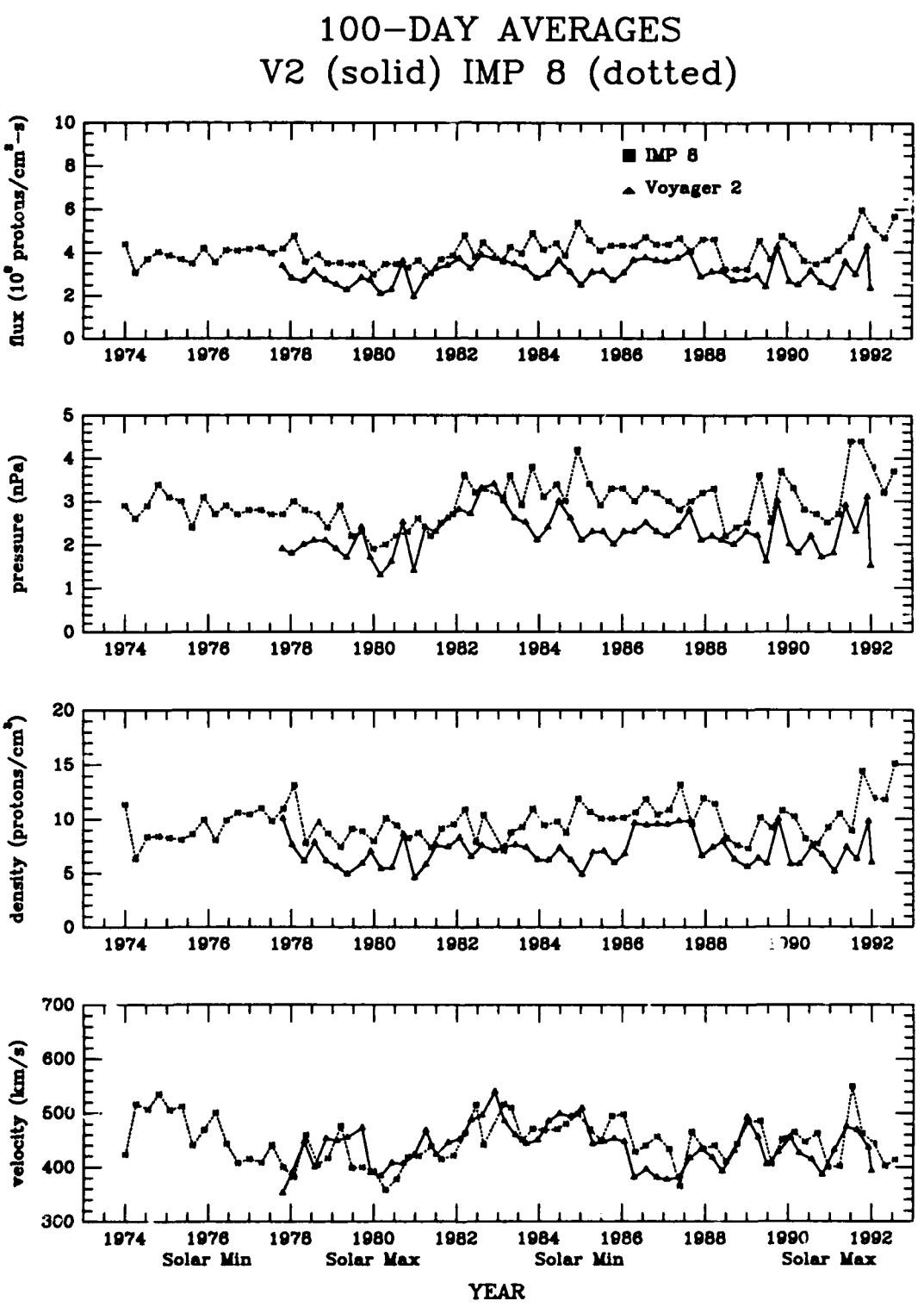

FIGURE 24. 100 Day-Averages for Voyager 2 and IMP 8. V2 data adjusted for propagation time.

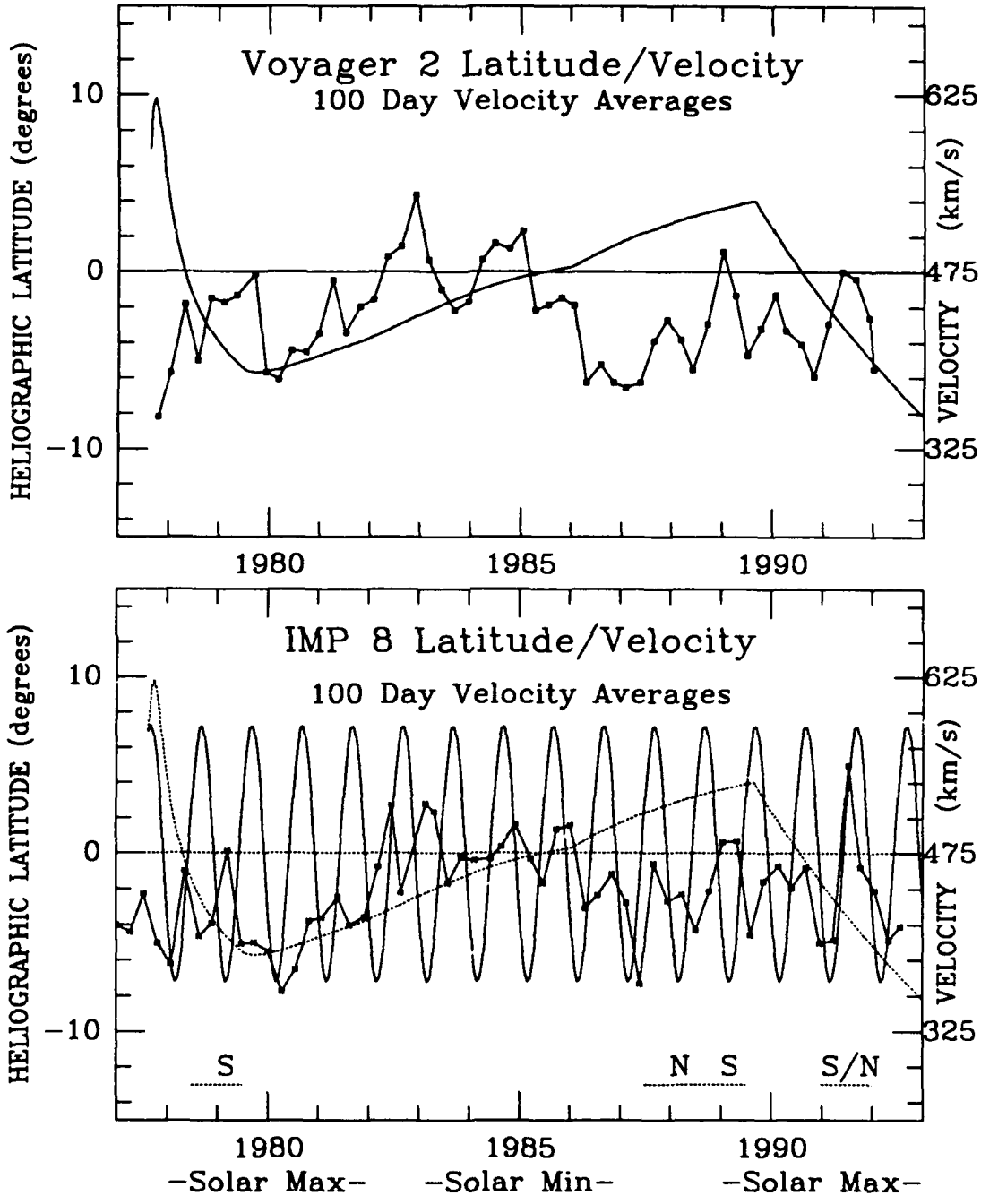

FIGURE 25. Heliographic latitude and velocity vs. year for Voyager 2 (top) and IMP 8 (bottom). Velocity corrected for propagation time; latitude not corrected. High speed sources labeled as N (north) and S (south).

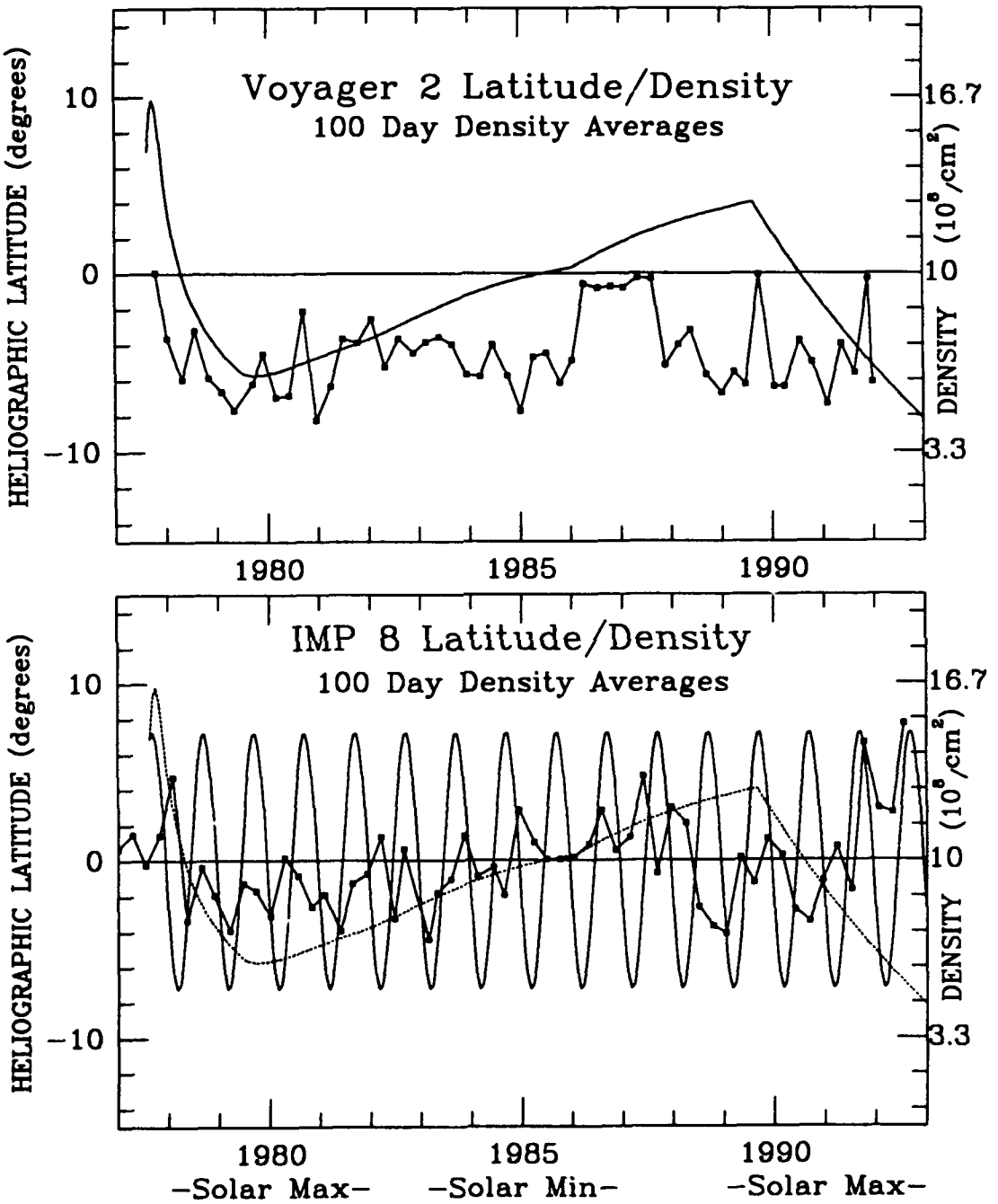

FIGURE 26. Heliographic latitude and normalized density vs. year for Voyager 2 (top) and IMP 8 (bottom). Density corrected for propagation time; latitude not corrected.

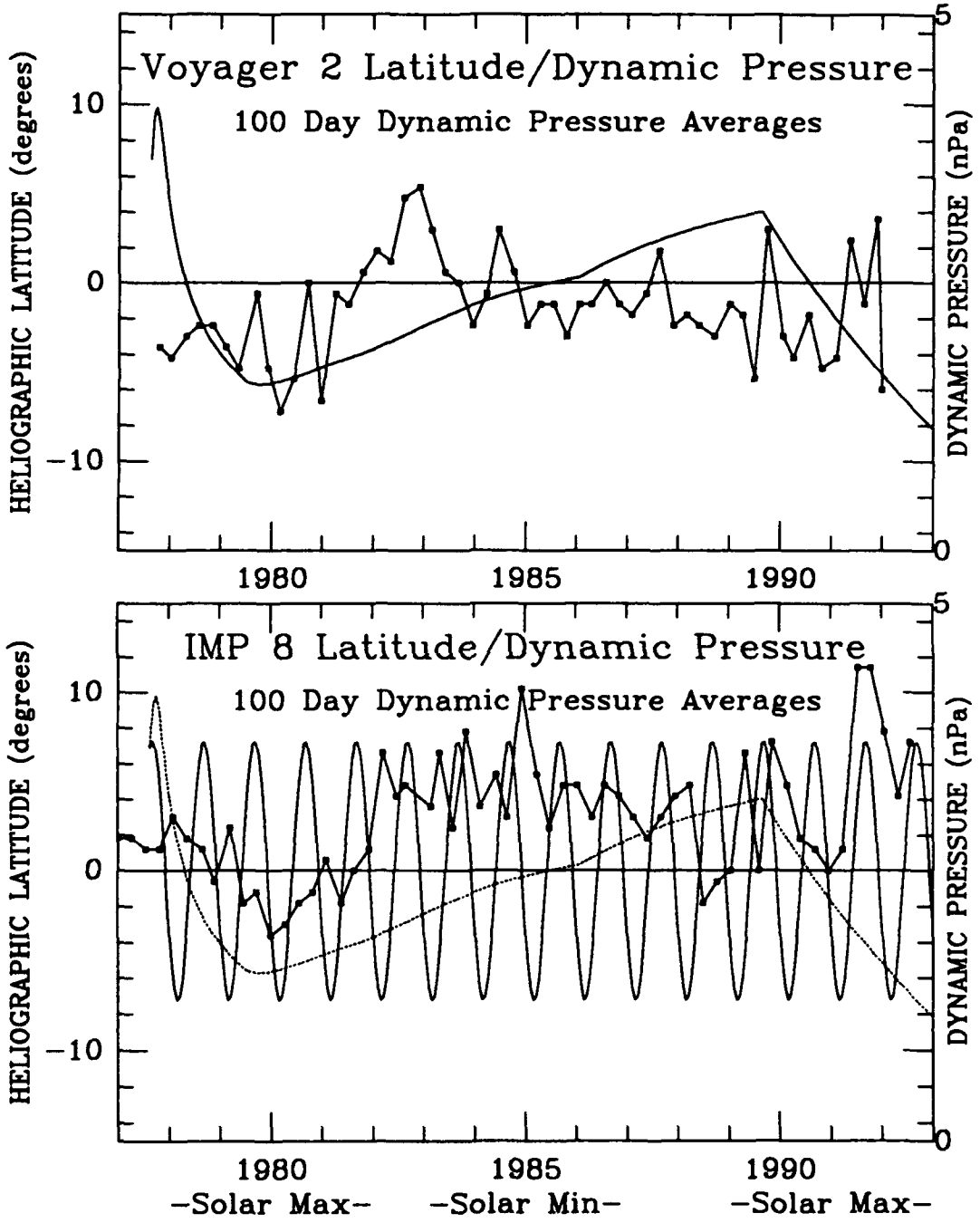

FIGURE 27. Heliographic latitude and dynamic pressure vs. year for Voyager 2 (top), IMP 8 (bottom). Pressure corrected for propagation time; latitude not corrected.

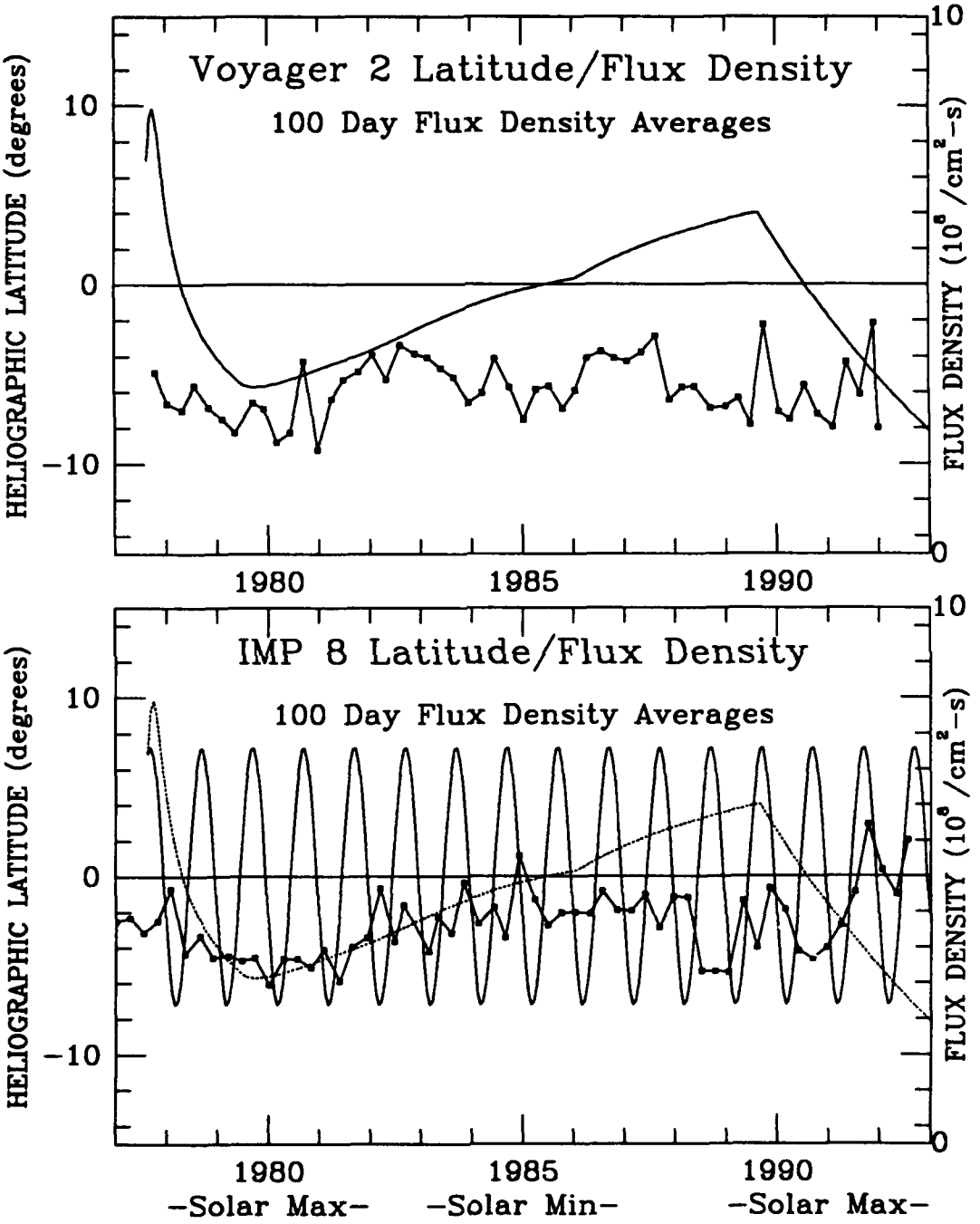

FIGURE 28. Heliographic latitude and flux density vs. year for Voyager 2 (top), IMP 8 (bottom). Flux density corrected for propagation time; latitude not corrected.

4.10. 200-DAY AVERAGES

This section examines solar wind parameters averaged over 200 day intervals, approximating eight solar rotations. Using this time resolution, essentially, there is no longer a difference between the average values measured by Voyagers 1 and 2. With the exception of average velocity, there is nearly a constant difference between the average parameters measured by the Voyagers and IMP 8. The nearly constant difference between spacecraft averages, as well as an approximate range for each of the average parameters, is provided in the following sections.

4.10.1. VELOCITY

Figure 29 shows that the velocity profiles for the three spacecraft are essentially the same, with a velocity variation between 380 and 460 km/s. There is one point, about 1979.6, where a difference between the spacecraft still exists. This difference, which was evident throughout all of the averaging intervals examined and is now about 13%, was caused by the Voyagers' measurement of a high speed stream moving more than 800 km/s which was not detected by IMP 8. A more detailed discussion of this time period is contained in Section 4.7.1.

4.10.2. DENSITY

Density ranged between 5 and 9 protons/cm^3 for the Voyagers and between 8 and 12 protons/cm^3 for IMP 8 during the period 1977-1981. This represents a nearly constant difference between the spacecraft of about 3 protons/cm^3 over this four year period. This means that IMP's 200 day average density was between 33% and 60% more than that recorded by the Voyagers. Averaging over this interval has helped to make this near constant difference of about 46% between the Voyagers and IMP more clear. Based upon this result, it becomes more convincing that there may have been some systematic processing

difference (e.g., calibration error, fitting program difference) between the spacecraft data sets which contributed to this difference.

4.10.3. DYNAMIC PRESSURE

Pressure remained nearly constant over this four-year period. The Voyagers recorded a dynamic pressure ranging between 1.6 and 2.2 nPa while IMP recorded a slightly higher variation between 2 and 2.8 nPa. This represents about a 30% average difference.

4.10.4. FLUX DENSITY

Flux remains nearly constant for both spacecraft at this time resolution. The Voyagers recorded a flux of about 3 protons/cm^2–s while IMP 8 recorded a flux of about 3.5 protons/cm^2–s. This translates to a difference of about 17%, due mainly to the difference in densities.

4.10.5. LONG-TERM VARIATIONS

Figure 30 covers the period 1973-1993. Velocity profiles are very similar and possible reasons for the differences have been discussed throughout this thesis. During this period, velocity varied between a minimum of 380 km/s to a maximum of about 520 km/s. Density varied between 5 and 10 protons/cm^3 for Voyager and between 7.5 and 12 protons/cm^3 for IMP (note that the end point is disregarded because it did not contain 200 days of data). Dynamic pressure ranged between 1.5 and 3.4 nPa for Voyager and between 2 and 4.4 nPa for IMP 8. Flux density varied between 2.5 and 4 protons/cm^2–s for Voyager and between 3 and 5.5 protons/cm^2–s for IMP 8. The differences between spacecraft average values have been accounted for by large data gaps, relatively long-term solar wind structures which may or may not be longitudinally dependent, and latitude velocity gradients.

4.10.6. LATITUDE GRADIENTS

Moving to Figure 31, it can be seen that by averaging over 200 day

intervals, much of the evidence for latitude velocity gradients has disappeared. Indications of velocity gradients around 1979.2, 1987.8, and 1991.5 can still be seen. Evidence of the other gradients, which probably did not persist long enough, have been averaged out.

Figures 32, 33, and 34 provide indications of gradients appearing in density, pressure, and flux. Looking at Figure 32, there is an indication of a source of higher density in the north about 1989.5. Because of the time resolution, it is very difficult to pinpoint other possible high density source locations. In Figure 33, indications are that there is a pressure gradient in the north around 1990, due no doubt to the high density seen during this time in Figure 32. Flux density is also effected by the higher density around 1989.5, as indicated in Figure 34.

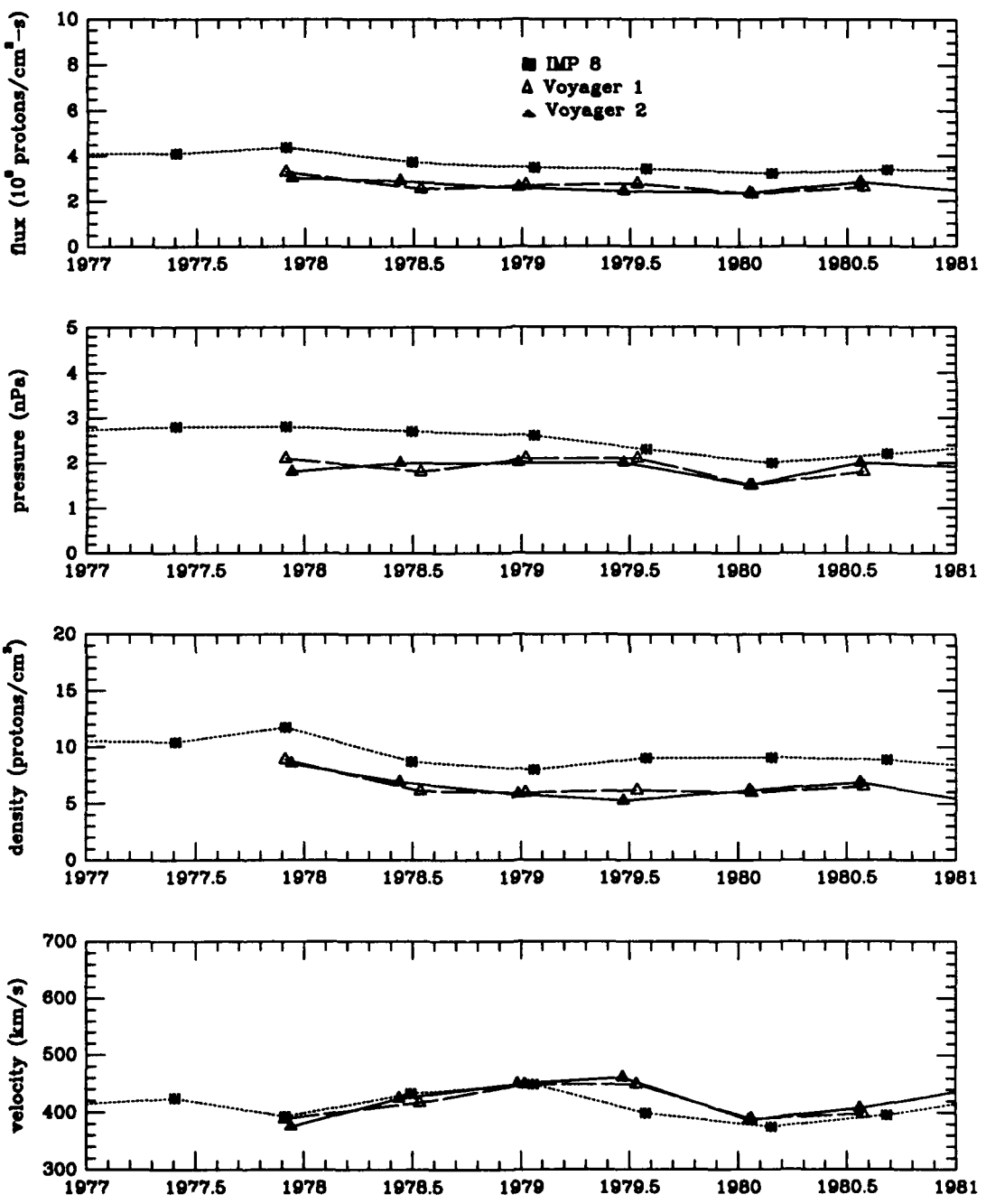

FIGURE 29. 200 Day Averages of flux density, ram pressure, normalized density, and velocity. All parameters adjusted for propagation time.

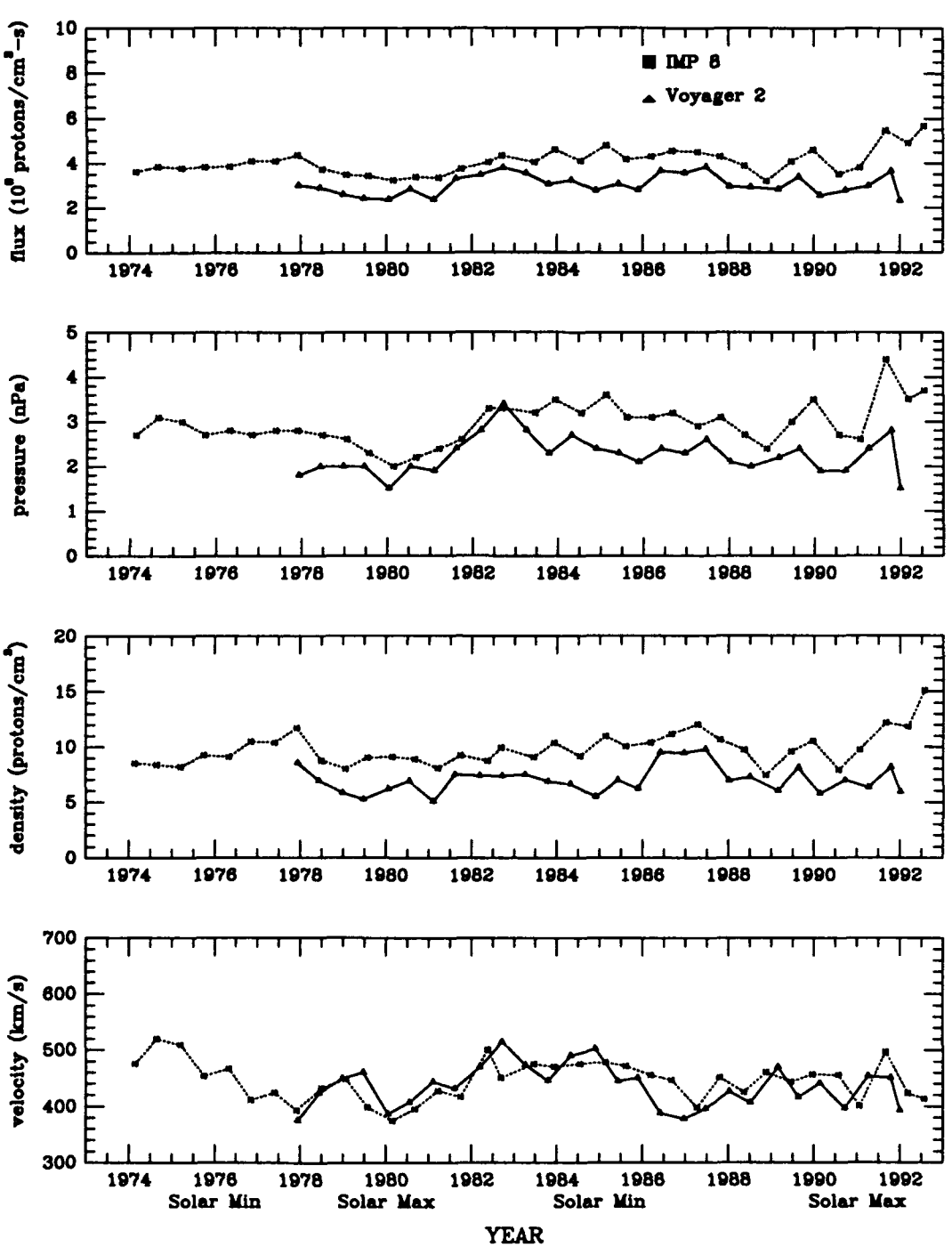

FIGURE 30. 200-Day Averages for Voyager 2 and IMP 8. V2 data adjusted for propagation time.

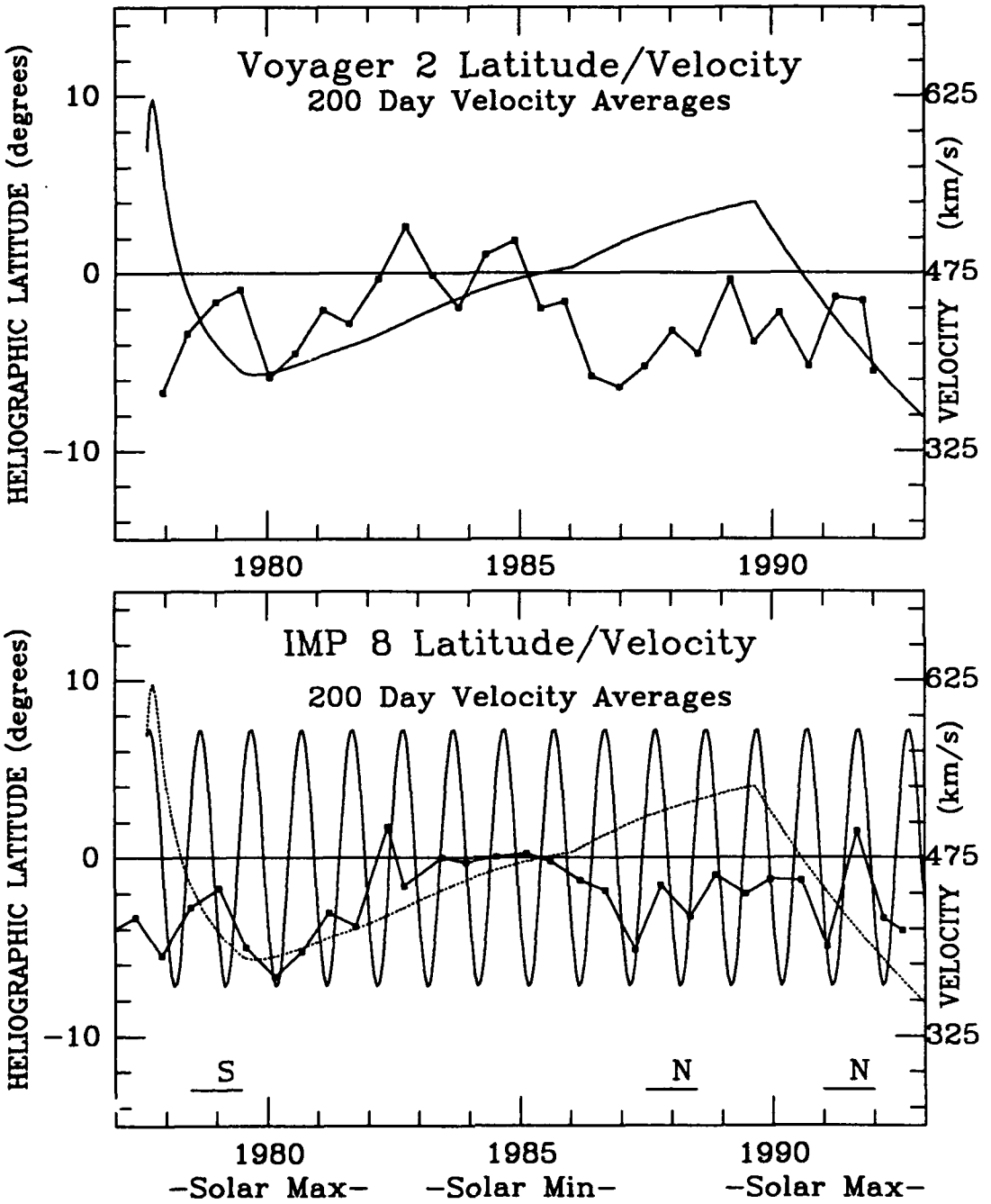

FIGURE 31. Heliographic latitude and velocity vs. year for Voyager 2 (top) and IMP 8 (bottom). Velocity corrected for propagation time; latitude not corrected. High speed sources labeled as N (north) and S (south).

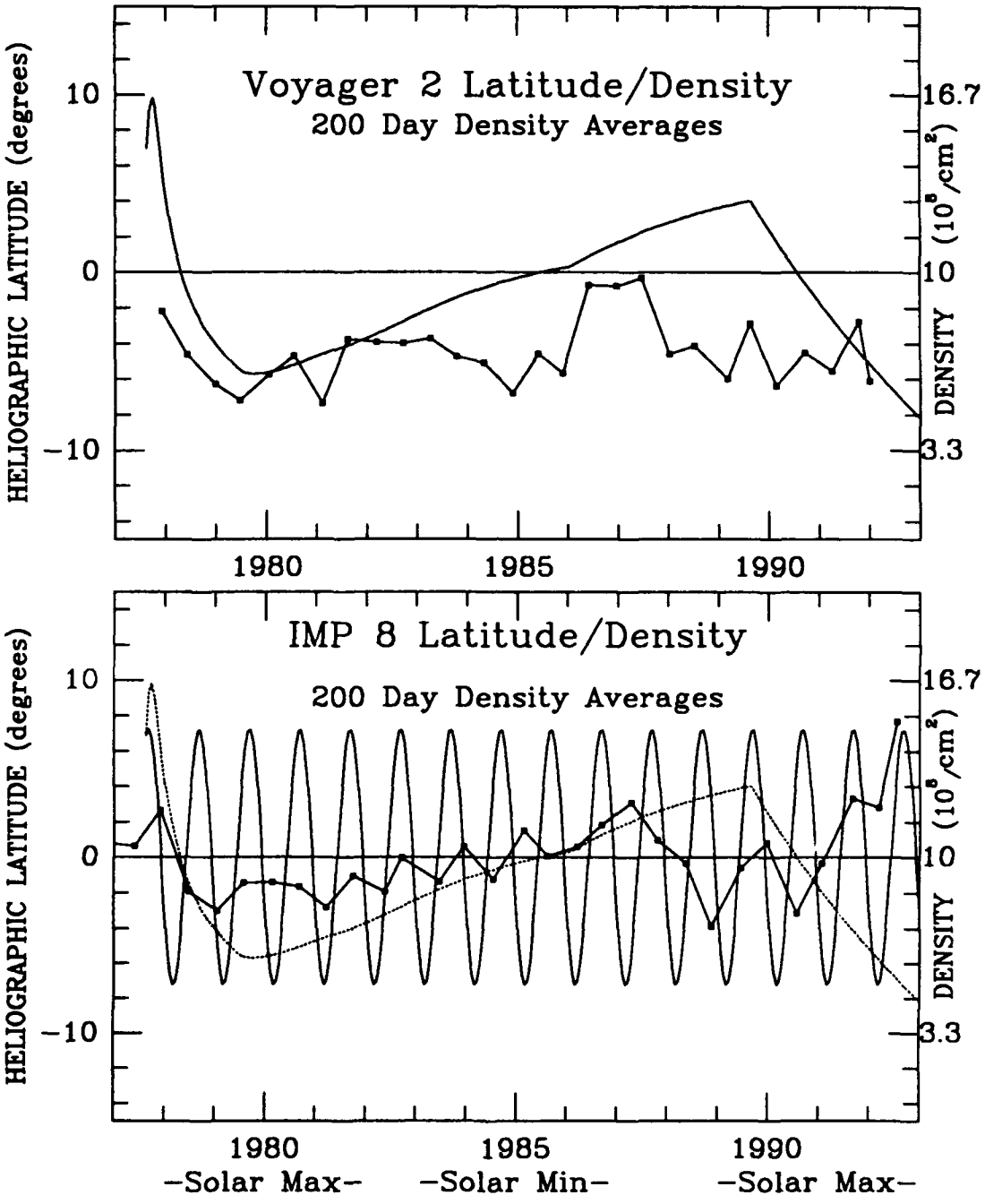

FIGURE 32. Heliographic latitude and density vs. year for Voyager 2 (top), IMP 8 (bottom). Density corrected for propagation time; latitude not corrected.

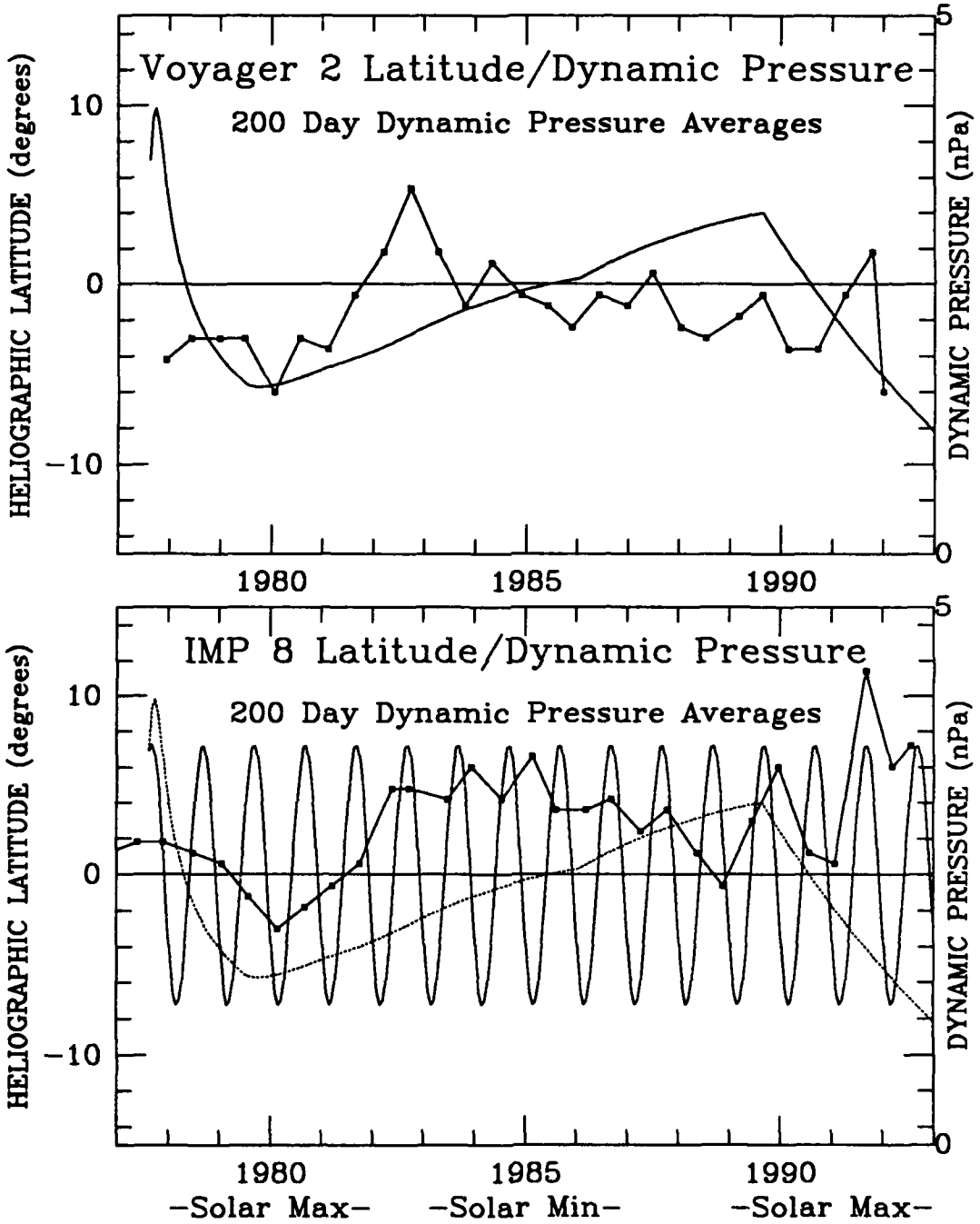

FIGURE 33. Heliographic latitude and dynamic pressure vs. year for Voyager 2 (top), IMP 8 (bottom). Pressure corrected for propagation time; latitude not corrected.

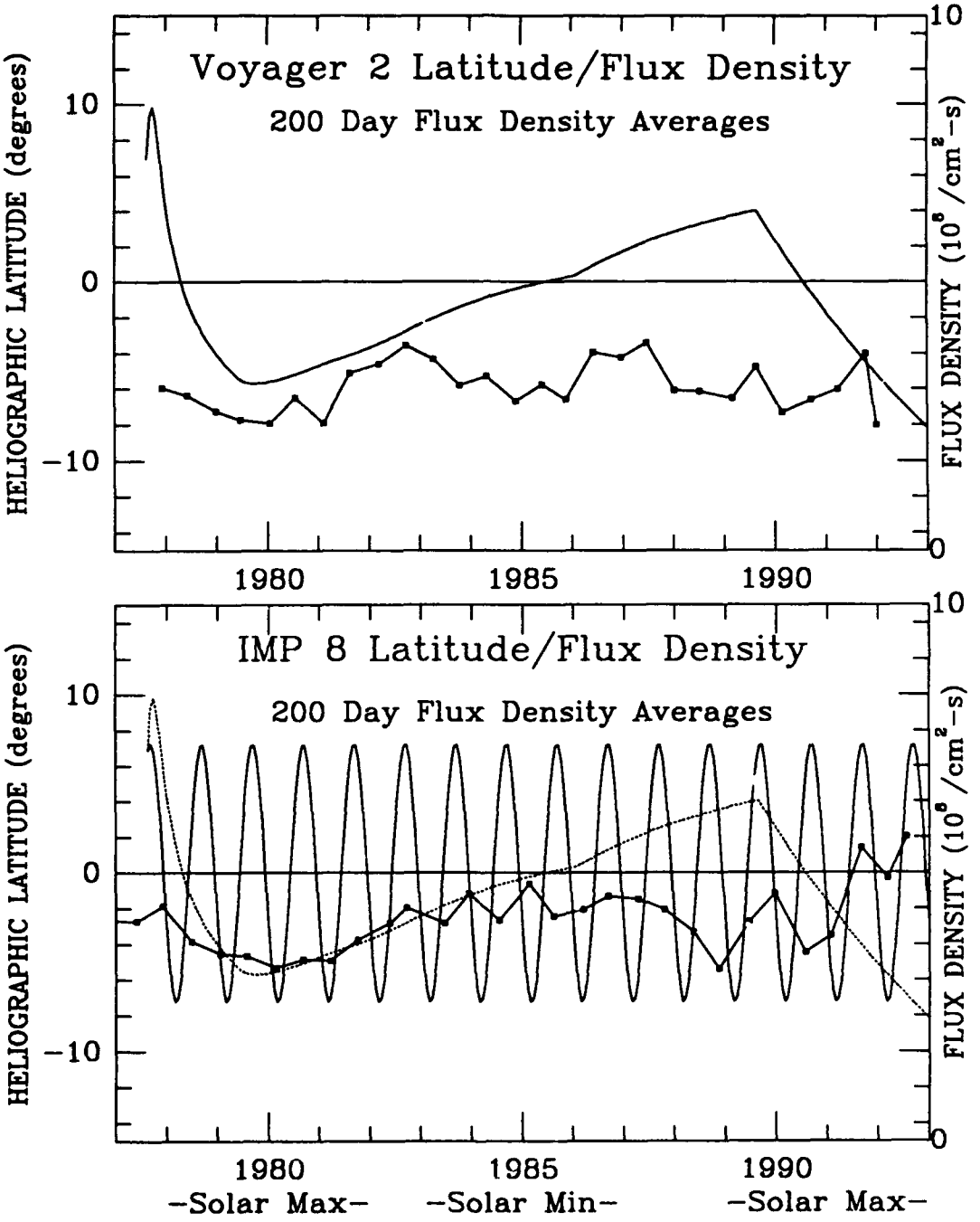

FIGURE 34. Heliographic latitude and flux density vs. year for Voyager 2 (top), IMP 8 (bottom). Flux density corrected for propagation time; latitude not corrected.

CONCLUSIONS

Generally, we have found that velocity measurements made by Voyagers 1 and 2 agreed with the measurements made by IMP 8, especially when averaged over 200 day intervals. On the other hand, there really was not good agreement between the Voyagers' and IMP's density values at any time resolution. These relatively minor differences in velocity and major differences in density further caused differences in calculated values of dynamic pressure and flux density. We can logically account for some of the discrepancies by the appearance of data gaps caused by equipment malfunction or tracking gaps. Other differences are attributed to solar wind structure seen by the Voyagers at large distances from Earth but missed by IMP 8. This structure is often longitude dependent and is nearly always affected by processing through interaction regions. Since IMP 8 remains at 1 AU, the effect of interaction regions is a minimum. Yet other differences result when high speed plasma sources appear above or below the heliographic equator, resulting in latitude dependent velocity gradients. Sometimes velocity differences are the result of the cyclic nature of the coronal neutral sheet which brings with it only low speed plasma streams. Still, there are some differences which cannot be so readily explained. One such difference is that seen in the density measurements. Since density differences cannot always be explained by reasons of solar wind structure, they may have to be attributed to some systematic difference in the Voyager and IMP data processing.

There are many processing steps between collecting solar wind data and creating hourly averages. First the solar wind is sampled by the spacecraft, then it is transmitted back to Earth, the raw data is analyzed and finally it is converted into hourly averages. Somewhere along this processing chain, there

may have been some slight difference between the IMP 8 and Voyager systematic analyses, giving rise to the density differences. Two factors are known which probably contributed to such large density differences. First, the fitting program used to create Voyager data produces density values about 7% lower than another, more accurate, fitting program. Second, a calibration error causes the IMP 8 density values to be about 8% too high. By accounting for these known data discrepancies, the differences in density values for IMP 8 and the Voyagers will become smaller.

There are drawbacks to averaging. We have looked at the same hourly data averaged over four periods: 25/27 days, approximating one solar rotation, 50/54 days, approximating two solar rotations, and 100 and 200 days, approximating four and eight solar rotations, respectively. We have found that using a shorter averaging interval provides more details of the short-term solar wind structure and is very sensitive to small-scale fluctuations in the solar wind but could cause us to lose sense of the long-term trends. The longer averaging periods are more useful if we are interested in looking at long term trends but we lose detail of some individual events. It is probably better, then, to use both shorter and longer averaging intervals as complements to each other. Another disadvantage of averaging over shorter time intervals is that the results are very sensitive to the start time. A starting time difference of only one day can change the average results significantly when averaging over a short time interval. Even with these limitations, averaging is the simplest method to use in analyzing trends in the solar wind.

There have been a couple of lessons learned. First, the technique applied to weight data according to the number of spectra is probably not advisable. Instead, future analyses probably should use each hourly average as equally significant, regardless of the number of spectra used in producing the hourly

average. Second, there should be a guideline established by which average points are discarded if less than 50% (or another agreed-to value) of the available data was used in computing their values. This problem often occurs when there are large data gaps caused by equipment malfunction or by encounters with planets. When the averaging interval is of a duration shorter than the duration of a data gap, there is a chance that the start and end times of the averaging interval will overlap most of the period of missing data and only catch a few hourly averages. The result is an average value calculated using a very small number of spectra. As the length of the averaging interval increases to twice the duration of the data gap, there is still a chance that a data point will be calculated using only 50% of the data normally found in an interval of that length. So, while this problem manifests itself when averaging over shorter periods, this problem is reduced as the averaging interval increases to a period much greater than the length of the data gap.

Using the methods described in this thesis, the following tables summarize the ranges of the average parameters studied, as measured by each spacecraft, for the four averaging periods examined.

TABLE I

25/27 Day Averages				
Spacecraft	Velocity (km/s)	Density (cm^{-3})	Pressure (nPa)	Flux (cm^{-2}–s^{-1})
IMP 8	350-600	4-19	1.6-6.5	2.5-7
Voyager 1	350-520	3-11	1-4.4	1.5-4.5
Voyager 2	340-600	1-15	0.2-5.2	0.5-7

TABLE II

50/54 Day Averages				
Spacecraft	Velocity (km/s)	Density (cm^{-3})	Pressure (nPa)	Flux (cm^{-2}–s^{-1})
IMP 8	360-580	5-17	1.8-5	2.6-7
Voyager 1	380-520	5-10	1.2-3.8	2-4.1
Voyager 2	370-600	4-12	1.2-4.2	1.5-5

TABLE III

100 Day Averages				
Spacecraft	Velocity (km/s)	Density (cm^{-3})	Pressure (nPa)	Flux (cm^{-2}–s^{-1})
IMP 8	360-550	6-14.5	2-4.4	3-6
Voyager 1	380-460	5-8	1.4-2.2	2-3.5
Voyager 2	350-540	5-10	1.4-3.3	2-4.2

TABLE IV

200 Day Averages				
Spacecraft	Velocity (km/s)	Density (cm^{-3})	Pressure (nPa)	Flux (cm^{-2}–s^{-1})
IMP 8	380-520	7.5-12	2-4.4	3.2-5.5
Voyager 1	390-450	6-9	1.8-2.2	2.5-3.5
Voyager 2	380-520	5-10	1.4-3.4	2.5-3.5

APPENDIX A

SOLAR WIND VELOCITY HOURLY AVERAGES

Presented on the next few pages are hourly averages of solar wind velocity. These are presented in order to provide the reader a reference for discussions within the text of this thesis. The Voyager data have not been adjusted to account for propagation time.

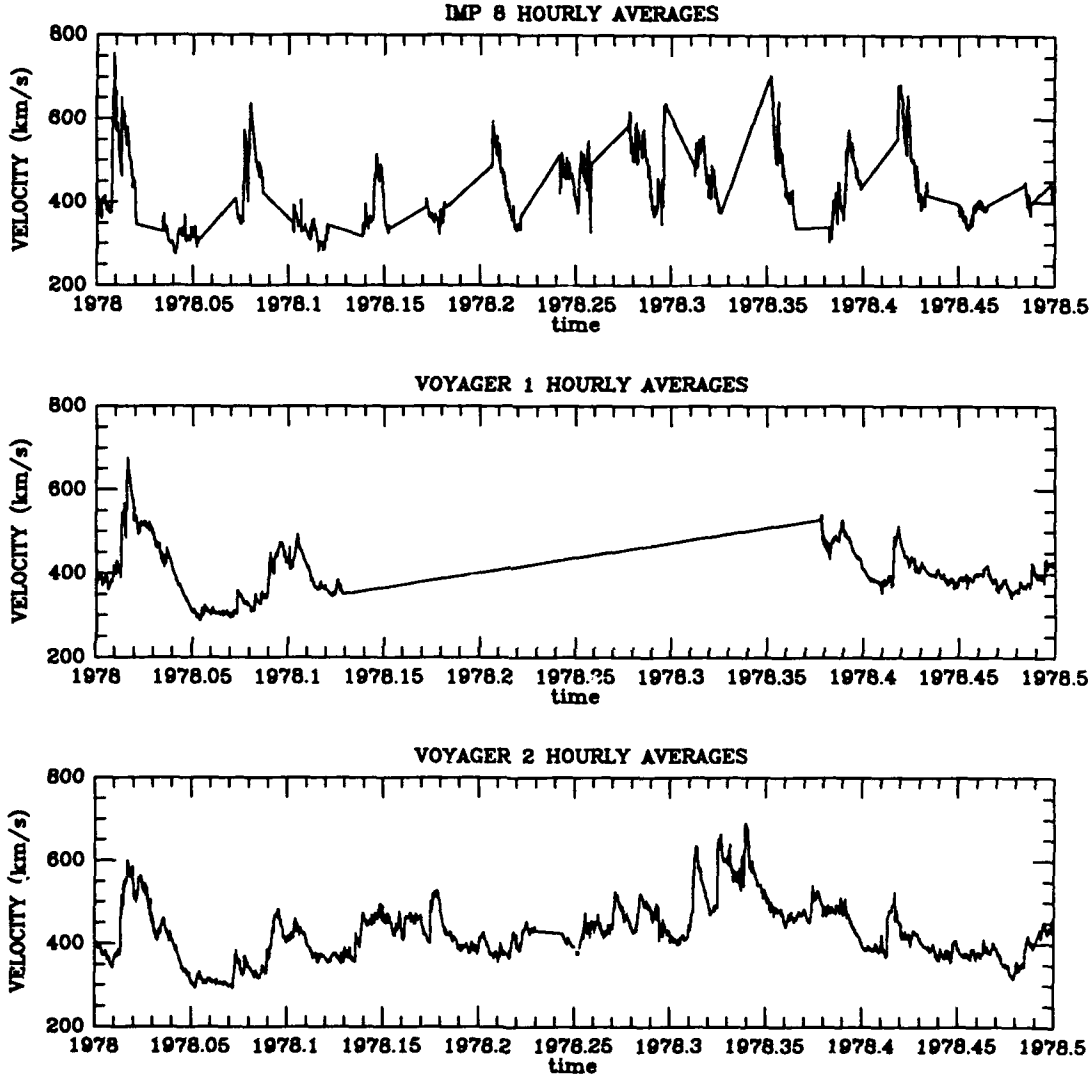

FIGURE A–1. Hourly Averages of Velocity for IMP 8 (Top), Voyager 1 (Middle), Voyager 2 (Bottom).

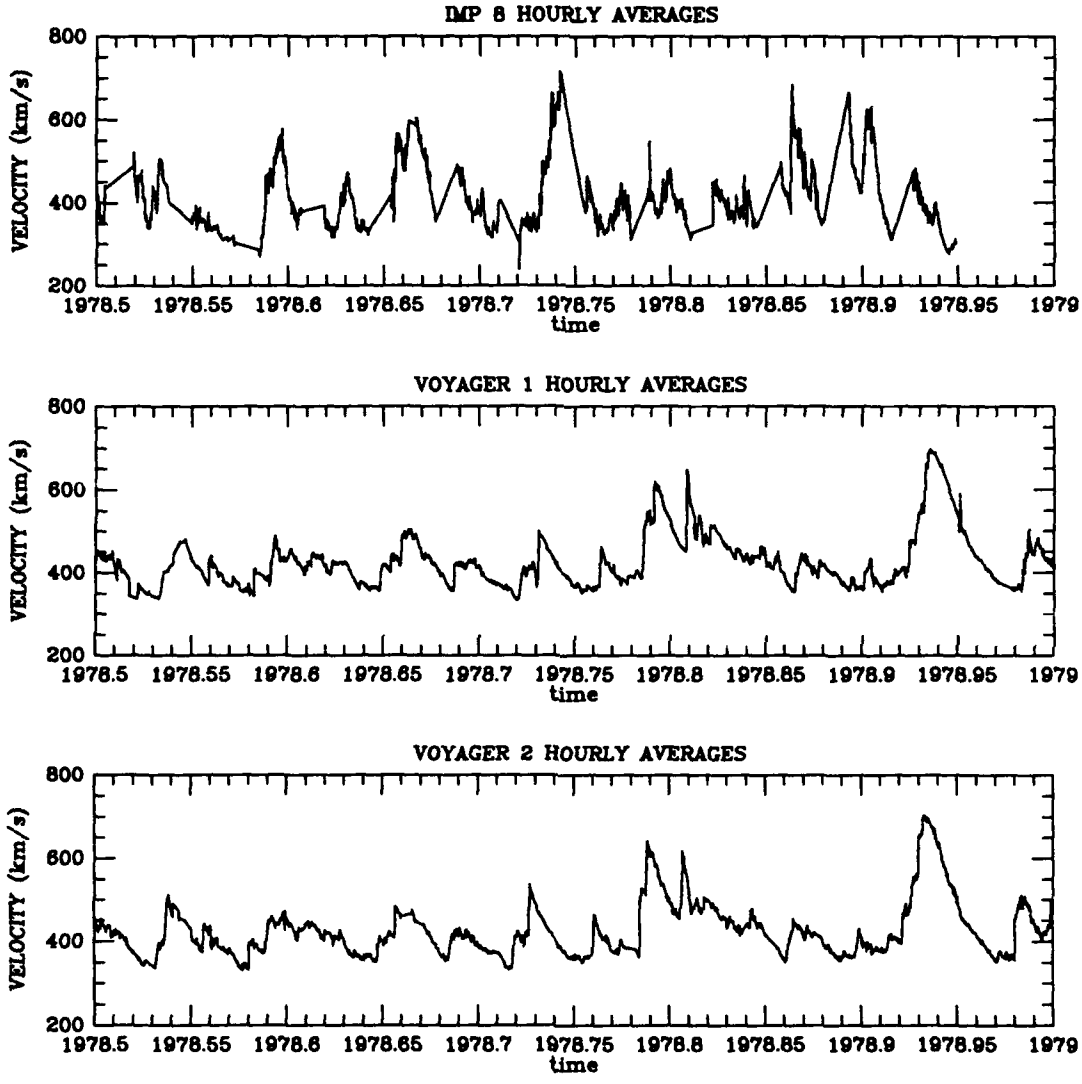

FIGURE A–2. Hourly Averages of Velocity for IMP 8 (Top), Voyager 1 (Middle), Voyager 2 (Bottom).

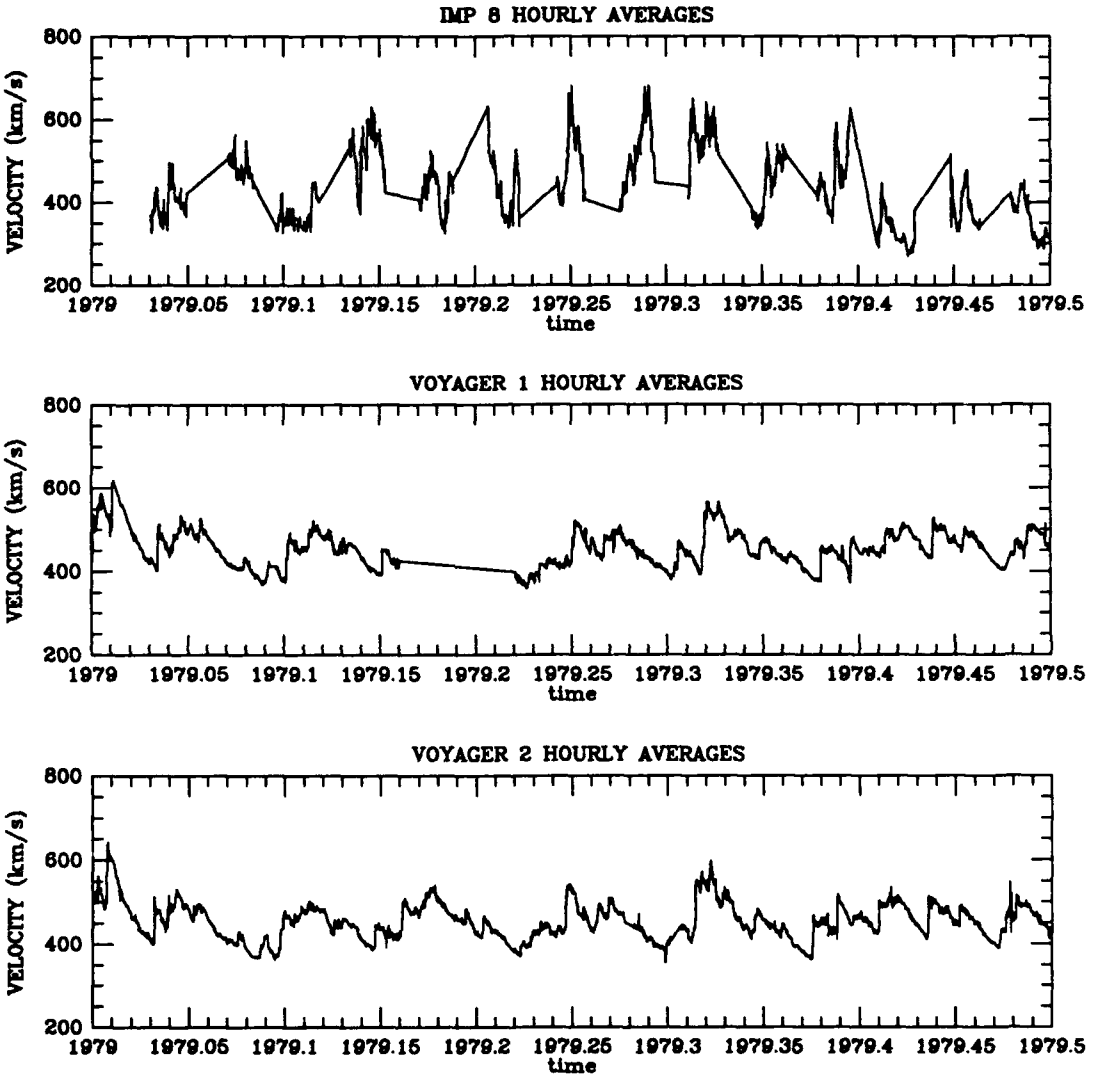

FIGURE A–3. Hourly Averages of Velocity for IMP 8 (Top), Voyager 1 (Middle), Voyager 2 (Bottom).

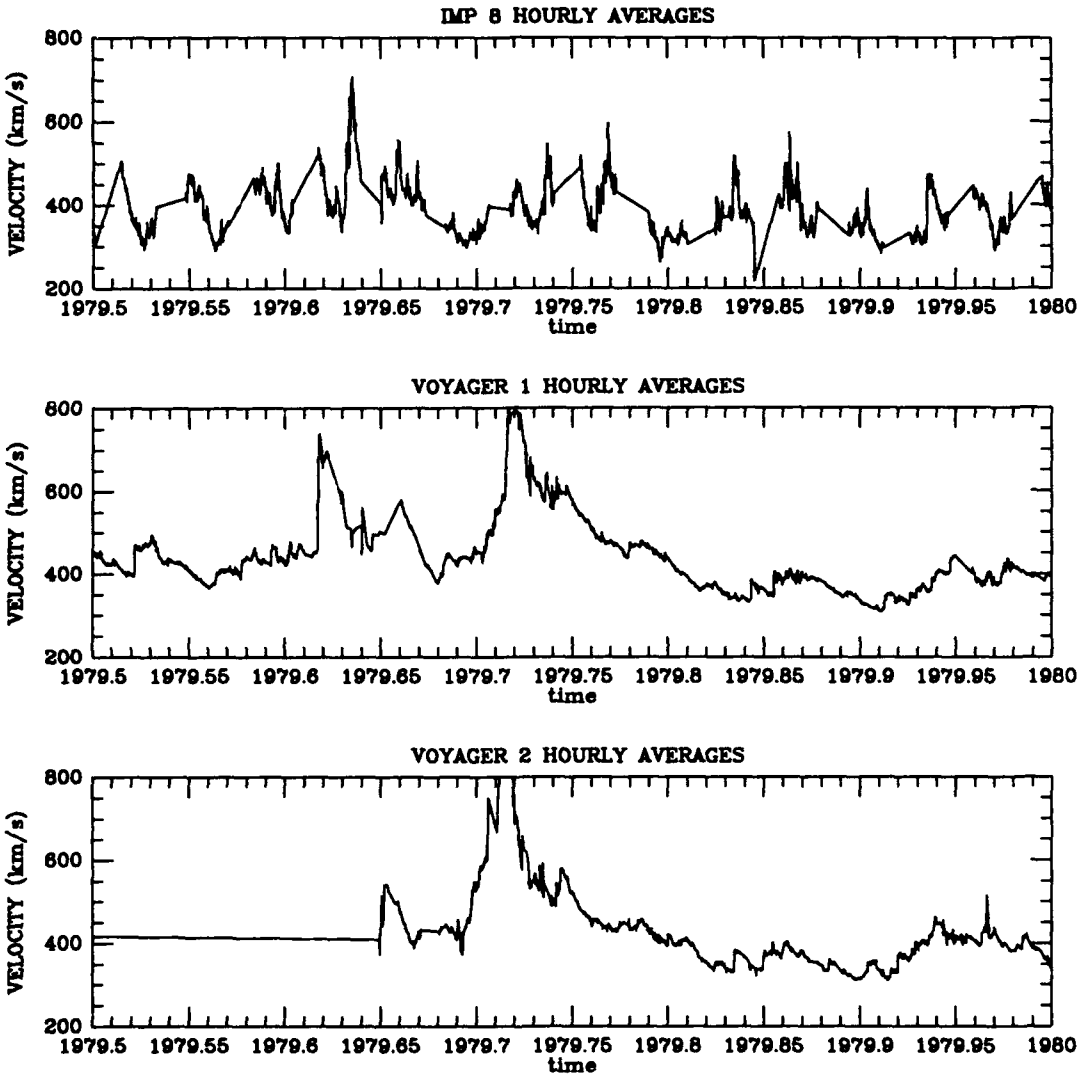

FIGURE A–4. Hourly Averages of Velocity for IMP 8 (Top), Voyager 1 (Middle), Voyager 2 (Bottom).

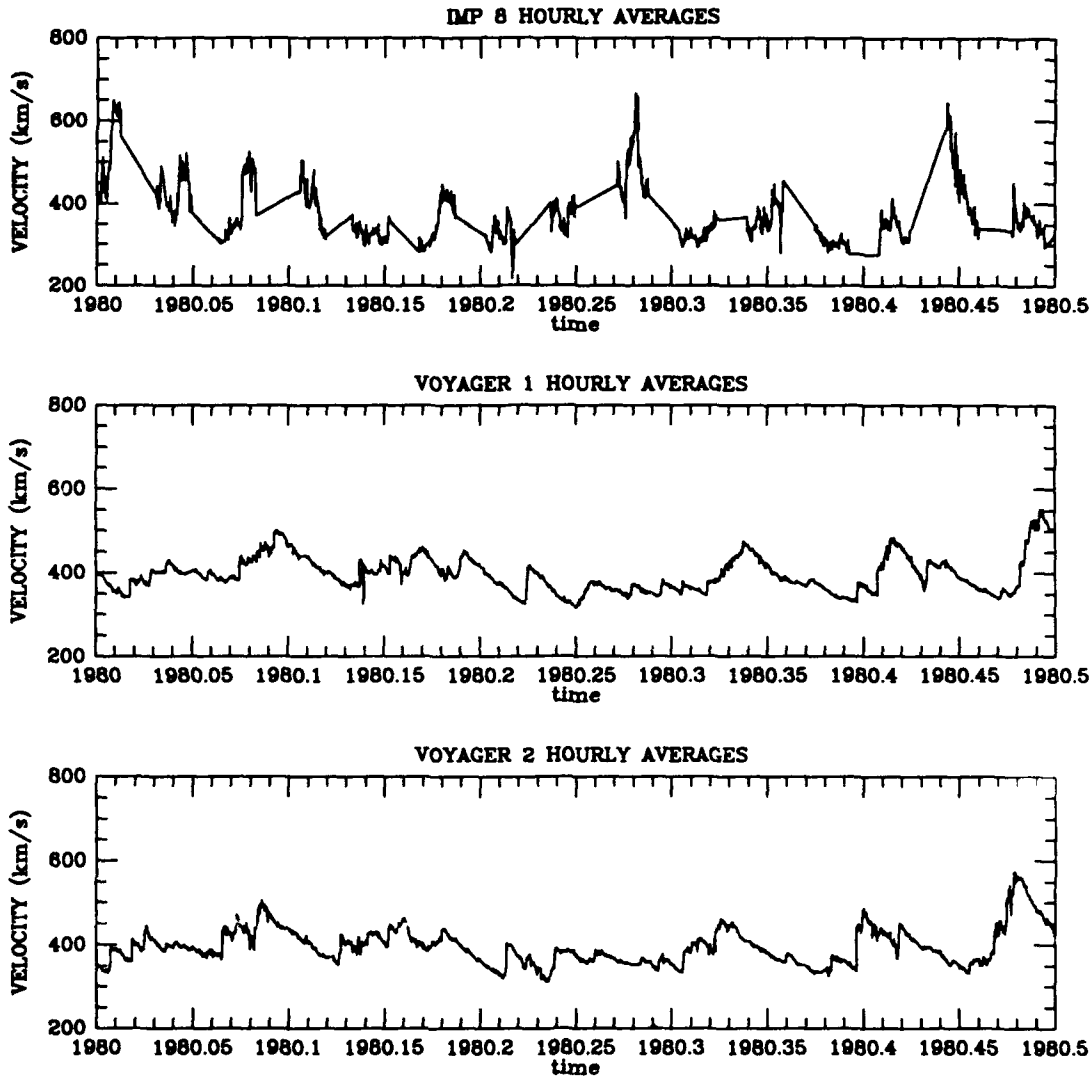

FIGURE A–5. Hourly Averages of Velocity for IMP 8 (Top), Voyager 1 (Middle), Voyager 2 (Bottom).

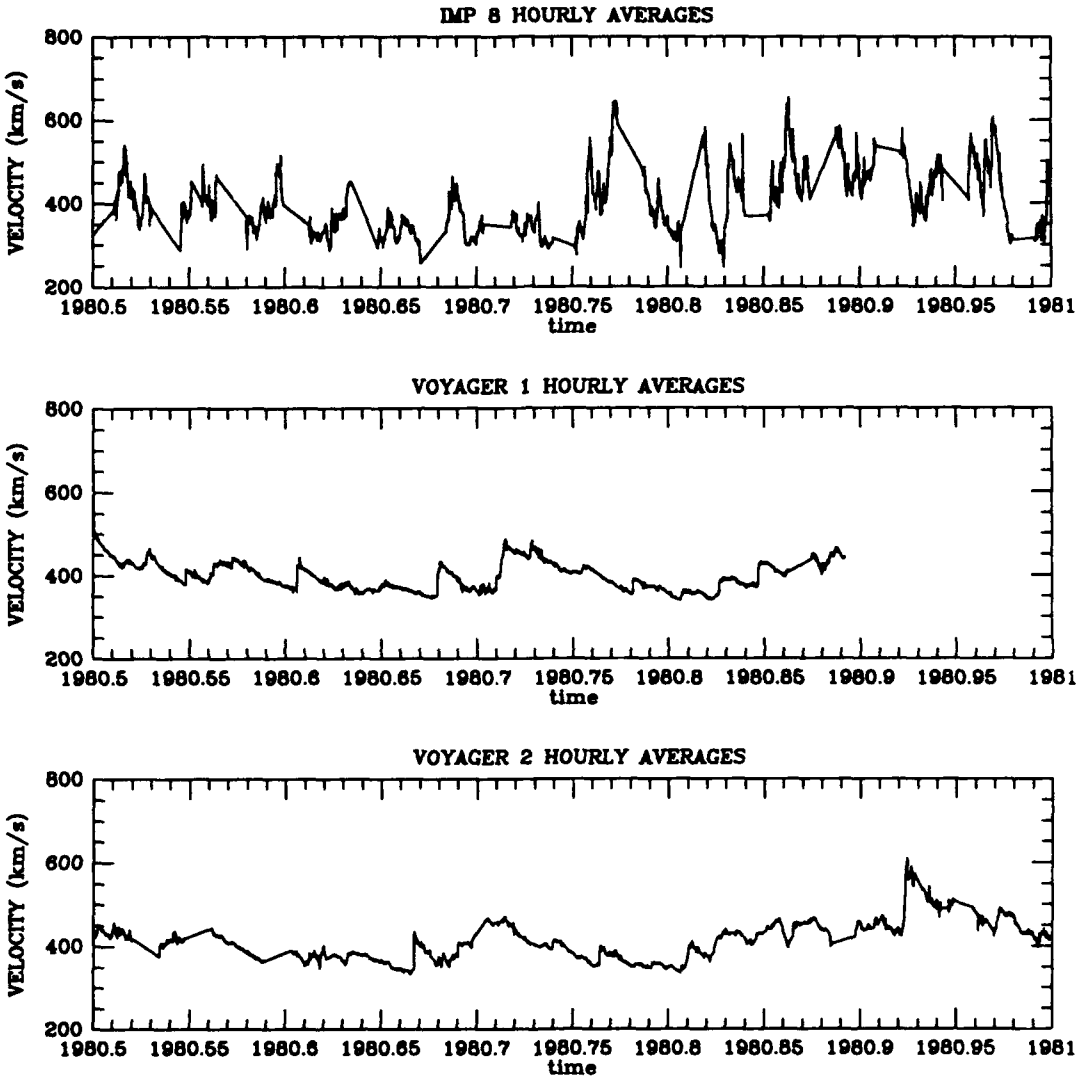

FIGURE A-6. Hourly Averages of Velocity for IMP 8 (Top), Voyager 1 (Middle), Voyager 2 (Bottom).

APPENDIX B

SOLAR WIND DENSITY HOURLY AVERAGES

Presented on the next few pages are hourly averages of solar wind density. These are presented in order to provide the reader a reference for discussions within the text of this thesis. The Voyager data have been normalized to 1 AU but propagation time has not been taken into account.

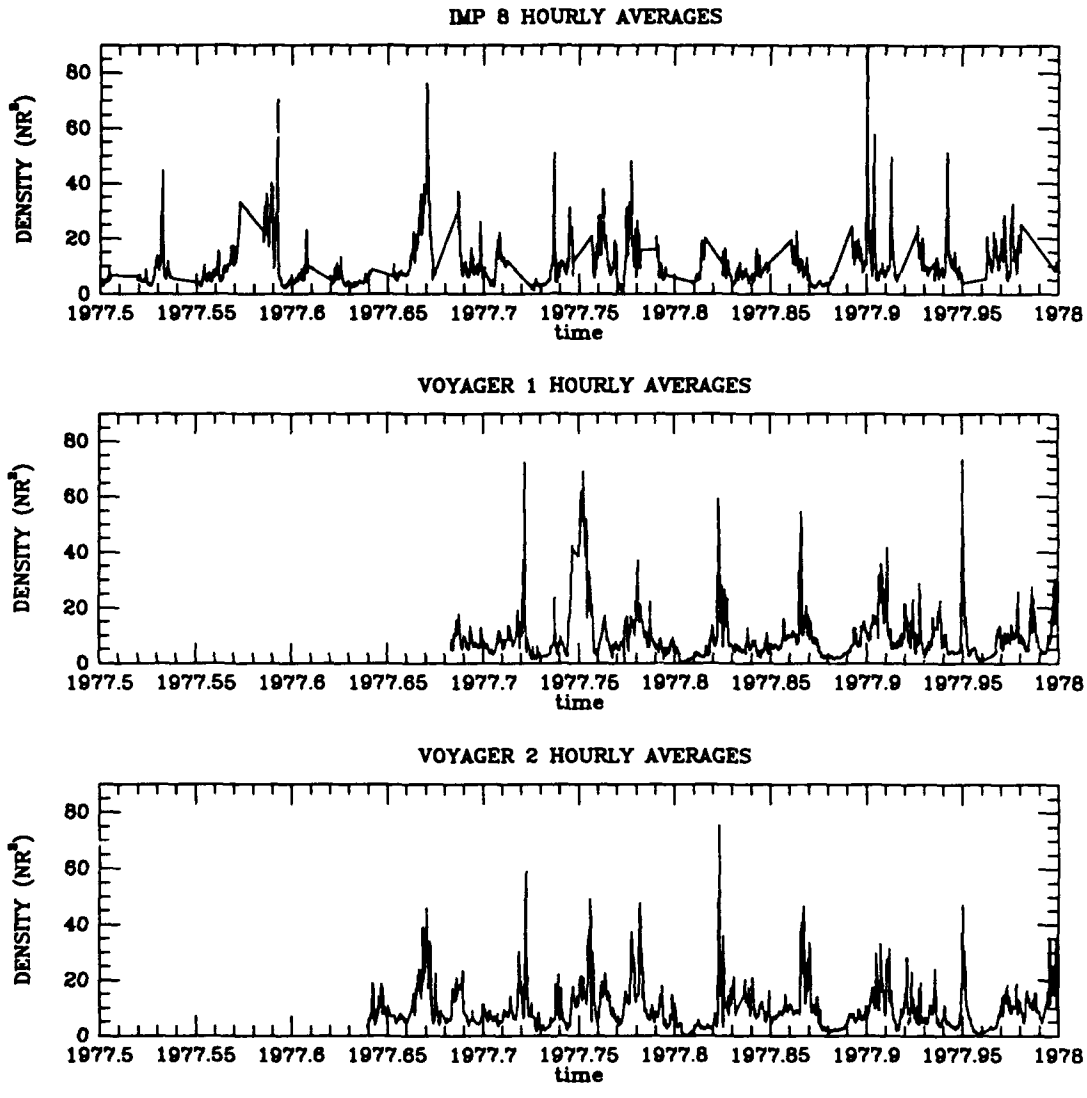

FIGURE B–1. Hourly Averages of Density for IMP 8 (Top), Voyager 1 (Middle), Voyager 2 (Bottom). Voyagers' density data normalized to 1 AU.

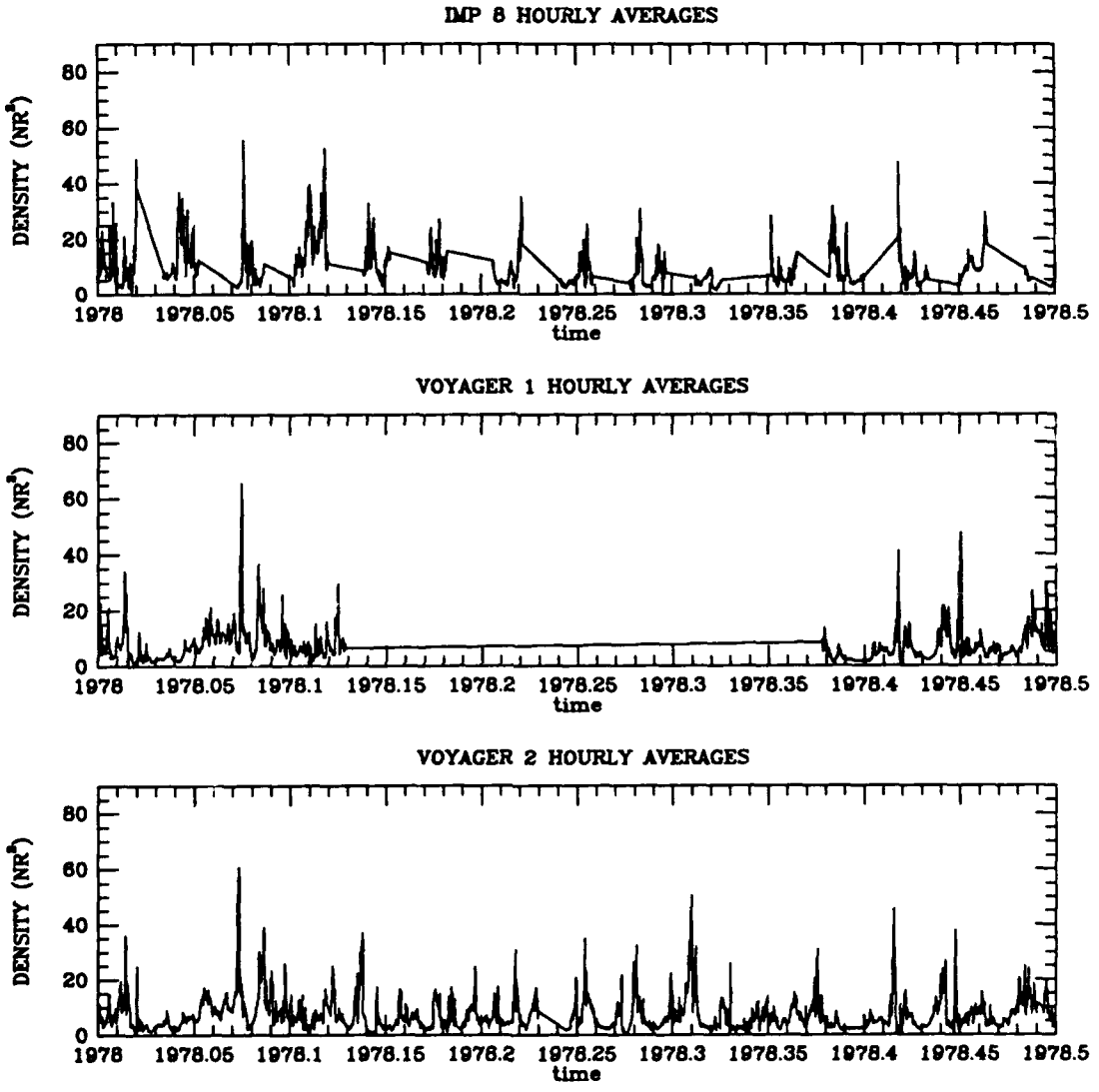

FIGURE B–2. Hourly Averages of Density for IMP 8 (Top), Voyager 1 (Middle), Voyager 2 (Bottom). Voyagers' density data normalized to 1 AU.

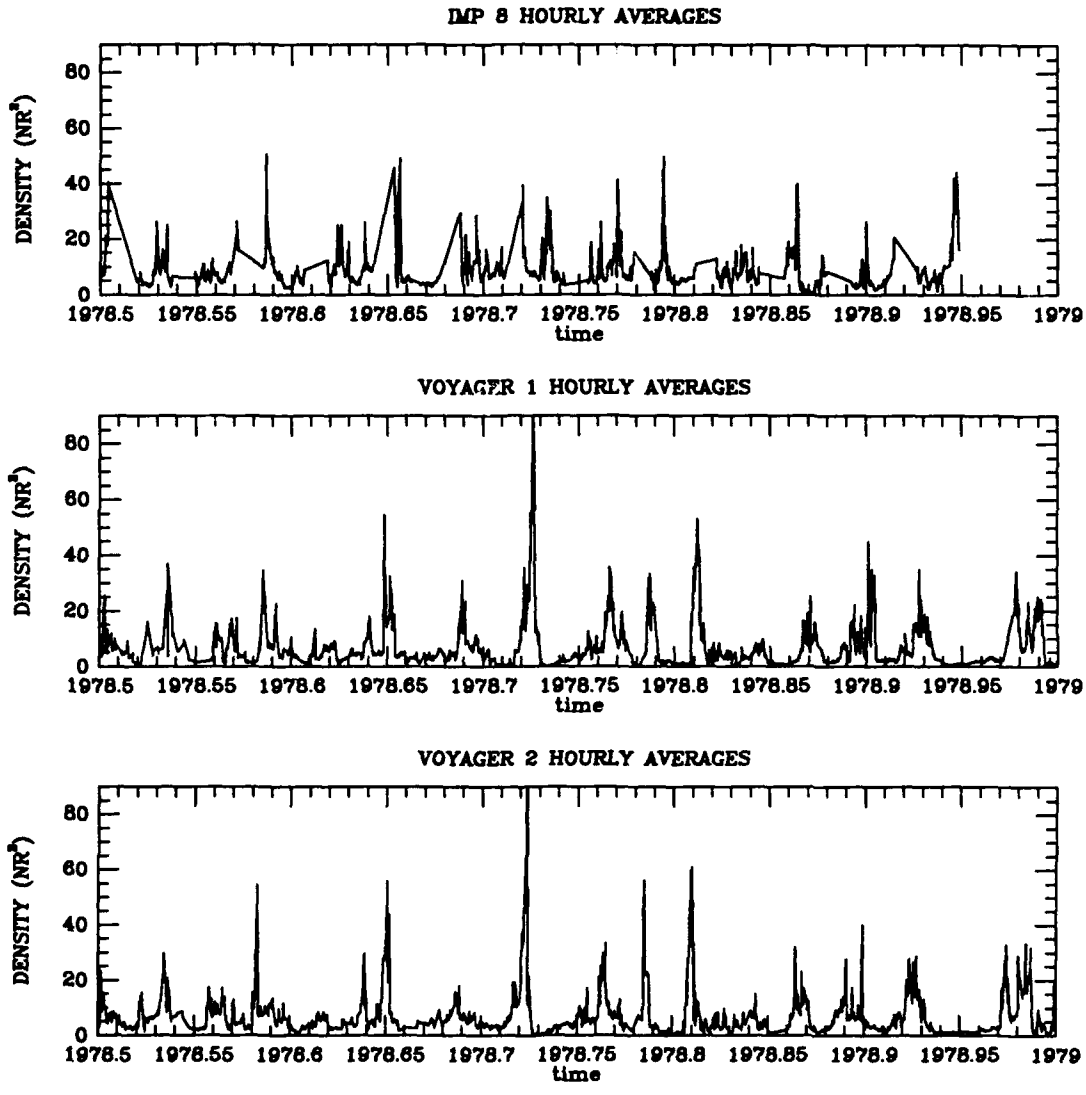

FIGURE B–3. Hourly Averages of Density for IMP 8 (Top), Voyager 1 (Middle), Voyager 2 (Bottom) Voyagers' density data normalized to 1 AU.

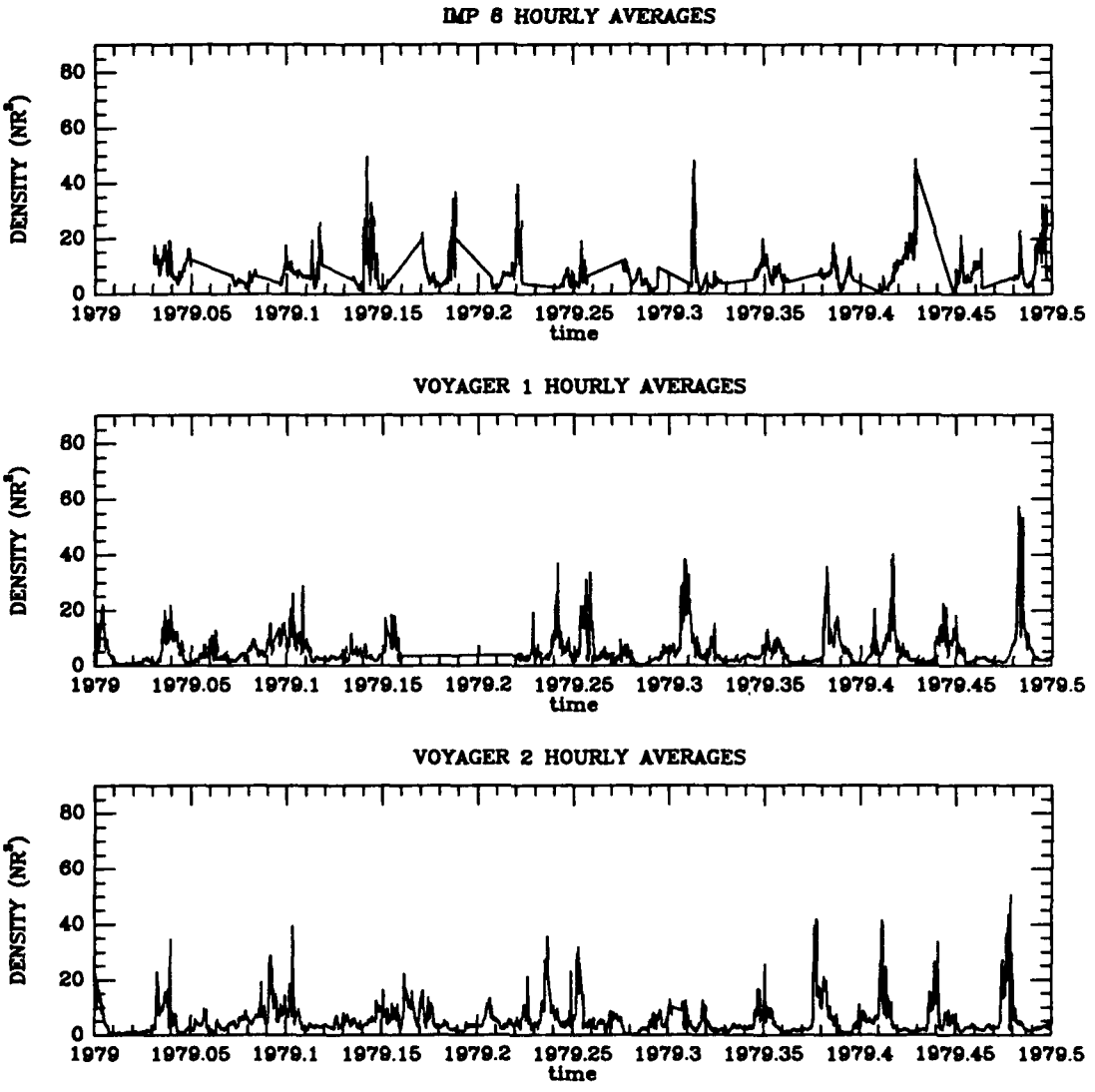

FIGURE B–4. Hourly Averages of Density for IMP 8 (Top), Voyager 1 (Middle), Voyager 2 (Bottom). Voyagers' density data normalized to 1 AU.

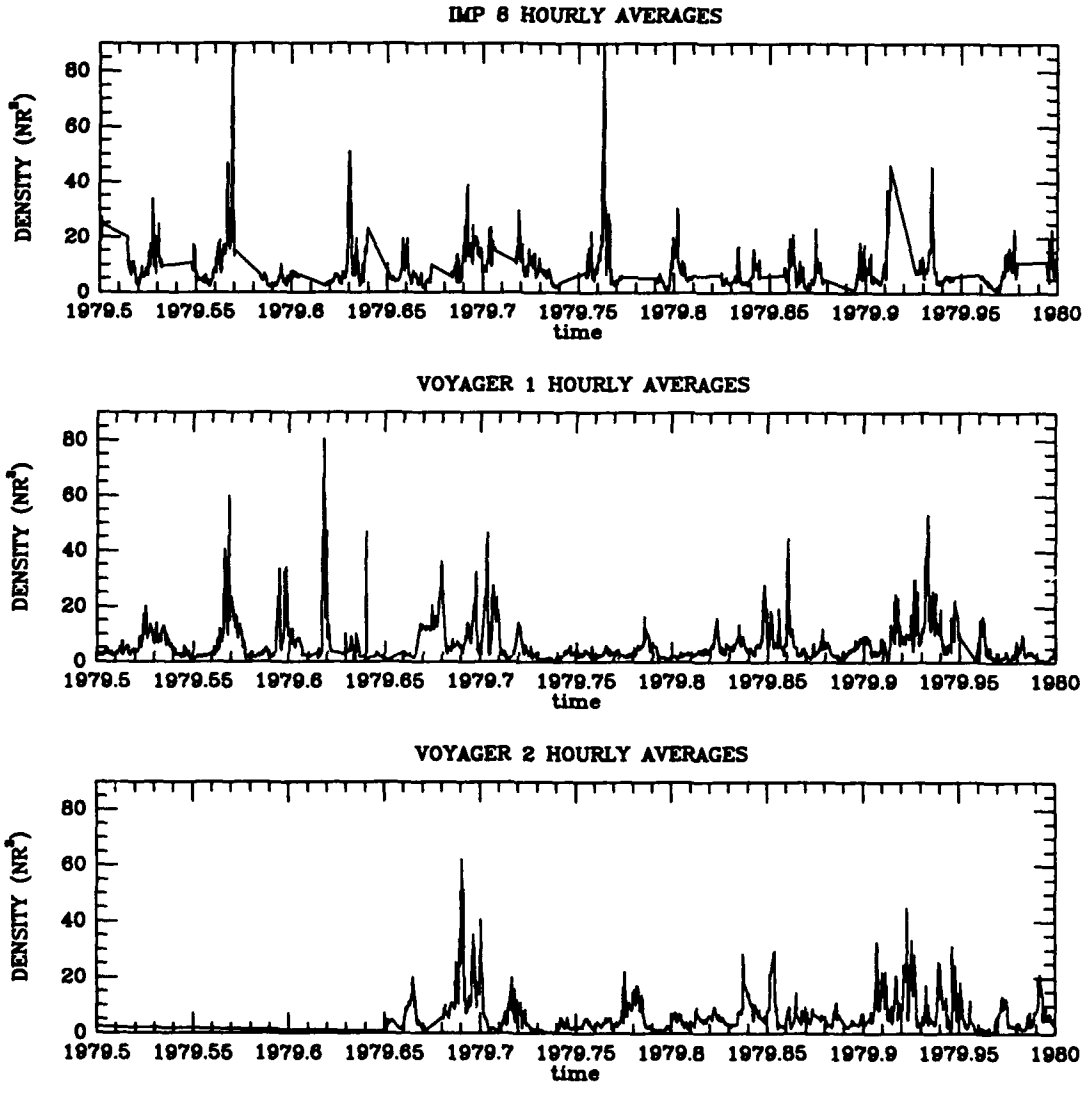

FIGURE B–5. Hourly Averages of Density for IMP 8 (Top), Voyager 1 (Middle), Voyager 2 (Bottom). Voyagers' density data normalized to 1 AU.

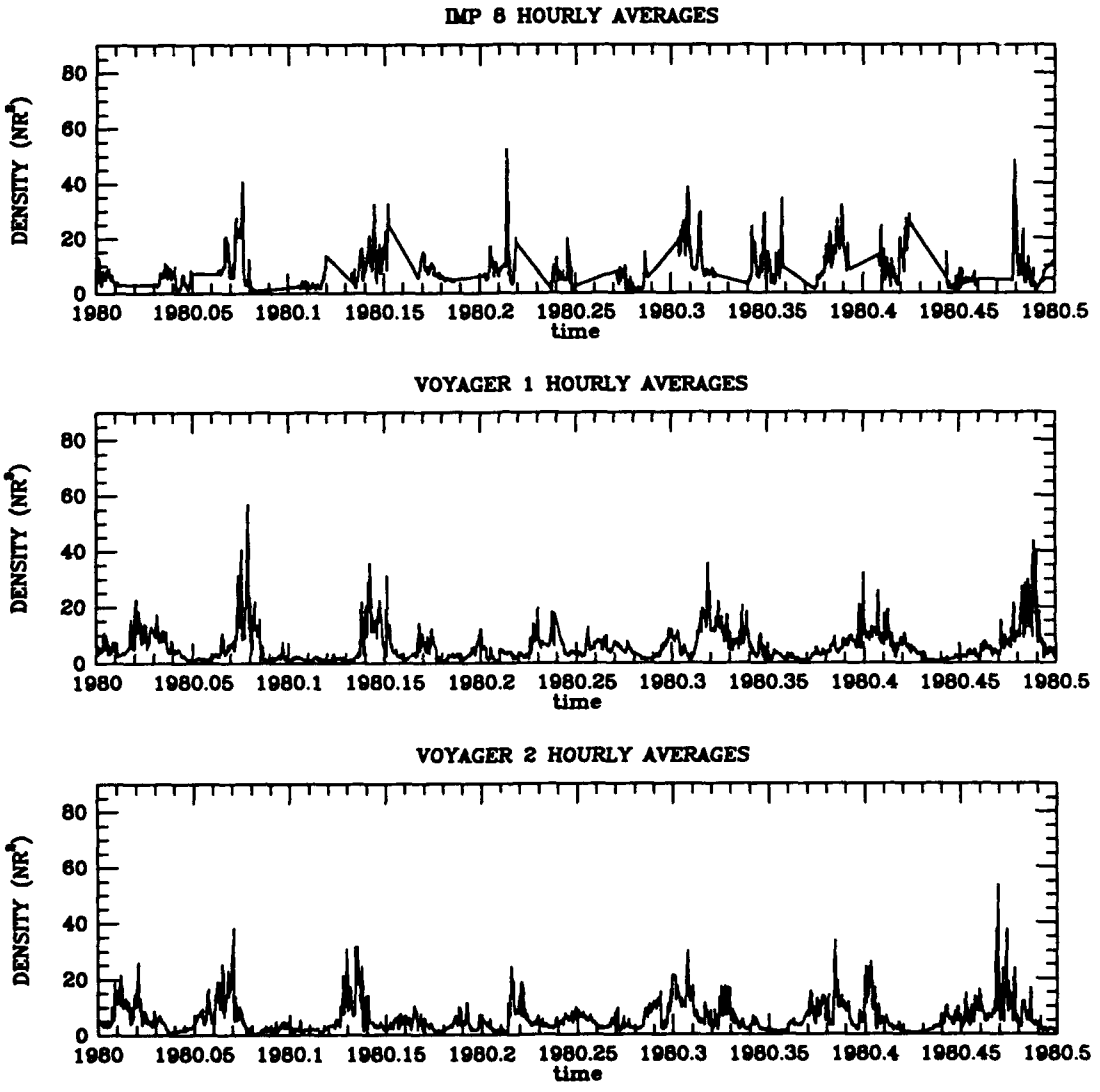

FIGURE B–6. Hourly Averages of Density for IMP 8 (Top), Voyager 1 (Middle), Voyager 2 (Bottom). Voyagers' density data normalized to 1 AU.

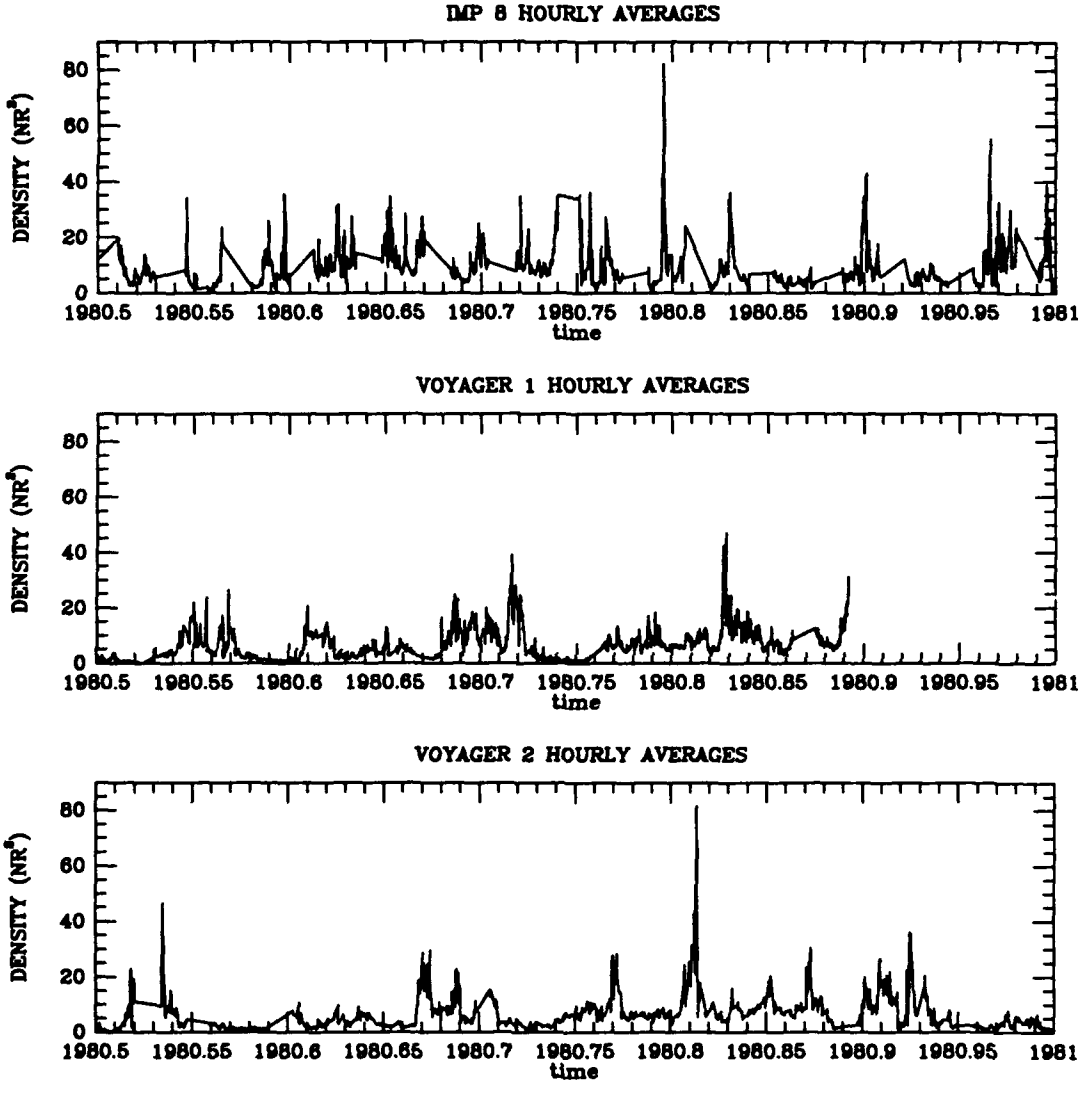

FIGURE B–7. Hourly Averages of Density for IMP 8 (Top), Voyager 1 (Middle), Voyager 2 (Bottom). Voyagers' density data normalized to 1 AU.

APPENDIX C

SOLAR WIND VELOCITY HOURLY AVERAGES (PROJECTED)

Presented on the next few pages are hourly averages of solar wind velocity. These have been adjusted to account for the time it takes for plasma to propagate to the spacecraft's location. These data are presented in order to provide the reader a reference for discussions within the text of this thesis.

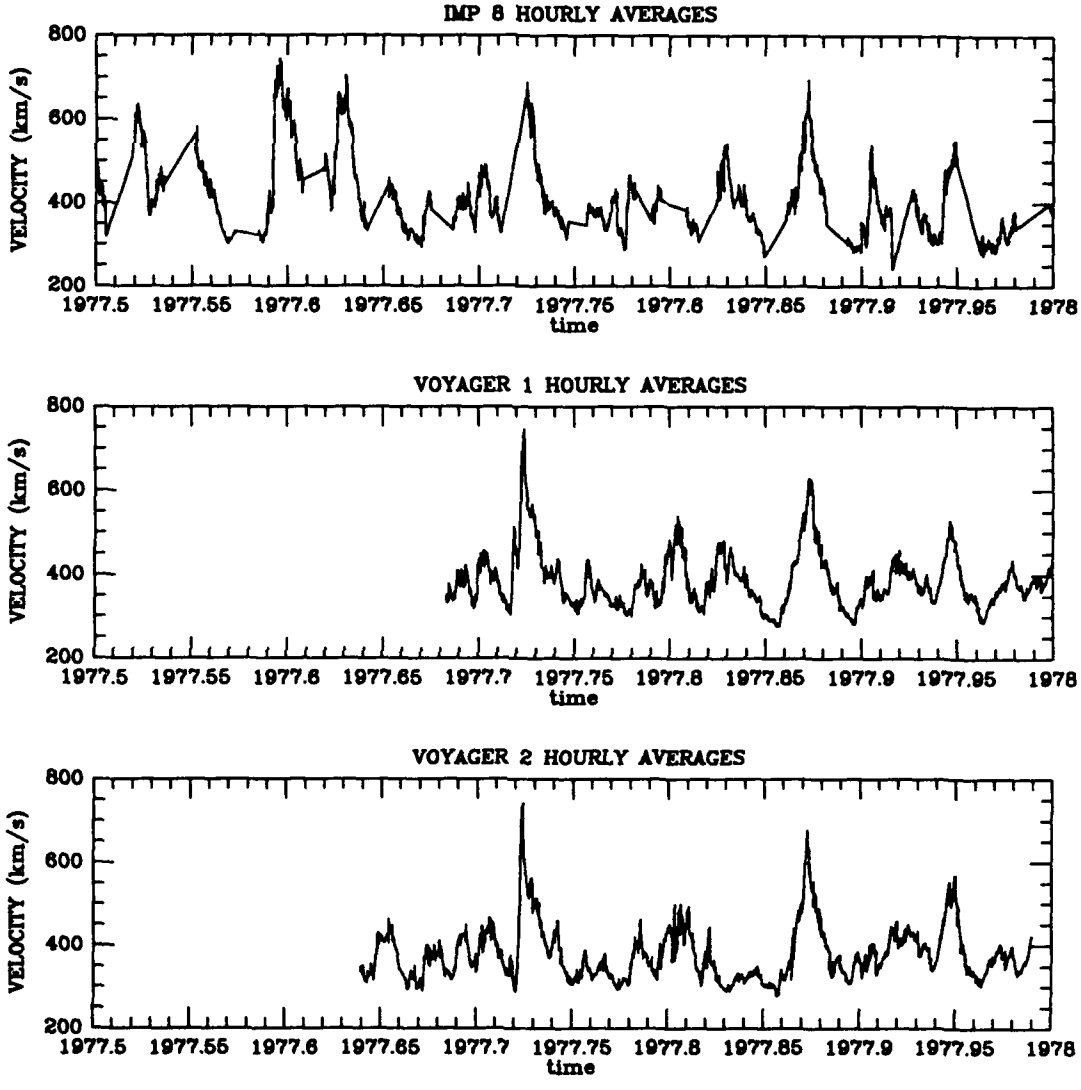

FIGURE C-1. Hourly Averages of Velocity for IMP 8 (Top), Voyager 1 (Middle), Voyager 2 (Bottom). Voyagers' velocity data projected to 1 AU.

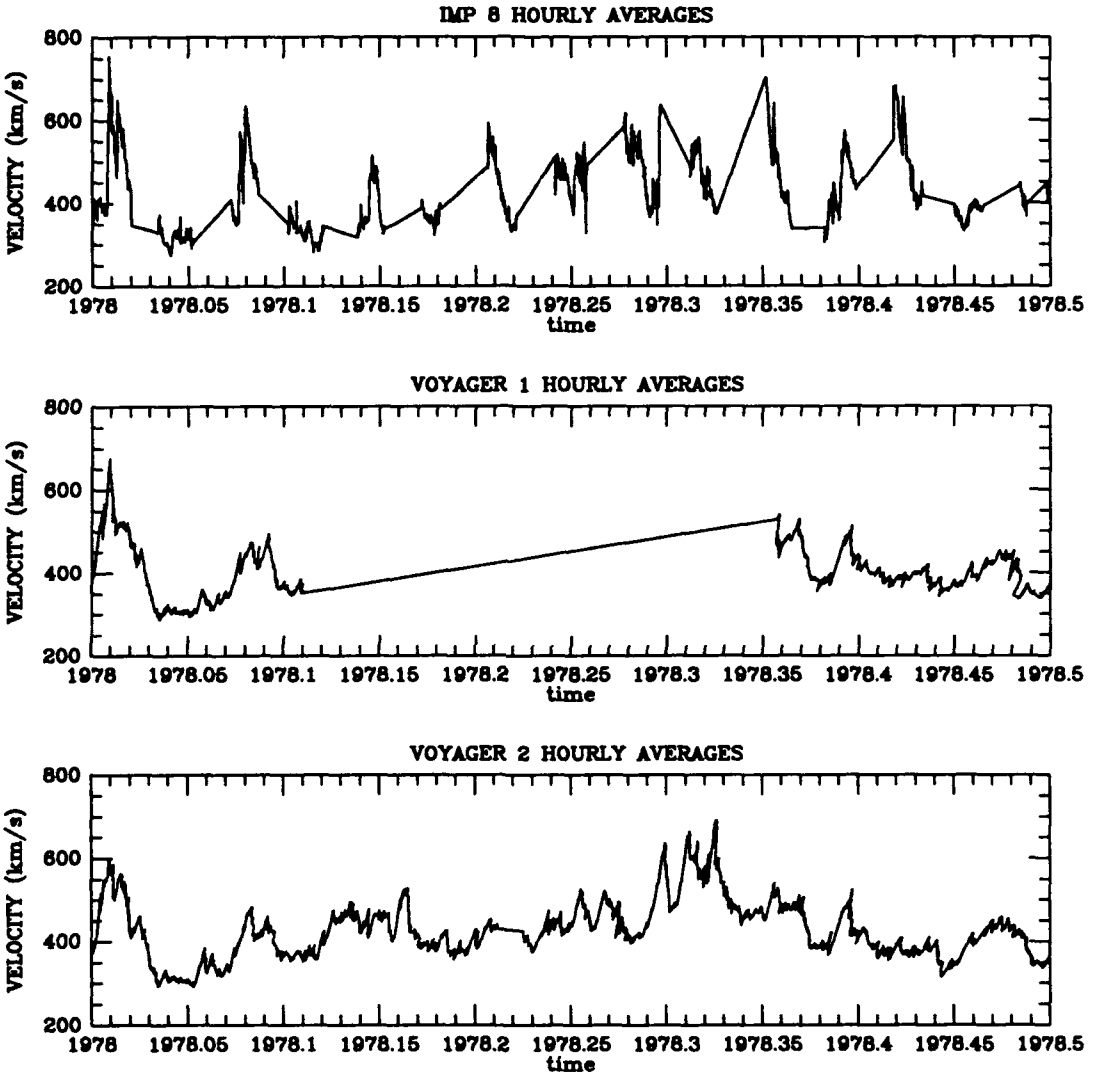

FIGURE C–2. Hourly Averages of Velocity for IMP 8 (Top), Voyager 1 (Middle), Voyager 2 (Bottom). Voyagers' velocity data projected to 1 AU.

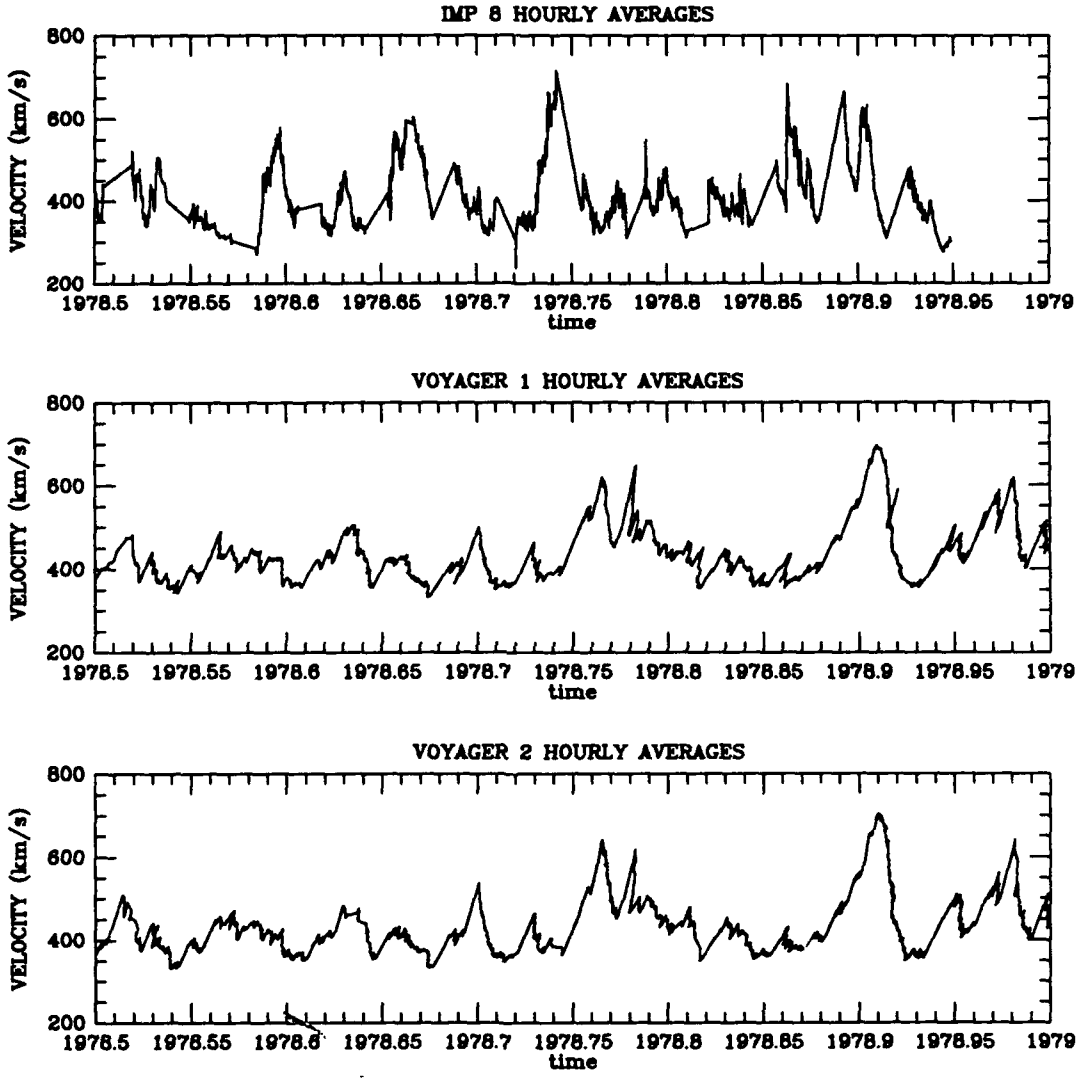

FIGURE C–3. Hourly Averages of Velocity for IMP 8 (Top), Voyager 1 (Middle), Voyager 2 (Bottom). Voyagers' velocity data projected to 1 AU.

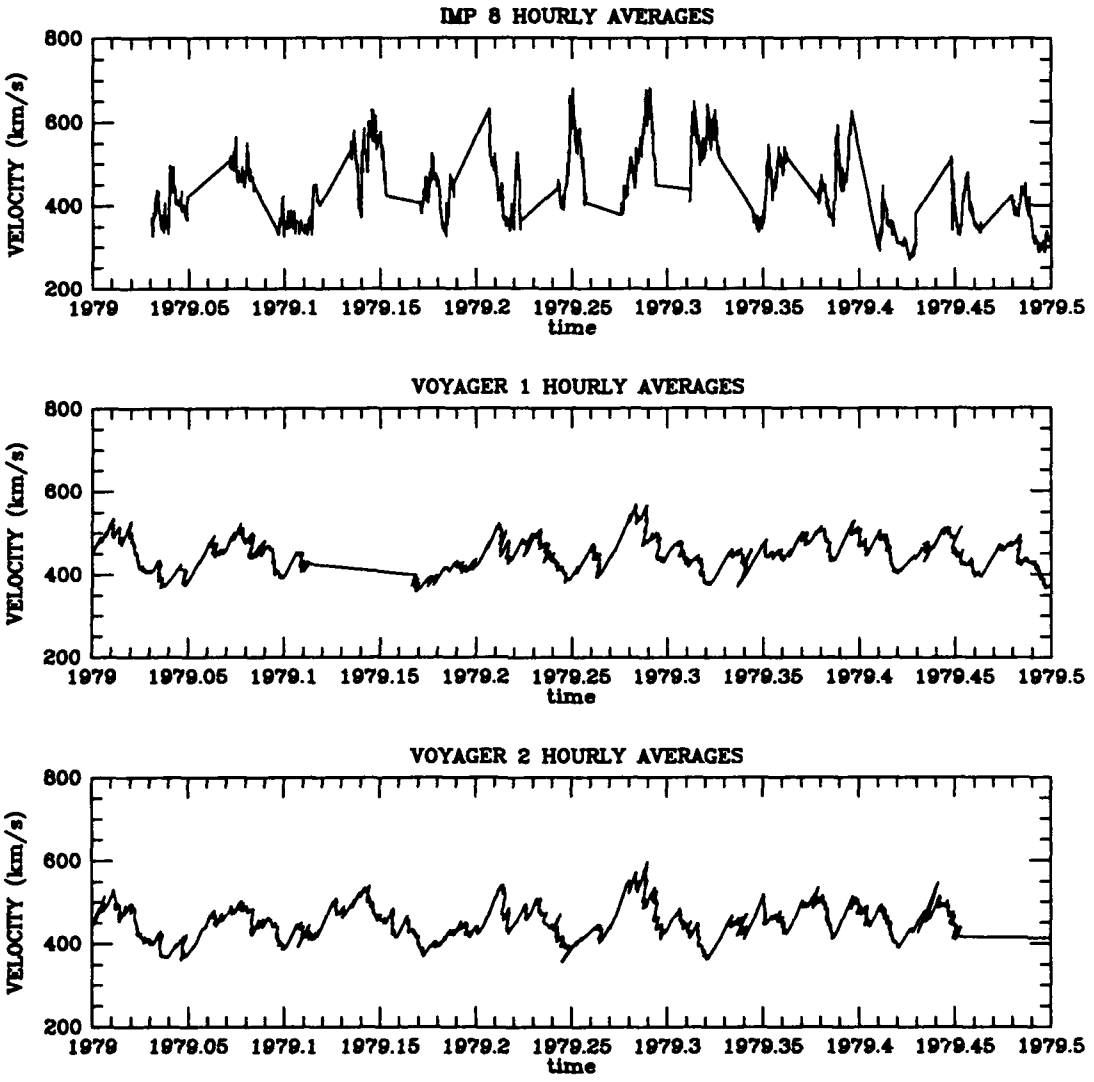

FIGURE C–4. Hourly Averages of Velocity for IMP 8 (Top), Voyager 1 (Middle), Voyager 2 (Bottom). Voyagers' velocity data projected to 1 AU.

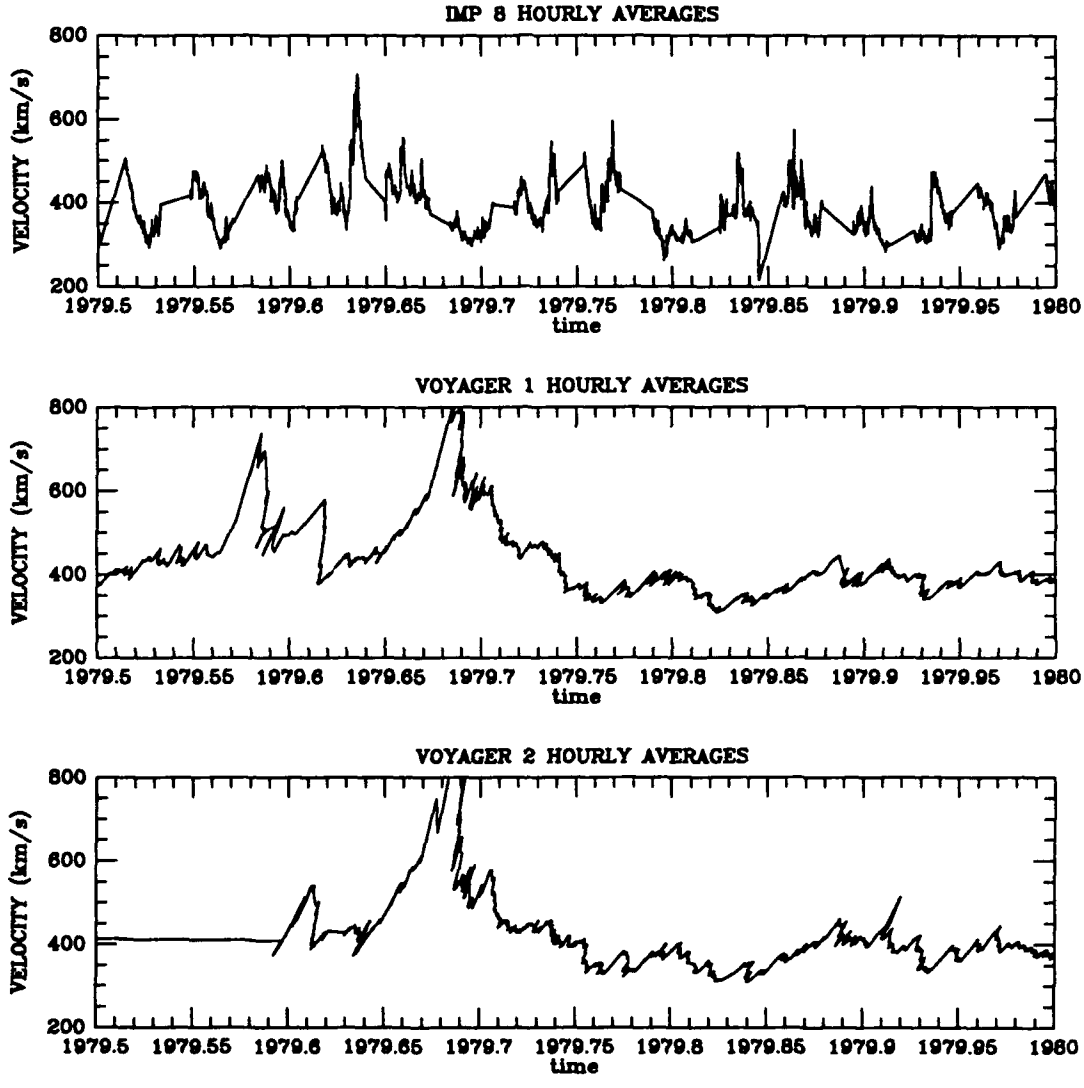

FIGURE C–5. Hourly Averages of Velocity for IMP 8 (Top), Voyager 1 (Middle), Voyager 2 (Bottom). Voyagers' velocity data projected to 1 AU.

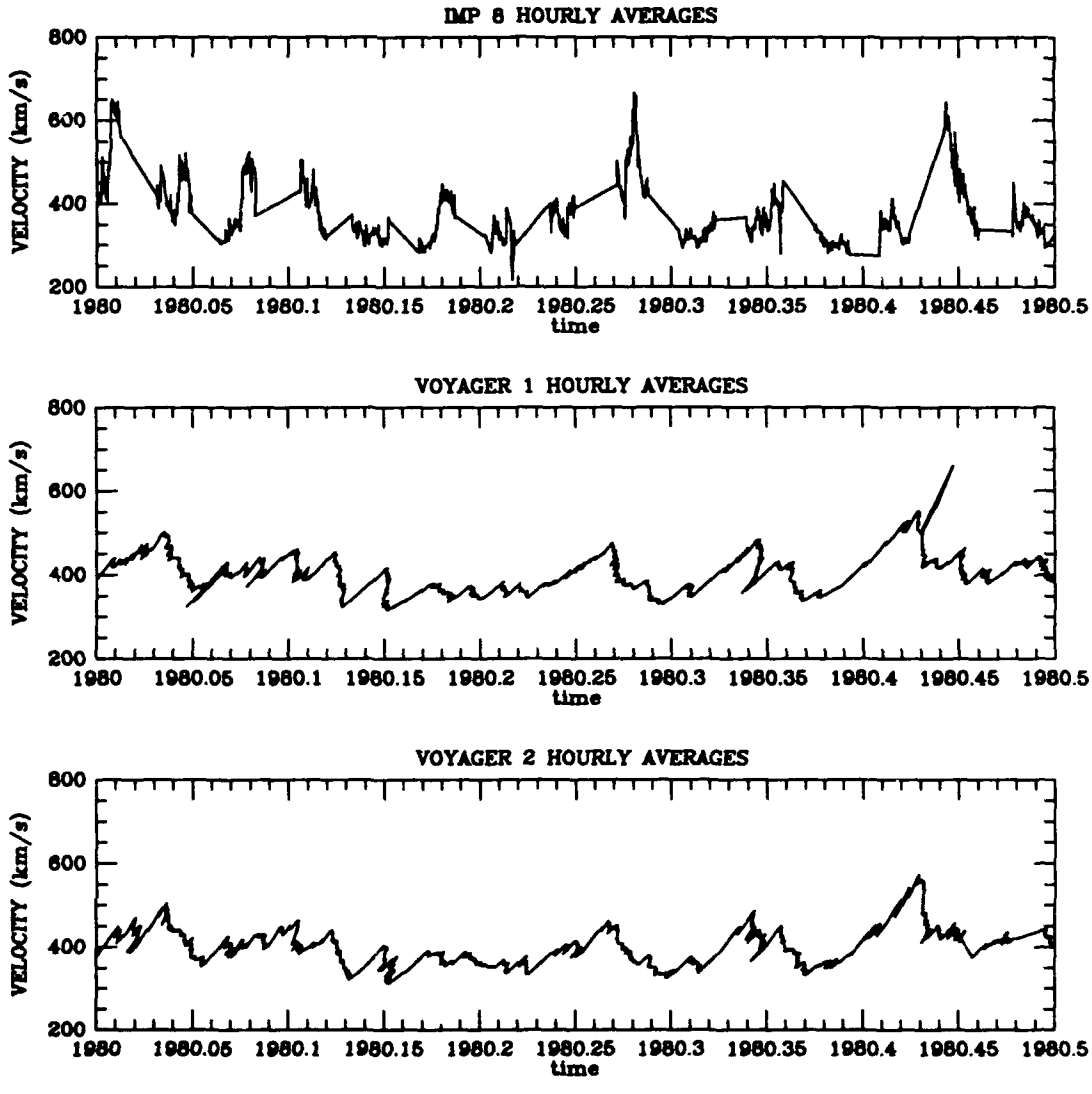

FIGURE C-6. Hourly Averages of Velocity for IMP 8 (Top), Voyager 1 (Middle), Voyager 2 (Bottom). Voyagers' velocity data projected to 1 AU.

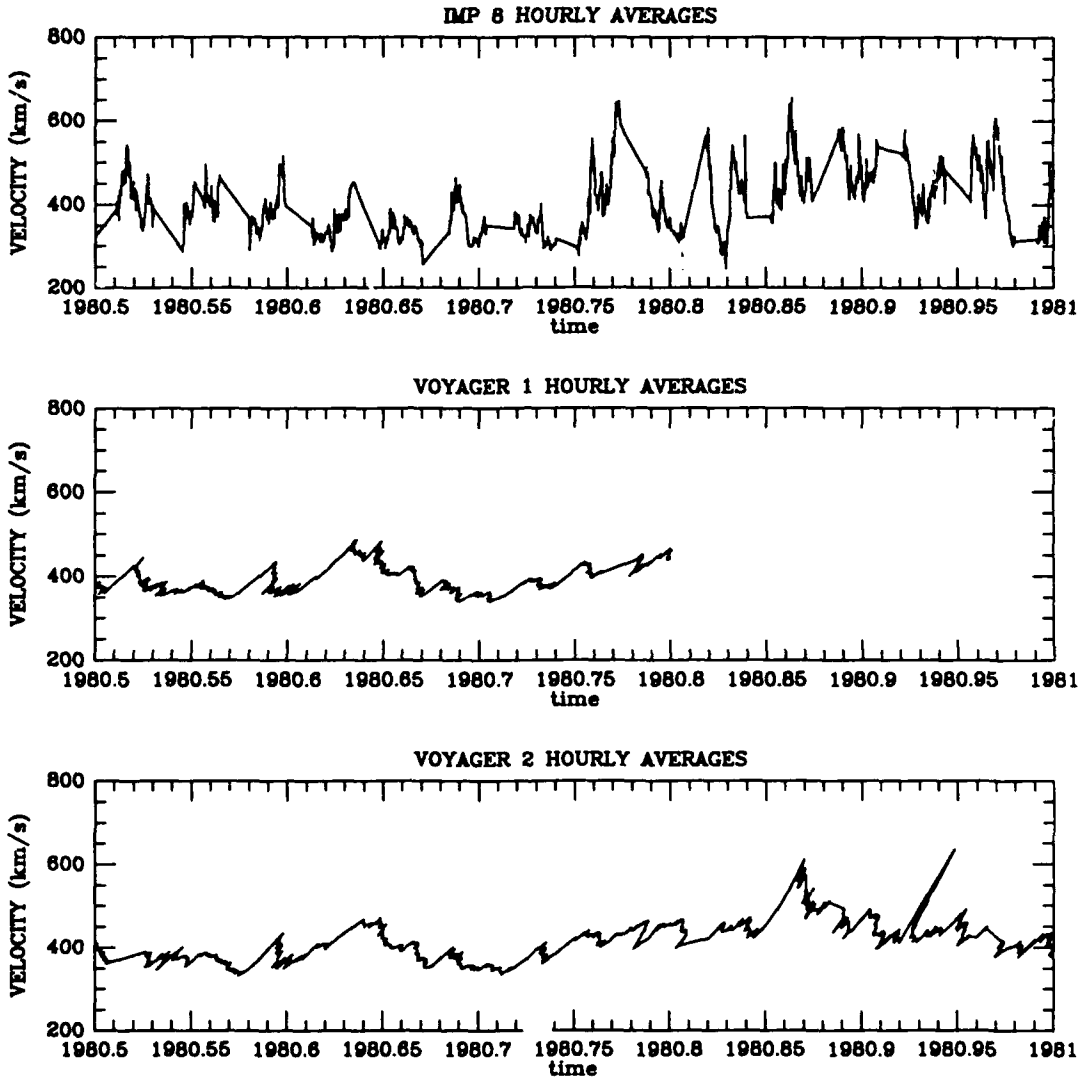

FIGURE C–7. Hourly Averages of Velocity for IMP 8 (Top), Voyager 1 (Middle), Voyager 2 (Bottom). Voyagers' velocity data projected to 1 AU.

APPENDIX D

SOLAR WIND DENSITY HOURLY AVERAGES (NORMALIZED)

Presented on the next few pages are hourly averages of solar wind density. These have been adjusted to account for the time it takes for plasma to propagate to the spacecraft's location and have been normalized to account for the fact that density varies approximately as R^{-2}. These data are presented in order to provide the reader a reference for discussions within the text of this thesis. Note how some data starts to get overwritten by other data beginning in 1978. This is a consequence of adjusting for plasma propagation time.

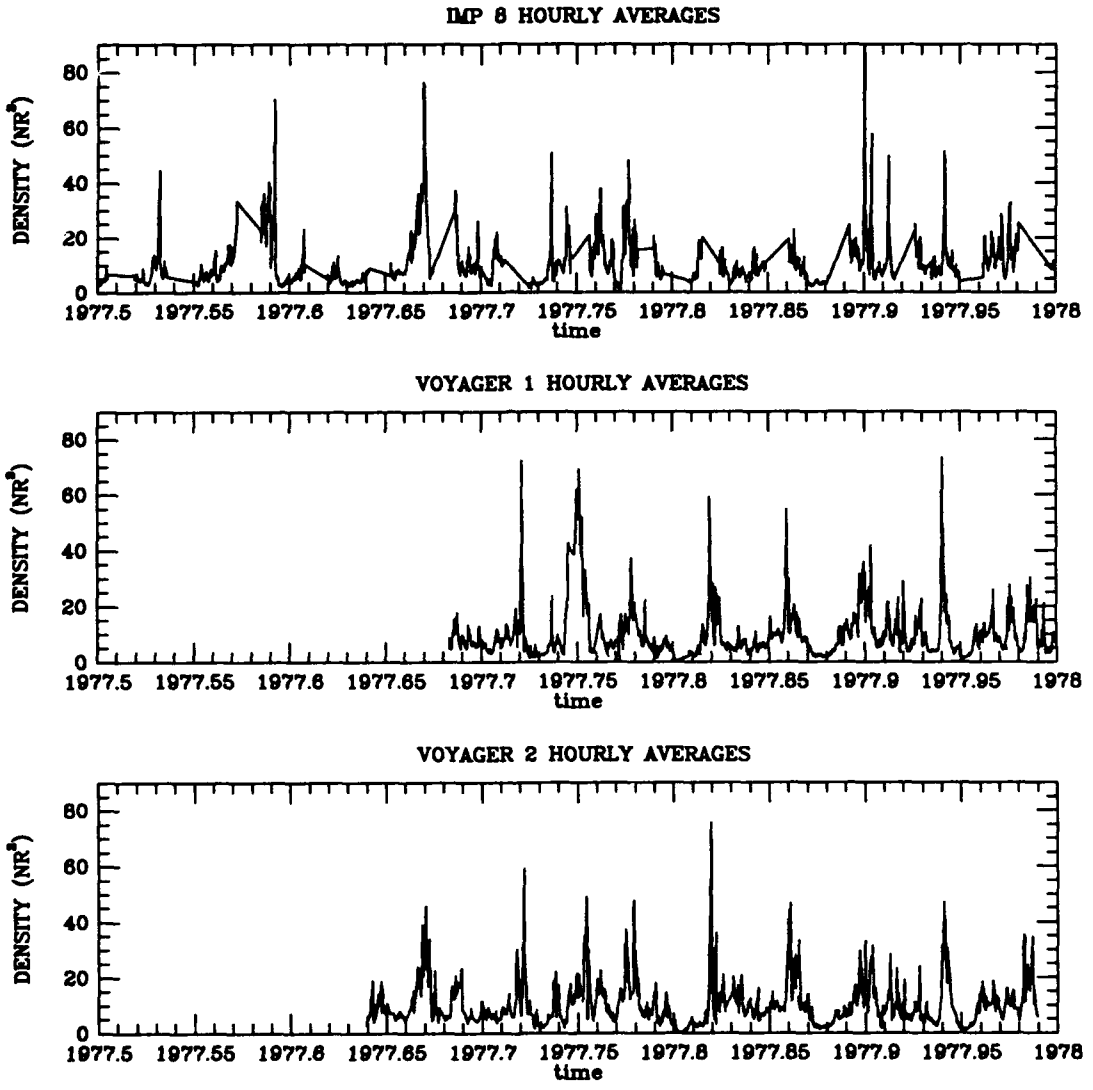

FIGURE D–1. Hourly Averages of Density for IMP 8 (Top), Voyager 1 (Middle), Voyager 2 (Bottom). Voyagers' density data normalized to 1 AU and corrected for Propagation Time.

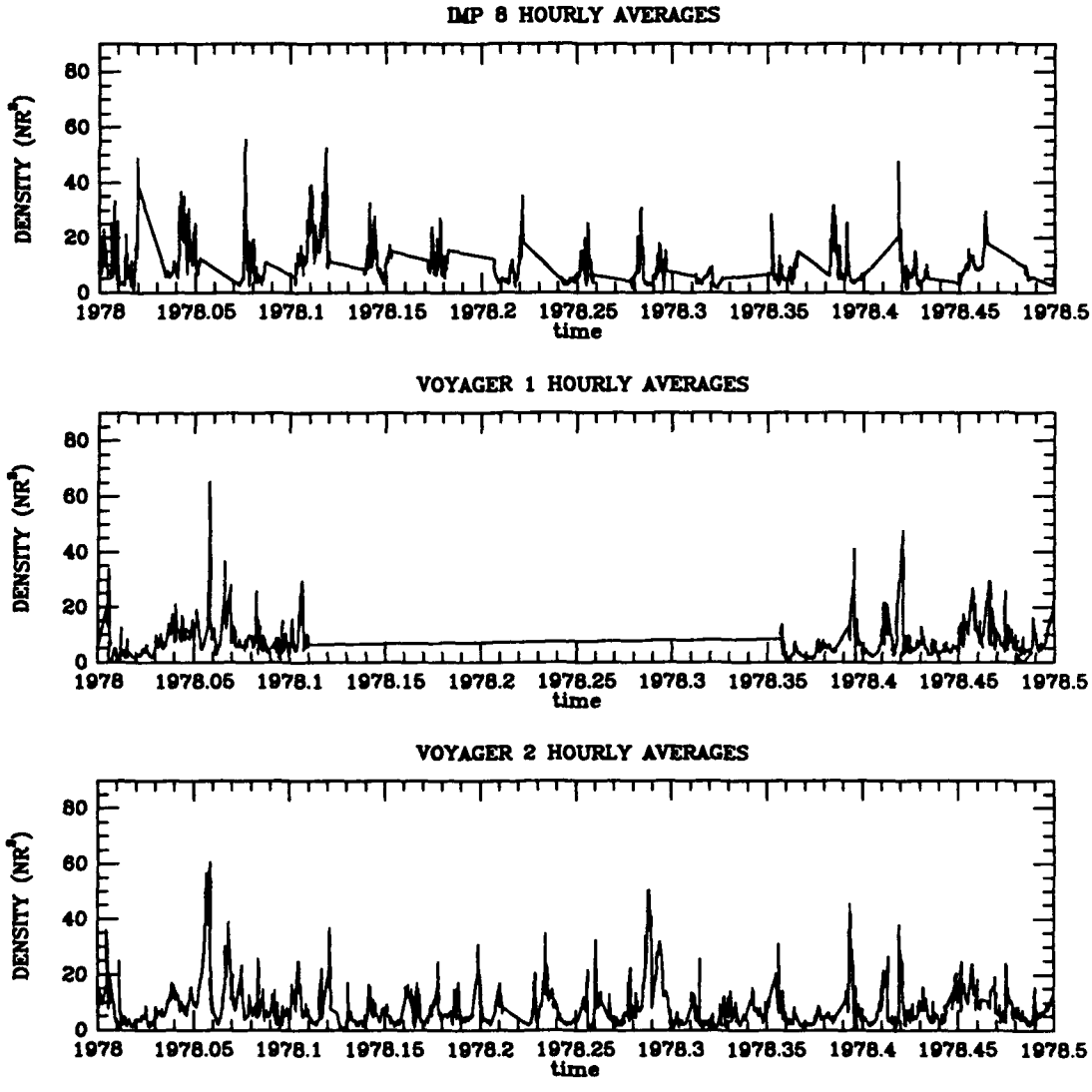

FIGURE D–2. Hourly Averages of Density for IMP 8 (Top), Voyager 1 (Middle), Voyager 2 (Bottom). Voyagers' density data normalized to 1 AU and corrected for Propagation Time.

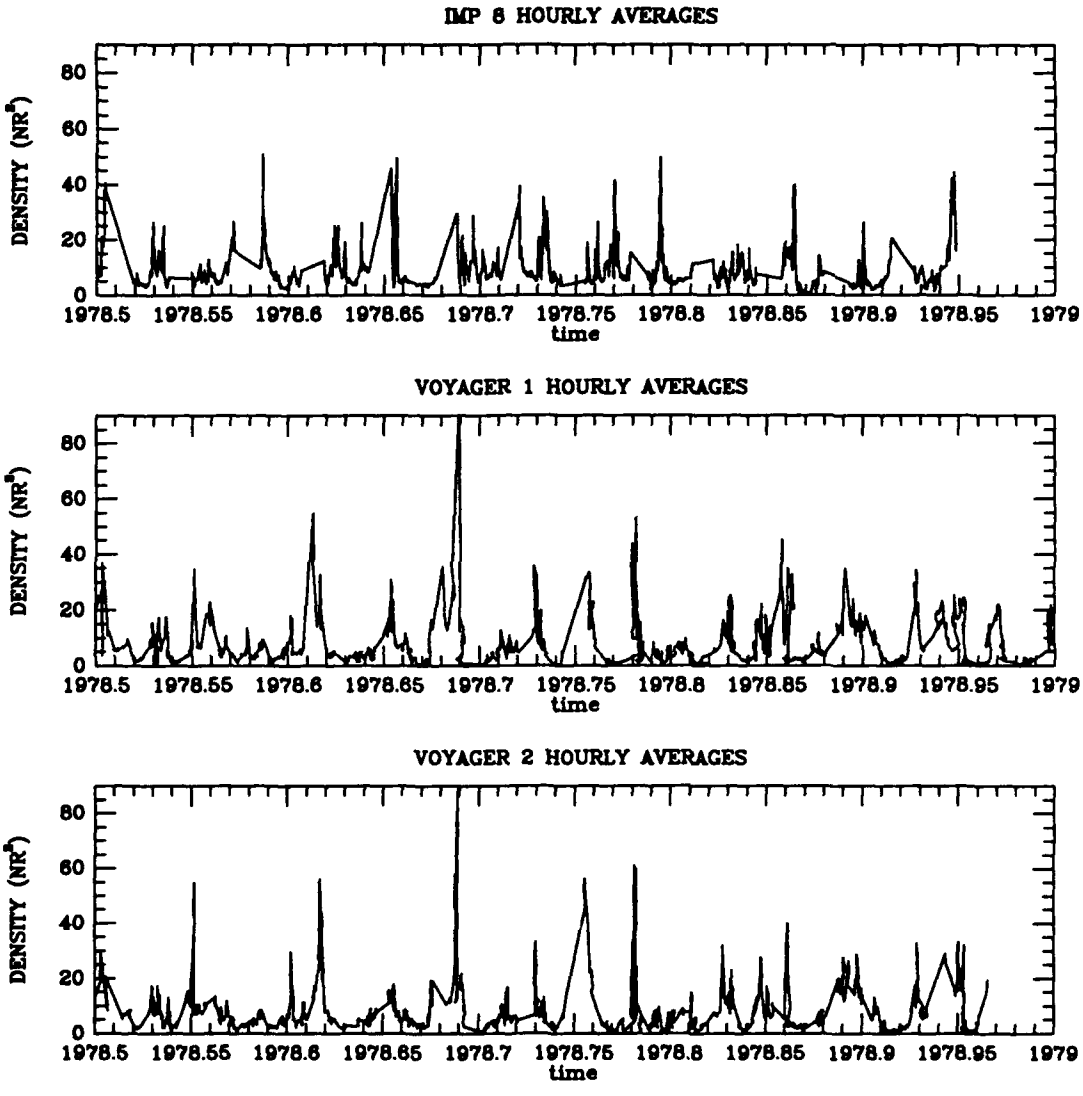

FIGURE D–3. Hourly Averages of Density for IMP 8 (Top), Voyager 1 (Middle), Voyager 2 (Bottom) Voyagers' density data normalized to 1 AU and Corrected for Propagation Time.

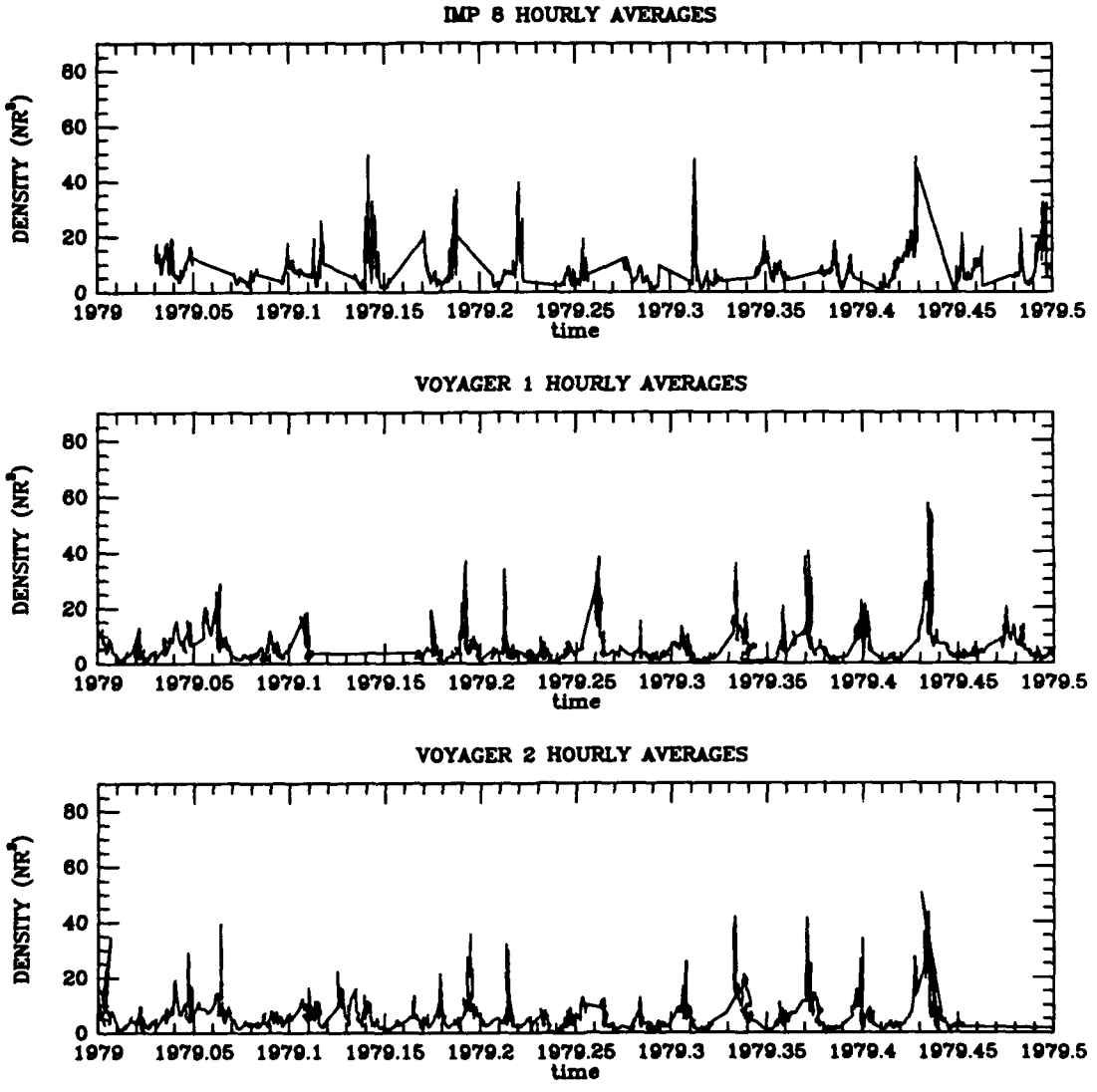

FIGURE D–4. Hourly Averages of Density for IMP 8 (Top), Voyager 1 (Middle), Voyager 2 (Bottom). Voyagers' density data normalized to 1 AU and Corrected for Propagation Time.

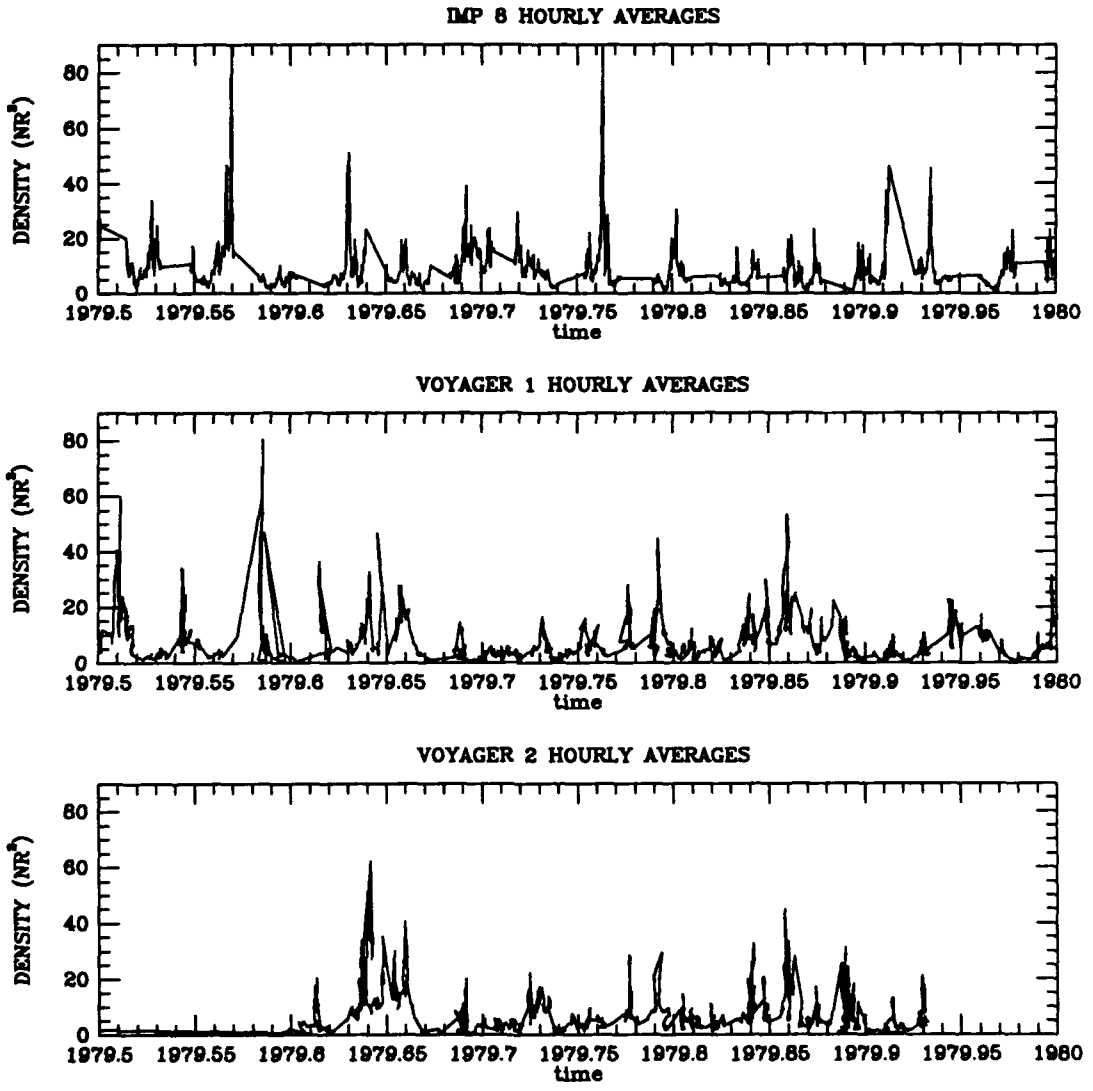

FIGURE D–5. Hourly Averages of Density for IMP 8 (Top), Voyager 1 (Middle), Voyager 2 (Bottom). Voyagers' density data normalized to 1 AU and Corrected for Propagation Time.

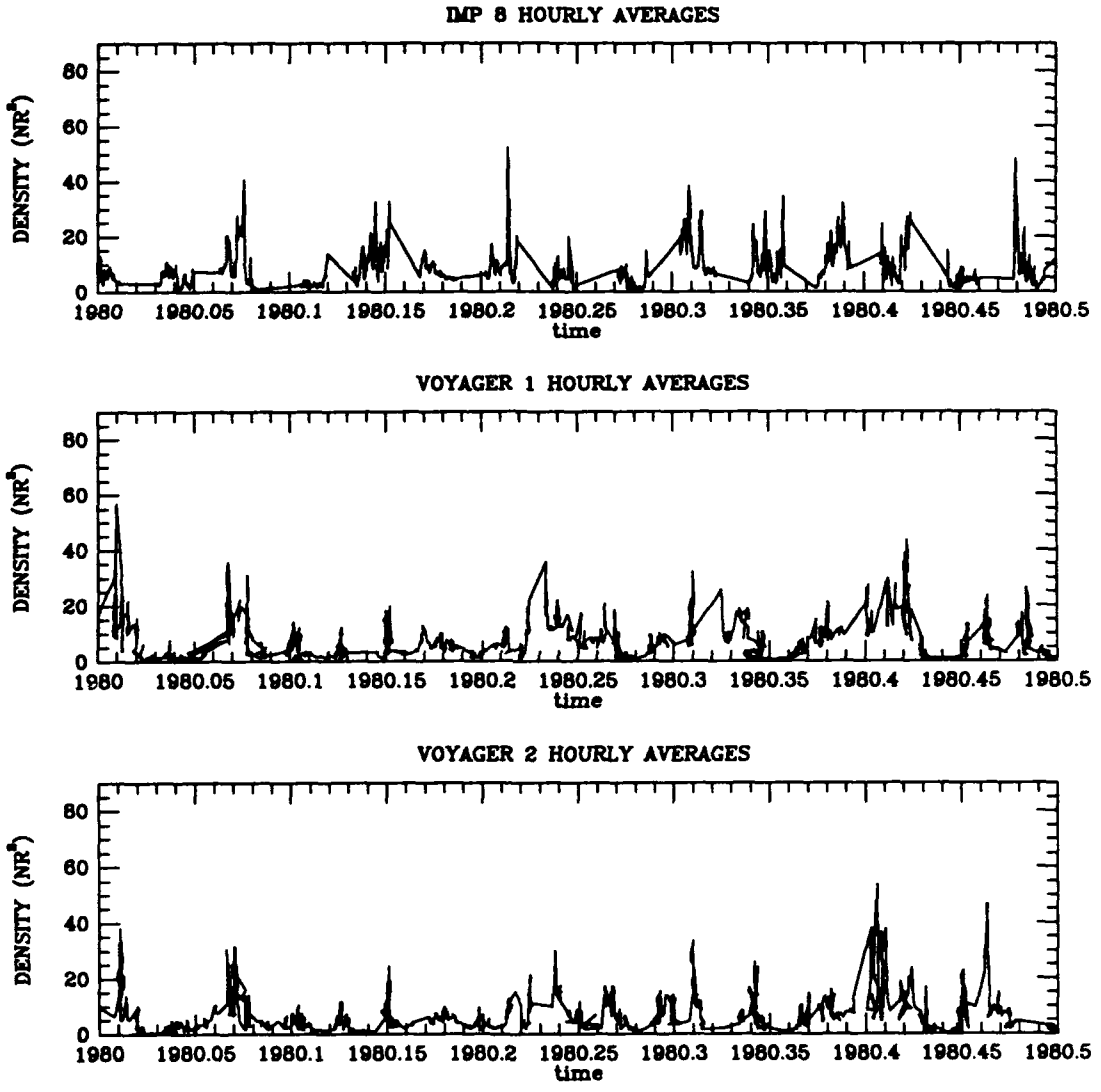

FIGURE D-6. Hourly Averages of Density for IMP 8 (Top), Voyager 1 (Middle), Voyager 2 (Bottom). Voyagers' density data normalized to 1 AU and Corrected for Propagation Time.

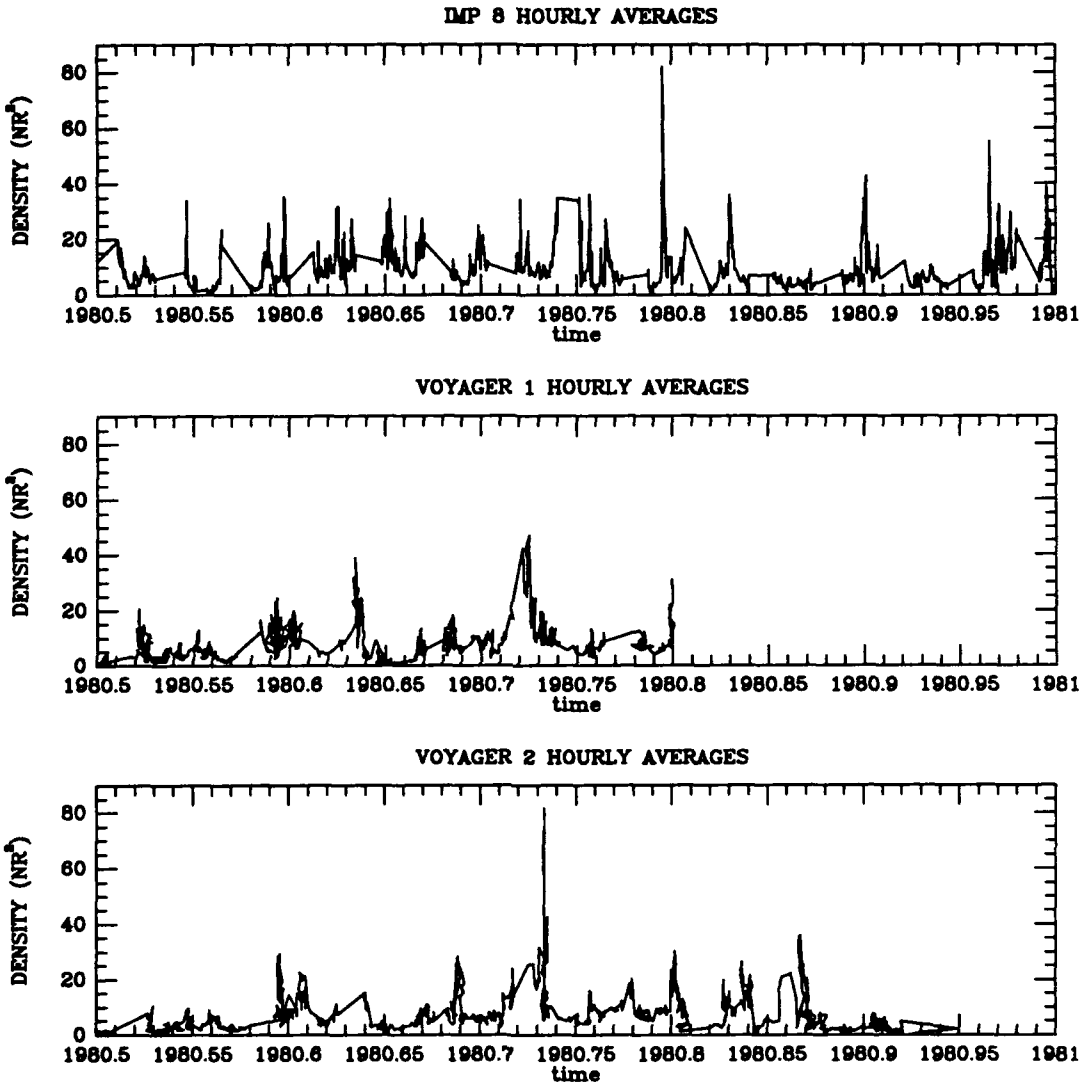

FIGURE D–7. Hourly Averages of Density for IMP 8 (Top), Voyager 1 (Middle), Voyager 2 (Bottom). Voyagers' density data normalized to 1 AU and Corrected for Propagation Time.

APPENDIX E

CORONAL HOLES AND HIGH SPEED STREAMS

Some of the differences between IMP 8 and Voyager 2 velocity measurements may be explained by examining latitudinal variations in the solar wind. In pursuit of this, I tried to correlate the location of coronal holes to the high speed streams measured by IMP 8.

Using an atlas of stackplots compiled by McIntosh et al. [1991], I examined plots of inferred magnetic fields and coronal holes within ± 25° of the heliographic equator for Carrington Rotations 1681-1787 (26 April 1979-22 April 1987). Using this range of latitude, I was assured of seeing all coronal holes which spanned the latitudinal range of IMP 8 (± 7.5°). I compared the times that IMP 8 recorded high velocity streams (those that peaked to 600 km/s or more) to the dates when coronal holes passed the central meridian. Allowing for approximately three to five days propagation time, I checked to see whether or not a coronal hole had passed the central meridian at a time coincident with the measurement of the high speed stream. For example, if IMP 8 measured a high speed stream between 20 and 27 June, I looked for a coronal hole to have passed the central meridian anytime between 15 and 24 June. Using this procedure, I looked at 152 periods when IMP 8 recorded a high speed stream. Coronal holes had been within three to five days of central meridian passage during 108 of these periods. This represents an overall average of about 71%. The table below summarizes the correlation of coronal holes and high speed streams by year between 1980 and 1986. The percentages for years 1979 and 1987 were omitted because data were available only for a partial year.

Year	Number Coronal Holes	Number High Speed Streams	Percentage
1980	4	6	67
1981	7	13	54
1982	23	28	82
1983	26	29	89
1984	23	27	85
1985	18	25	72
1986	4	17	23

The correlation between high speed streams and coronal holes increased after solar maximum and decreased after solar minimum. This result is expected because the number of coronal holes near the sun's equator increased near solar minimum and decreased near solar maximum. Since there were so many coronal holes present near the equator between 1982 and 1985, it was easy to find one passing the central meridian near the dates when IMP 8 measured the high speed streams.

In general, the correspondence between high speed streams and coronal holes is best when there are several large coronal holes, persisting for multiple Carrington Rotations. In the absence of such coronal hole structure, there is not always a one-to-one correspondence. According to Bravo et al. [1991], solar wind divergence can be great. Starting from a coronal hole only 10° wide, solar wind can diverge so that it appears as if it came from an angular width as wide as 100°. Considering this divergence, we could expect that some of the high speed streams originated from coronal holes outside of the region studied and coronal holes within this region produced high speed streams which propagated outside of this region.

In summary, a better method should be used to establish the relationship between high speed plasma streams and the existence of coronal holes. The method used in this thesis is too inexact. There are methods of tracking plasma streams back to the individual coronal holes which are more accurate, but more

time-consuming and difficult.

APPENDIX F

DELETED VOYAGER DATA

The tables below list the larger time intervals of data which have been removed from the Voyager 1 and Voyager 2 data sets. The reasons for deletion are indicated.

Table I. Voyager 1 Deletion Times

Reason	Start Time			End Time		
	Year	Day	Hour	Year	Day	Hour
Malfunction	1978	049	00	1978	138	00
Jupiter encounter	1979	059	14	1979	081	13
Saturn encounter	1980	316	23	1980	321	06
Malfunction	1980	328	00	1980	366	23

Table II. Voyager 2 Deletion Times

Reason	Start Time			End Time		
	Year	Day	Hour	Year	Day	Hour
Jupiter encounter	1979	183	16	1979	238	00
Saturn encounter	1981	236	13	1981	243	01
Uranus encounter	1986	024	07	1986	029	06
Neptune encounter	1989	236	14	1989	240	06
Jovian Tail	1979	258	20	1979	260	06
	1980	157	19	1980	157	23
	1980	324	03	1980	328	14
	1980	347	07	1980	350	16
	1981	014	08	1981	015	19
	1981	016	16	1981	021	06
	1981	043	15	1981	056	00
	1981	066	08	1981	072	05
	1981	094	15	1981	098	01
	1981	100	08	1981	103	09
	1981	106	18	1981	108	21
	1981	118	14	1981	119	09
	1981	140	08	1981	148	20
	1981	167	16	1981	170	06

REFERENCES

Belcher, J. W., Lazarus, A. J., McNutt, R., and Gordon, G. Jr., Solar Wind Conditions in the Outer Heliosphere and the Distance to the Termination Shock, submitted to *JGR*, 1992.

Bohlin, J. D., An Observational Definition of Coronal Holes, in *Coronal Holes and High Speed Wind Streams*, p. 29, Colorado Associated University Press, Boulder, 1977.

Bravo, S., Mendoza, B., and Perez-Enriquez, R., Coronal Holes as Sources of Large-Scale Wind Disturbances and Geomagnetic Perturbations, *JGR*, 96, A4, 1991.

Bridge, H. S., Lazarus, A. J., and Lyons, E. F., Proposal to the National Aeronautics and Space Administration for a Plasma Experiment on IMP-H and IMP-J, December 5, 1967.

Bridge, H. S., Belcher, J. W., Butler, R. J., Lazarus, A. J., Mavretic, A. M., Sullivan, J. D., Siscoe, G. L., and Vasyliunas, V. M., The Plasma Experiment on the 1977 Voyager Mission, *Space Science Review*, 21, 1977.

Farquhar, R. W., editor, Handbook on Trajectories, Mission Design, and Operations, 2d ed, Vol I, prepared by Working Group 3 of the Inter-Agency Consultative Group (IACG) for Space Science, 1990.

Gazis, P.R., Pioneer Venus and IMP 8 Observations of the Latitude Dependence of the Solar Wind, submitted to *JGR*, 1993.

Gurnette, B. L. and Woolley, R. v. d. R., editors, Explanatory Supplement to the Astronomical Ephemeris and the American Ephemeris and Nautical Almanac, p.

489, Her Majesty's Stationery Office, London, 1961.

Hundhausen, A. J., An Interplanetary View of Coronal Holes, in *Coronal Holes and High Speed Streams*, edited by J. B. Zirker, p. 225, Colorado Associated University Press, Boulder, 1977.

Lazarus, A. J., B. Yedidia, L. Villaneuva, R. L. McNutt, Jr., J. W. Belcher, U. Villante, and L. F. Burlaga, Meridional Plasma Flow in the Outer Heliosphere, *Geophysical Research Letters*, 15, 1519, 1988.

McIntosh, P.S., Thompson, R. J., and Willock, E. C., Atlas of Stackplots derived from Solar Synoptic Charts, World Data Center A for Solar- Terrestrial Physics, Boulder, 1991.

Miyake, W. et al., Multi-Spacecraft Observations of Heliographic Structure of the Solar Wind Speed, *Planetary and Space Science*, 36, 12, 1988.

Neugebauer, M., Quasi-Stationary and Transient States of Solar Winds, *Science*, 252, 1991.

Parker, E. N., Interplanetary Dynamical Processes, edited by R. E. Marshak, p. 139, John Wiley & Sons, Inc., New York, 1963.

Peratt, Anthony, L., Physics of the Plasma Universe, Springer-Verlag, New York, 1992.

Smith, Edward J., The Sun in Time, in *The Sun and Interplanetary Magnetic Field*, edited by C. P. Sonett, M. S. Giampapa, and M. S. Matthews, p. 176, University of Arizona Press, 1991.

Suess, S. T., The Heliopause, *Reviews of Geophysics*, 28, 1, 1990.

Suess, S. T., McComas, D. J., Hoeksema, J. T., Prediction of the Heliospheric Current Sheet Tilt 1992-1996, *Geophysical Research Letters*, 20, 1993.

Vasyliunas, Vytenis M., Deep Space Plasma Measurements, in *Methods of Experimental Physics* Vol. 9B, edited by R. H. Lovbergs, pp. 49-87, Academic Press, Inc., New York, 1971.

ACKNOWLEDGEMENTS

Special thanks goes to Dr. Alan J. Lazarus, whose patience, understanding, and mentoring made it possible for me to complete this thesis. Also thanks to Professor John W. Belcher and all the members of MIT's Interplanetary Plasma Group for their support and encouragement. Thanks to Dr. George Gordon, who kept the computers running and the data flowing. Thanks to Pam Milligan for providing IMP 8 and Voyager data. Thanks to Louis Villaneuva for his help on numerous occasions, especially with the section on moment and fit calculations.

BIOGRAPHY

Steve Simmerer graduated from the United States Military Academy at West Point, New York, in May, 1981, with a B.S. in Engineering and was commissioned in the United States Army's Corps of Engineers. Since graduation, he has served in a variety of assignments such as platoon leader, project engineer, company commander, and staff officer in several locations including Germany, Egypt, Belgium, and the United States. Upon receiving a Master of Science in Physics, Steve will teach physics at West Point. Steve has published the following articles:

Lunar Construction: The Countdown Begins, in *The Military Engineer*, 79, 1987.

Preparing to Bridge the Lunar Gap, in *Journal of Aerospace Engineering*, 1, 1988.